Supporting Information

for

Efficient synthesis of cyclic carbonates and oxazolidinones by simple zinc guanidinato complexes.

Carlos Ginés,[a] Blanca Parra-Cadenas,[a] David Elorriaga,[b] Daniel García-Vivó,[c] Rafael Fernández-Galán,[a] Alberto Ramos,[a] Fernando Carrillo-Hermosilla.*[,a]

E-mail: Fernando.Carrillo@uclm.es

a Departamento de Química Inorgánica, Orgánica y Bioquímica-Centro de Innovación en Química Avanzada (ORFEO−CINQA), Facultad de Ciencias y Tecnologías Químicas, Universidad de Castilla-La Mancha, 13071 Ciudad Real, Spain

b Departamento de Química Inorgánica, Orgánica y Bioquímica-Centro de Innovación en Química Avanzada (ORFEO−CINQA), Facultad de Ciencias Ambientales y Bioquímica, Universidad de Castilla-La Mancha, 45071 Toledo, Spain

c Departamento de Química Orgánica e Inorgánica/IUQOEM, Universidad de Oviedo, 33071 Oviedo, Spain.

Table of Contents

1. General information

All manipulations were performed under nitrogen atmosphere, due to the sensitivity of the reagents and some products, using dual-manifold (N_2/vacuum) Schlenk line and a glovebox MBRAUN. The solvents and reagents were obtained from Sigma Aldrich and were used without previous purification. The commercial anhydrous solvents were kept on activated molecular sieves (4 Å) under inert atmosphere. The precursor 2-(diphenylphosphino)aniline was synthesized adapting a previously published experimental procedure.[1] Guanidines were synthesized using a procedure previously published by our research group.[2]

NMR spectra were recorded on a Bruker Avance Neo 500 spectrometer, using standard TOPSPIN 4.0 software. The chemical shifts were assigned based on homo- and heteronuclear 2D NMR experiments (COSY, HSQC, HMBC). Elemental analysis data were recorded on a Foss-Heraeus CHNO-Rapid analyzer.

2. Synthesis of 2-(diphenylphosphino)aniline precursor

In a Schlenk, CuI (0.193 g, 1 mmol), $HPPh_2$ (3.825 mL, 22 mmol) and DMEDA (0.77 mL, 7 mmol) were added in 40 mL of toluene, stirring for 10 minutes. Then, 2-iodoaniline (4.385 g, 20 mmol) and Cs_2CO_3 (13.050 g, 40 mmol) were added, stirring at 110 ºC for 20h. H_2O (20 mL) was added, and the suspension stirred for 30 min. Then, it was extracted with ethyl acetate (2x20 mL) and the organic phase was dried over $MgSO_4$. The solvent was removed in vacuum forming a viscous residue, which was purified by chromatography in a hexane/ethyl acetate mixture (9:1). The solution was concentrated and kept at -20 ºC and white solid was obtained. Yield: 3.20 g, 58%. The ^1H and ^{31}P NMR data agree with those described in bibliography.

3. Synthesis and characterization of L^1H, L^2H, L^3H, L^4H.

In a Schlenk, the corresponding aniline (3.14 mmol), diisopropylcarbodiimide (3.14 mmol) and $ZnEt_2$ as catalyst (0.094 mmol, 1.1 M in toluene) were added to 10 ml of toluene. The reaction mixture was stirred at 70°C for 5h. The solution was concentrated; pentane was added and kept at -20ºC to obtain a white solid. Yield: 0.51 g (91%) for L^1H, 0.69 g (93%) for L^2H, 0.45 g (80%) for L^3H, 0.92 g (90%) for L4H.

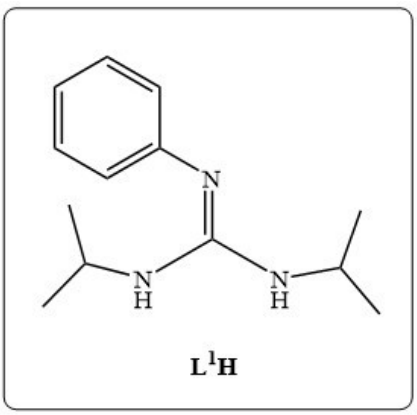

L^1H

^1H NMR (500 MHz, 298 K, C_6D_6) δ (ppm) = 7.26 (m, 2H, *H*-arom.), 7.13 (m, 2H, *H*-arom.), 6.92 (tt, 1H,

$^{3}J_{HH}$ = 7.4, $^{3}J_{HH}$ = 1.2, *H*-arom.), 3.64 (m, 2H, HNC*H*$(CH_3)_2$), 3.43 (d, 2H, $^{3}J_{HH}$ = 7.2, *H*NCH$(CH_3)_2$), 0.89 (d, 12H, $^{3}J_{HH}$ = 6.4, HNCH(C*H*$_3)_2$).

^{13}C{^{1}H} NMR (126 MHz, 298 K, C_6D_6) δ (ppm) = 151.7 (s, *C*-arom.), 149.5 (s, *C*N_3), 129.6 (s, *C*-arom.), 123.7 (s, *C*-arom.), 121.3 (s, *C*-arom.), 43.2 (s, HNC*H*$(CH_3)_2$), 23.2 (s, HNCH(*C*$H_3)_2$).

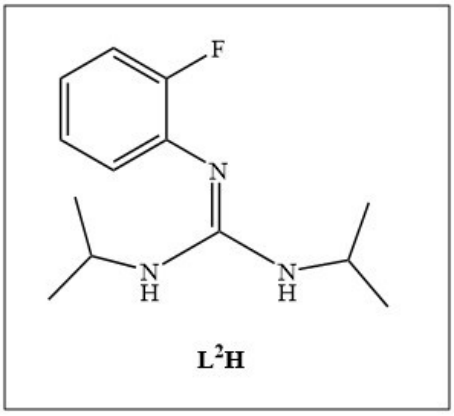

L^{2}H

^{1}H NMR (500 MHz, 298 K, C_6D_6) δ (ppm) = 7.53 (m, 4H, *H*-arom.), 7.15-7.13(m, 1H, *H*-arom.), 7.04-7.00 (m, 8H, *H*-arom), 6.94-6.91 (m, 1H, *H*-arom.), 6.73-6.68 (m, 1H, *H*-arom.), 3.64 (m, 2H, HNC*H*$(CH_3)_2$), 3.37 (d, 2H, *H*NCH$(CH_3)_2$), 0.89 (d, 12H, HNCH(C*H*$_3)_2$).

^{13}C{^{1}H} NMR (101 MHz, 298 K, C_6D_6) δ (ppm) = 157.20 (s, *C*N_3), 155.28 (s, *C*-arom.), 139.15 (s, *C*-arom.), 126.4 (s, *C*-arom.), 124.9 (s, *C*-arom.), 122.1 (s, *C*-arom.), 116.3 (s, *C*-arom.), 43.4 (s, HNC*H*$(CH_3)_2$), 23.2 (s, HNCH(*C*$H_3)_2$).

^{13}F{^{1}H} NMR (471 MHz, 298 K, C_6D_6) δ (ppm) = -125.27.

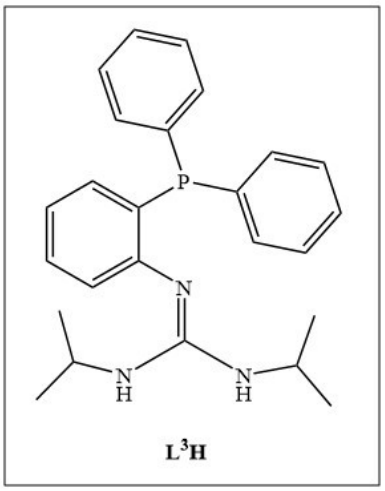

L^{3}H

^{1}H NMR (500 MHz, 298 K, C_6D_6) δ (ppm) = 7.53 (m, 4H, *H*-arom.), 7.18 (m, 1H, *H*-arom.), 7.00-7.15 (m, 8H, *H*-arom), 6.79 (m, 1H, *H*-arom.), 3.45 (m, 2H, HNC*H*$(CH_3)_2$), 3.37 (d, 2H, *H*NCH$(CH_3)_2$), 0.82 (d, 12H, HNCH(C*H*$_3)_2$).

^{13}C{^{1}H} NMR (101 MHz, 298 K, C_6D_6) δ (ppm) = 154.12 (s, *C*-arom.), 148.6 (s, *C*N_3), 139.6 (s, *C*-arom.), 134.6 (s, *C*-arom.), 124.1 (s, *C*-arom.), 133.0 (s, *C*-arom.), 129.9 (s, *C*-arom.), 128.5 (s, *C*-arom.), 128.2 (s, *C*-arom.), 121.7 (s, *C*-arom.), 121.6 (s, *C*-arom.), 43.1 (s, HNC*H*$(CH_3)_2$), 23.4 (s, HNCH(*C*$H_3)_2$).

^{31}P{^{1}H} NMR (162 MHz, 298 K, C_6D_6): δ -13.2.

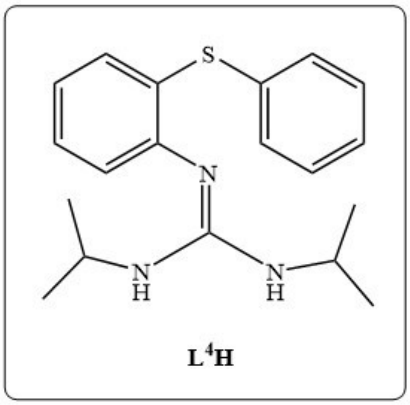

L^4H

^{1}H NMR (500 MHz, 298 K, C_6D_6) δ (ppm) =7.50-7.47 (m, 1H, *H*-arom.), 7.26-7.24 (m, 1H, *H*-arom.), 7.06-7.05 (m, 2H, *H*-arom.), 7.03-6.99 (m, 2H, *H*-arom.), 6.96-6.93 (m, 1H, *H*arom), 6.73-6.75 (m, 1H, *H*-arom.), 3.67-3.60 (m, 2H, HNC*H*$(CH_3)_2$), 3.42 (d, 2H, *H*NCH$(CH_3)_2$), 0.91 (d, 12H, HNCH(C*H*$_3)_2$).

^{13}C{^{1}H} NMR (101 MHz, 298 K, C_6D_6) δ (ppm) = 149.7 (s, *C*N_3), 149.4 (s, *C*-arom.), 136.4 (s, *C*-arom.), 132.8 (s, *C*-arom.), 131.7 (s, *C*-arom.), 130.5 (s, *C*-arom.), 129.3 (s, *C*-arom.), 127.5 (s, *C*-arom.), 127.0 (s, *C*-arom.), 123.1 (s, *C*-arom.), 122.1 (s, *C*-arom.), 43.3(s, HNC*H*$(CH_3)_2$), 23.4 (s, HNCH(*C*$H_3)_2$).

4. Synthesis and characterization of the complexes

The corresponding guanidine (2.5 mmol) and dimethylzinc (2.5 mmol) were added to a Schlenk, with the minimal amount of toluene, completing the reaction in 10 minutes. The solution was concentrated, hexane was added, obtaining a white solid which was filtered and dried in vacuum. Yields: 0.72 g (97%) for complex **1**, 0.73 g (93%) for complex **2**, 0.78 g (91%) for complex **3**, 0.96 g (95%) for complex **4.**

Complex **1**. Elem. Anal. Calc. for [$C_{14}H_{23}N_3Zn$]: C, 56.29; H, 7.76; N, 14.07. Found: C, 56.38; H, 7.82; N, 14.10.

Complex **2**. Elem. Anal. Calc. for [$C_{14}H_{22}FN_3Zn$]: C, 53.09; H, 7.00; N, 13.27. Found: C, 53.12; H, 7.10; N, 13.40.

Complex **3**. Elem. Anal. Calc. for [$C_{26}H_{32}N_3PZn$]: C, 64.67; H, 6.68; N, 8.70. Found: C, 64.38; H, 6.82; N, 8.10.

Complex **4**. Elem. Anal. Calc. for [$C_{20}H_{27}N_3SZn$]: C, 59.04H, 6.69; N, 10.33. Found: C, 59.18; H, 6.82; N, 10.40.

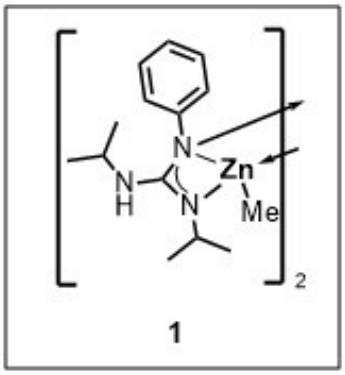

1

^{1}H NMR (500 MHz, 298 K, C_6D_6) δ (ppm) = 7.21-7.12 (m, 4H, *H*-arom.), 6.81-6.80 (m, 1H, *H*-arom.), 3.48 (m, 2H, *H*NC*H*$(CH_3)_2$), 3.11-3.05 (m, 1H, HNC*H*$(CH_3)_2$), 1.08 (d, 6H, HNCH(C*H*$_3)_2$), 0.60 (d, 6H, HNCH(C*H*$_3)_2$), -0.11 (s, 3H, ZnC*H*$_3$).

^{13}C{^{1}H} NMR (101 MHz, 298 K, C_6D_6) δ (ppm) = 161.5 (s, *C*N_3), 151.1(s, *C*-arom.), 129.2 (s, *C*-arom.), 122.3 (s, *C*-arom.), 120.7 (s, *C*-arom.), 46.7 (s, HNC*H*$(CH_3)_2$), 44.8 (s, HNC*H*$(CH_3)_2$), 24.5 (s, HNCH(*C*$H_3)_2$), 23.5 (s, HNCH(*C*$H_3)_2$), -12.0 (s, Zn*C*H_3).

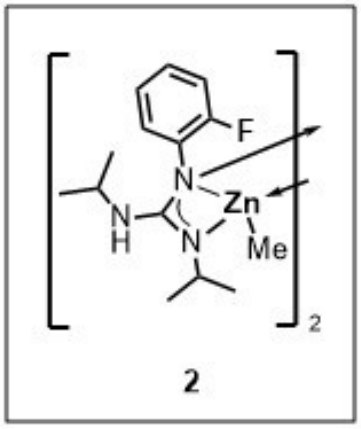

2

^{1}H NMR (500 MHz, 298 K, C_6D_6) δ (ppm) = 7.16 (m, 1H, *H*-arom.), 6.94-6.90 (m, 1H, *H*-arom.), 6.84-6.81 (m, 1H, *H*-arom.), 6.64-6.61 (m, 1H, *H*-arom.), 3.51-3.45 (m, 2H, *H*NC*H*$(CH_3)_2$), 3.13-3.10 (m, 1H, HNC*H*$(CH_3)_2$), 1.10 (d, 6H, HNCH(C*H*$_3)_2$), 0.63 (d, 6H, HNCH(C*H*$_3)_2$), -0.14 (s, 3H, ZnC*H*$_3$).

^{13}C{^{1}H} NMR (101 MHz, 298 K, C_6D_6) δ (ppm) = 162.4 (s, *C*N_3), 157.4(s, *C*-arom.), 155.6(s, *C*-arom.), 124.7(s, *C*-arom.), 115.6(s, *C*-arom.), 115.4 (s, *C*-arom.), 46.9 (s, HNC*H*$(CH_3)_2$), 45.3 (s, HNC*H*$(CH_3)_2$), 24.1 (s, HNCH(*C*$H_3)_2$), 23.5 (s, HNCH(*C*$H_3)_2$), -14.8(s, Zn*C*H_3).

^{13}F{^{1}H} NMR (471 MHz, 298 K, C_6D_6) δ (ppm) = -125.27.

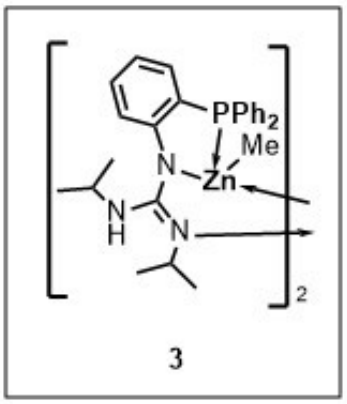

3

^{1}H NMR (500 MHz, 298 K, C_6D_6) δ (ppm) = 7.79-7.75 (m, 1H, *H*-arom.), 7.42-7.38 (m, 1H, *H*-arom.), 7.12-6.99 (m, 9H, *H*-arom.), 6.69-6.65 (m, 1H, *H*-arom.), 6.52-6.49(m, 1H, *H*-arom.), 6.45-6.41 (m, 1H, *H*-arom.), 3.68 (d, 1H, *H*NCH$(CH_3)_2$), 3.48-3.42 (m, 1H, HNC*H*$(CH_3)_2$), 3.12-3.03 (m, 1H, HNC*H*$(CH_3)_2$), 1.51 (d, 3H, HNCH(C*H*$_3)_2$), 1.36 (d, 3H, HNCH(C*H*$_3)_2$), 0.60 (d, 3H, HNCH(C*H*$_3)_2$), 0.44(d, 3H, HNCH(C*H*$_3)_2$), 0.02 (d, 3H, ZnC*H*$_3$).

^{13}C{^{1}H} NMR (101 MHz, 298 K, C_6D_6) δ (ppm) = 163.7 (s, *C*N_3), 158.7 (s, *C*-arom.), 136.4 (s, *C*-arom.), 136.3 (s, *C*-arom.), 135.4 (s, *C*-arom.), 135.3 (s, *C*-arom.), 133.9 (s,

C-arom.), 132.9 (s, *C*-arom.), 131.0 (s, *C*-arom.), 130.0 (s, *C*-arom.), 128.8 (s, *C*-arom.), 128.7 (s, *C*-arom.),128.5 (s, *C*-arom.), 120.2 (s, *C*-arom.), 116.6 (s, *C*-arom.), 49.8 (s, HN*C*H(CH_3)$_2$), 45.1 (s, HN*C*H(CH_3)$_2$), 25.4 (s, HNCH(*C*H_3)$_2$), 24.2 (s, HNCH(*C*H_3)$_2$), 24.0 (s, HNCH(*C*H_3)$_2$), 22.2 (s, HNCH(*C*H_3)$_2$), -6.08 (s, Zn*C*H_3).

^{31}P{^{1}H} NMR (162 MHz, 298 K, C_6D_6): δ -24.17.

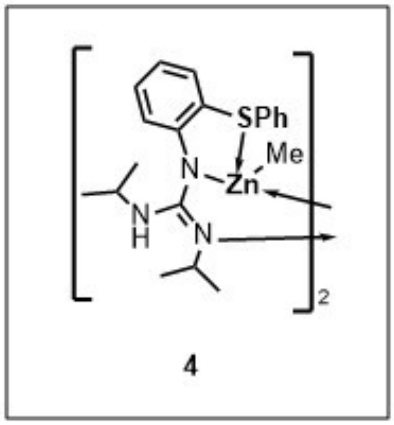

4

^{1}H NMR (500 MHz, 298 K, C_6D_6) δ (ppm) = 7.39-7.37 (m, 1H, *H*-arom.), 7.23-7.22 (m, 2H, *H*-arom.), 6.97-6.94 (m, 2H, *H*-arom.), 6.88-6.86 (m, 1H, *H*-arom.), 6.67-6.64 (m, 1H, *H*-arom.), 6.43-6.40 (m, 2H, *H*-arom.), 3.54-3.46 (m, 2H, *H*NC*H*(CH_3)$_2$), 3.16-3.11 (m, 1H, HNC*H*(CH_3)$_2$), 1.54-1.50 (dd, 6H, HNCH(C*H*$_3$)$_2$), 0.56-0.54(dd, 6H, HNCH(C*H*$_3$)$_2$), -0.27 (s, 3H, ZnC*H*$_3$).

^{13}C{^{1}H} NMR (101 MHz, 298 K, C_6D_6) δ (ppm) = 162.3 (s, *C*N_3), 154.7 (s, *C*-arom.), 137.8 (s, *C*-arom.), 137.6 (s, *C*-arom.), 131.4 (s, *C*-arom.), 128.9 (s, *C*-arom.), 127.1 (s, *C*-arom.), 126.0 (s, *C*-arom.), 120.7 (s, *C*-arom.), 117.0 (s, *C*-arom.), 115.5 (s, *C*-arom.), 50.0 (s, HN*C*H(CH_3)$_2$), 45.3 (s, HN*C*H(CH_3)$_2$), 25.3 (s, HNCH(*C*H_3)$_2$), 25.2 (s, HNCH(*C*H_3)$_2$), 24.5 (s, HNCH(*C*H_3)$_2$), 21.8 (s, HNCH(*C*H_3)$_2$), -8.4 (s, Zn*C*H_3).

5. Synthesis and characterization of cyclic carbonates

5.1. Synthesis of cyclic carbonates

In a 300 mL J. Young Schlenk flask, 1 mol% of catalyst **1** ($49.5 \cdot 10^{-3}$ mmol), 2 mol% of TBAI ($100 \cdot 10^{-3}$ mmol), the corresponding epoxide (5 mmol), and an atmospheric CO_2 pressure were added. The reaction mixture was heated at 100 °C for 24 hours. In the case of the epichlorohydrin precursor, dry 2-MeTHF was used as solvent. Afterwards, the conversion to the corresponding cyclic carbonates was determined by ^{1}H NMR spectroscopy after dissolving the crude product in $CDCl_3$.

5.2. NMR details of cyclic carbonates

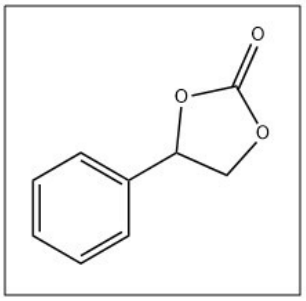

4-phenyl-1,3-dioxolan-2-one (6a): ^{1}H NMR ($CDCl_3$) δ (ppm) = 7.32-7.29 (m, 3H), 7.25-7.26 (m, 3H), 5.58 (t, 1H), 4.69 (t, 1H), 4.18 (t, 1H).

4-(4-chlorophenyl)-1,3-dioxolan-2-one (6b): ^{1}H NMR ($CDCl_3$) δ (ppm) = 7.43-7.41 (m, 3H), 7.32-7.21 (m, 3H), 5.66 (t, 1H), 4.80 (t, 1H), 4.30 (t, 1H).

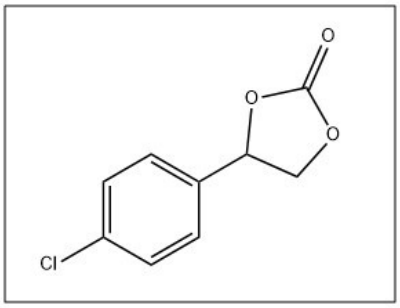

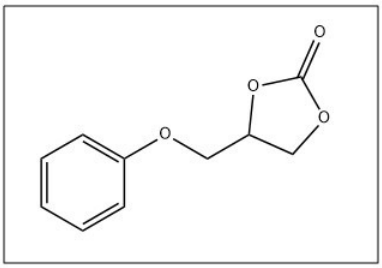

4-(4-(phenoxymethyl)phenyl)-1,3-dioxolan-2-one (6c): ^{1}H NMR ($CDCl_3$) δ (ppm) = 7.32-7.29 (m, 2H), 7.03-7.00 (m, 1H), 6.92-6.90 (m, 2H) 5.04-5.00 (m, 1H), 4.62-4.51 (dt, 2H), 4.25-4.12 (dt, 2H).

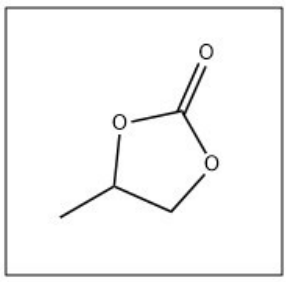

4-methyl-1,3-dioxolan-2-one (6d): ^{1}H NMR ($CDCl_3$) δ (ppm) = 4.88-4.81 (m, 1H), 4.54 (t, 1H), 4.01 (t, 1H), 1.48 (t, 3H).

4-ethyl-1,3-dioxolan-2-one (6e): ^{1}H NMR ($CDCl_3$) δ (ppm) = 4.69-4.63 (m, 1H), 4.52 (t, 1H), 4.08 (t, 1H), 1.85-1.75 (m, 2H), 1.03 (t, 3H).

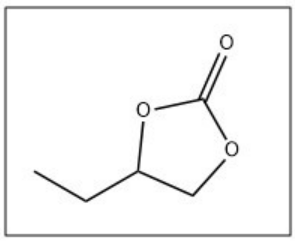

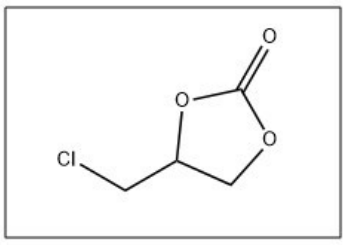

4-(chloromethyl)-1,3-dioxolan-2-one (6f): ^{1}H NMR ($CDCl_3$) δ (ppm) = 4.98-4.94 (m, 1H), 4.58 (t, 1H), 4.40 (t, 1H), 3.79-37 (dd, 2H).

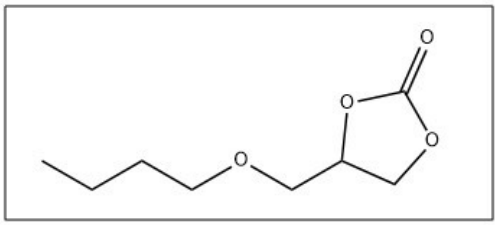

4-(butoxymethyl)-1,3-dioxolan-2-one (6g): ^{1}H NMR ($CDCl_3$) δ (ppm) = 4.75-4.70 (m, 1H), 4.39 (t, 2H), 4.25 (t, 1H), 3.56 (dd, 1H), 3.46 (dd, 1H), 3.38 (tt, 2H), 1.45-1.39 (m, 2H), 1.27-1.21 (m, 2H), 0.78 (t, 3H).

Table S1. Reported catalysts for the coupling of CO_2 and epoxides at atmospheric pressure.

Catalyst (mol%)	Cocatalyst (mol%)	Temperature (°C)	Time (h)	Solvent	Conversion (%)	TON	TOF (h^{-1})	Reference
$[Zn_4(OCOCF_3)_6O]$ carboxylato cluster (2)	I^- (4)	25	20	Neat	94	47	2.4	3a
$[Zn(DIP_2pyr)_2]$ N.N-bischelato complex (2.5)	Br^- (5)	105	2	Neat	86	34	17.2	3b
$[Zn(OH\text{-}salC_2NH_2Am]$ salicylato bifunctional complex (0.5)	Br^- (0.5)	120	12	DMF	90	180	15.0	3c
[Zn(N.N.O)(N.O)] Schiff base bischelato complex (0.14)	Br^- (0.2)	100	24	Neat	77	550	22.9	3d
Bis-(Zn-salphen) dinuclear complex (2)	I^- (2.7)	95	2	Neat	91	46	22.8	3e
Bifunctional Zn(II) porphyrin complex (0.05)	Br^- (0.05)	20	48	Neat	82	1640	34.2	3f
[Zn(NCP)Cl] porphyrin complex (0.004)	Br^- (0.0169)	120	24	Neat	97	24250	1010.4	3g
In situ generated catalyst from Zn. DMF and BnBr (5)	Br^- (5)	80	12	DMF	>99	20	1.7	3h
$[Zn(Brpy_2\text{-}pyr)_2$ Tridentate bispyridylpyrrole complex (0.1)	Br^- (10)	25	48	Neat	>99	990	20.6	3i
$[ZnMe(N.N.O\text{-}scorpionate)(ZnMe_2)]Br$ Bifunctional complex (5)	Br^- (10)	25	24	Neat	53	11	0.4	3j

$[Hmim]_2[ZnBr_4]$ Metal-ionic liquid (5)	Br^- (5)	25	5	Neat	>99	20	4.0	3k
$AsC(O)(OCO_2)Zn$ Ascorbato complex (16)	Br^- (32)	50	17	Neat	88	6	0.3	3l
$[Zn_4(L)_4(OH_2)_2(O)](TEAH)_2$ Tetranuclear Schiff base complex (0.01)	Br^- (2)	80	4	Neat	81	8100	2025.0	3m
$[\{ZnBr(DBM)\}_2]Br_2$ Diketone bifunctional complex (15)	Br^- (15)	60	16	Neat	97	6	0.4	3n
$[Zn(Me_6Tren)I]I$ Bifunctional complex (1)	I^- (1)	80	6	Neat	>99	99	16.5	3o
La_2Zn(N.O-ligand)$(OBn)_2$ Heterobimetallic diglycolamine bridged bis(phenolato) complex (0.5)	Br^- (2)	25	24	Neat	93	186	7.8	3p
$Zn(betaine)_2Br_2$ Bischelato complex (2)	Br^- (2)	40	24	Neat	>99	50	2.1	3q
$[ZnMe(\kappa^3$-cis-bpmy$)]$ Scorpionato complex (5)	Br^- (5)	25	24	Neat	71	14	0.6	3r
Catalyst 1 **(1)**	I^- **(2)**	**100**	**24**	**Neat**	**91**	**91**	**3.8**	**This work**

6. Synthesis and characterization of oxazolidinones

6.1. Synthesis of oxazolidinones

Syntheses of compounds **8a-i**, **9a-g** were performed under N_2 atmosphere. In the glovebox, 1 equivalent of the appropriate isocyanate (**7a-f**, $50 \cdot 10^{-3}$ mmol) was added into a Schlenk and dissolved in 2-MeTHF (5 mL). Subsequently, 2 mol % of catalyst **1** and cocatalyst, Bu_4NI, were added in a 1:2 ratio (0.006 g ($10 \cdot 10^{-3}$ mmol) and 0.007 g ($20 \cdot 10^{-3}$ mmol), respectively). Finally, 1 equivalent of the corresponding epoxide (**5a-d,f**, $50 \cdot 10^{-3}$ mmol) was added. The reaction mixture was heated at 100ºC for 24 hours. Afterwards, the conversion to the corresponding oxazolidinones was determined by ^1H NMR spectroscopy after dissolving the crude product in $CDCl_3$. Separation and purification of compounds **8a-i**, **9a-g** were carried out using TLC glass plate silica (employing hexane:ethyl acetate mixtures). Purification of compounds **8g** and **8i** were done by crystallization of these compounds in saturated solutions in 2-MeTHF.

6.2. NMR details of oxazolidinones

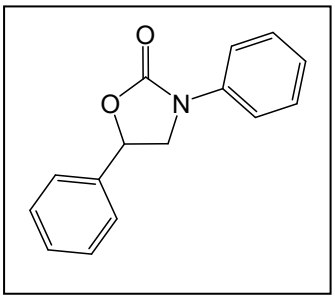

3,5-diphenyloxazolidin-2-one (8a): ^1H NMR ($CDCl_3$) δ (ppm) = 3.97 (dd, 1H, CH_2, J = 7.5, 8.9 Hz), 4.38 (t, 1H, CH, J = 8.8 Hz), 5.64 (dd, 1H, CH_2, J = 7.6, 8.6 Hz), 7.13-7.17 (m, 1Harom), 7.37-7.44 (m, 7Harom), 7.55-7.57 (m, 2Harom). $^{13}C\{^1H\}$ NMR ($CDCl_3$) δ (ppm) = 52.8, 74.2, 118.4, 124.3, 125.8, 129.2, 129.3, 138.2, 128.3, 154.8.

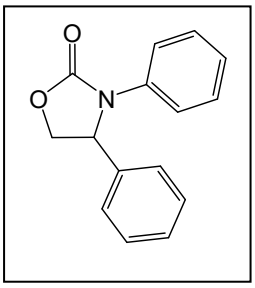

3,4-diphenyloxazolidin-2-one (9a): ^1H NMR ($CDCl_3$) δ (ppm) = 4.35 (dd, 1H, CH_2, J = 7.9, 8.6 Hz), 4.80 (t, 1H, CH J = 8.4 Hz), 5.67 (t, 1H, CH_2, J = 8.0 Hz), 7.07-7.14 (m, 1Harom), 7.33-7.37 (m, 5Harom), 7.43-7.49 (m, 4Harom). $^{13}C\{^1H\}$ NMR ($CDCl_3$) δ (ppm) = 66.4, 71.3, 121.3, 124.5, 126.0, 128.6, 129.5, 129.9, 135.9, 154.9.

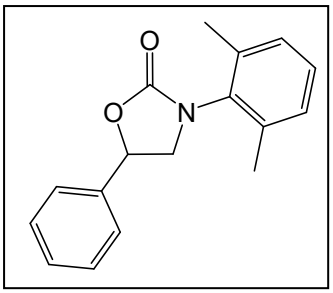

3-(2,6-dimethylphenyl)-5-phenyloxazolidin-2-one (8b): ^1H NMR ($CDCl_3$) δ (ppm) = 2.21 (s, 6H, CH_3), 3.72 (dd, 1H, CH_2, J = 7.4, 9.0 Hz), 4.17 (t, 1H, J = 8.9 Hz), 5.75 (dd, 1H, CH_2, J = 7.4, 8.8 Hz), 7.06-7.19 (m, 3Harom), 7.44-7.47 (m, 5Harom). $^{13}C\{^1H\}$ NMR ($CDCl_3$) δ (ppm) = 17.9, 53.9, 75.1,

125.6, 127.8, 128.8, 128.9, 129.0, 129.2, 133.9, 136.9, 137.0, 139.0, 156.2.

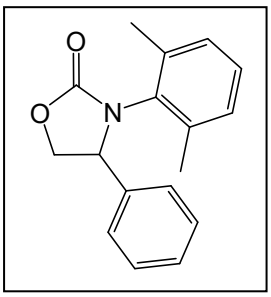

3-(2,6-dimethylphenyl)-4-phenyloxazolidin-2-one (9b): ^{1}H NMR ($CDCl_3$) δ (ppm) = 1.73 (s, 3H, CH_3), 2.40 (s, 4H, CH_3), 4.74 (dd, 1H, CH_2, *J* = 5.8, 9.2 Hz), 4.88 (t, 1H, *J* = 9.0 Hz), 5.07 (dd, 1H, CH_2, *J* = 5.8, 8.8 Hz), 6.88-6.89 (m, 1Harom), 7.06-7.07 (m, 2Harom), 7.24-7.33 (m, 5Harom). ^{13}C{^{1}H} NMR ($CDCl_3$) δ (ppm) = 18.4, 18.6, 61.9, 69.1, 125.6, 128.2, 128.6, 128.9, 129.0, 129.4, 133.1, 135.9, 137.3, 138.5, 156.2.

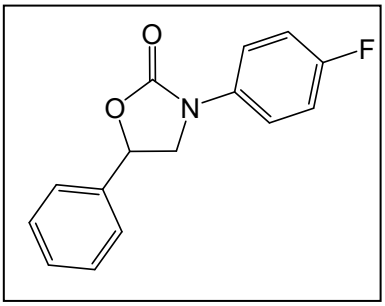

3-(4-fluorophenyl)-5-phenyloxazolidin-2-one (8c): ^{1}H NMR ($CDCl_3$) δ (ppm) =3.95 (t, 1H, CH_2, *J* = 8.2 Hz), 4.36 (t, 1H, *J* = 8.8 Hz), 5.65 (dd, 1H, CH_2, *J* = 8.1 Hz), 7.06-7.09 (m, 2Harom), 7.39-7.46 (m, 5Harom), 7.50-7.53 (m, 2Harom). ^{13}C{^{1}H} NMR ($CDCl_3$) δ (ppm) = 53.1, 74.2, 115.9, 120.2, 125.8, 129.2, 129.3, 134.4, 138.1, 154.9, 160.7. ^{19}F{^{1}H} NMR ($CDCl_3$) δ (ppm) = -118.2.

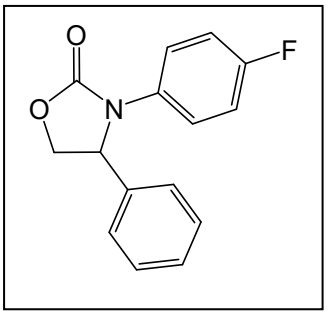

3-(4-fluorophenyl)-4-phenyloxazolidin-2-one (9c): ^{1}H NMR ($CDCl_3$) δ (ppm) = 4.22 (dd, 1H, CH_2, *J* = 6.3, 8.7 Hz), 4.79 (t, 1H, *J* = 8.7 Hz), 5.34 (dd, CH_2, 1H, *J* = 6.3, 8.7 Hz), 6.93-6.96 (m, 2Harom), 7.28-7.38 (m, 7Harom). ^{13}C{^{1}H} NMR ($CDCl_3$) δ (ppm) = 61.3, 69.9, 115.7, 123.1, 126.5, 129.2, 129.6, 133.1, 137.9, 156.2, 161.1. ^{19}F{^{1}H} NMR ($CDCl_3$) δ (ppm) = -117.3.

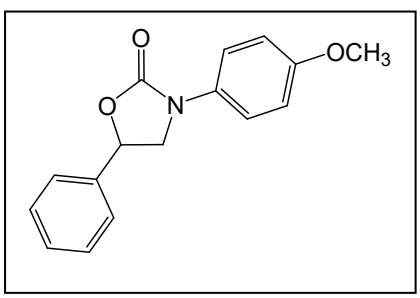

3-(4-methoxyphenyl)-5-phenyloxazolidin-2-one (8d): ^{1}H NMR ($CDCl_3$) δ (ppm) = 3.80 (s, 3H, CH_3O), 3.93 (dd, 1H, CH_2, *J* = 7.6, 8.8 Hz), 4.34 (t, 1H, *J* = 8.8 Hz), 5.63 (dd, 1H, CH_2, *J* = 7.6, 8.6 Hz), 6.91-6.93 (m, 2Harom), 7.37-7.45 (m, 7Harom). ^{13}C{^{1}H} NMR ($CDCl_3$) δ (ppm) = 53.4, 55.7, 74.1, 114.5, 120.5, 125.8, 129.1, 129.2, 131.5, 155.2, 156.6.

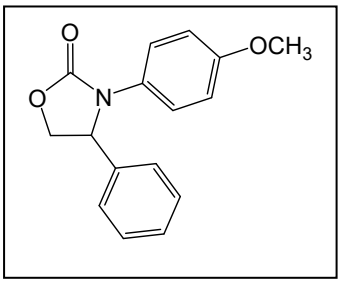

3-(4-methoxyphenyl)-4-phenyloxazolidin-2-one (9d): ^{1}H NMR ($CDCl_3$) δ (ppm) = 3.73 (s, 3H, CH_3O), 4.22 (dd, 1H, CH_2, J = 6.4, 8.6 Hz), 4.77 (t, 1H, J = 7.4 Hz), 5.31 (dd, CH_2, 1H, J = 6.4, 8.7 Hz), 6.78-6.80 (m, 2Harom), 7.24-7.34 (m, 7Harom). ^{13}C{^{1}H} NMR ($CDCl_3$) δ (ppm) = 55.5, 61.6 ,69.9, 114.4, 123.5, 126.0, 126.7, 129.0, 129.5, 138.4, 156.5, 157.1.

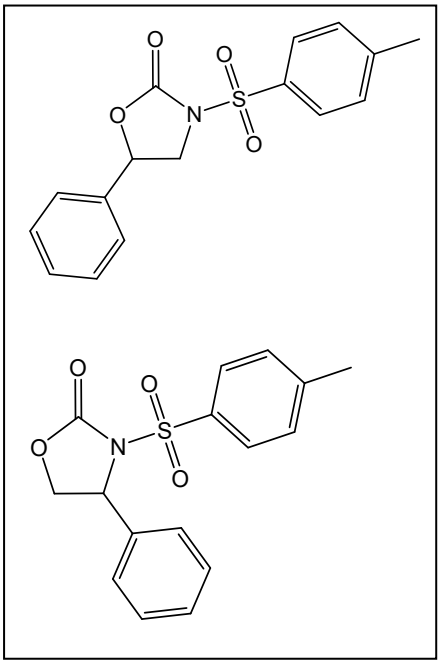

mixture of 5-phenyl-3-tosyloxazolidin-2-one (8e) and 4-phenyl-3-tosyloxazolidin-2-one (9e): ^{1}H NMR ($CDCl_3$) δ (ppm) = 2.37 (s, 3H, CH_3), 2.47 (s, 3H, CH_3), 3.89 (dd, 1H, CH_2, J = 8.0, 9.2 Hz), 4.28 (dd, 1H, CH_2, J = 3.3, 8.8 Hz), 4.43 (t, 1H, CH, J = 8.8 Hz), = 4.72 (t, 1H, CH J = 8.7 Hz), 5.43 (t, 1H, CH_2, J = 3.3, 8.5 Hz), 5.53 (t, 1H, CH_2, J = 8.0 Hz), 7.11-7.95 (m, 18Harom). ^{13}C{^{1}H} NMR ($CDCl_3$) δ (ppm) = 21.8, 21.9, 51.9, 60.4, 70.5, 75.6, 125.7, 127.2, 128.4, 128.5, 129.3, 129.4, 129.7, 130.1, 134.0, 134.9, 136.3, 137.8, 145.3, 146.0, 151.7, 152.1.

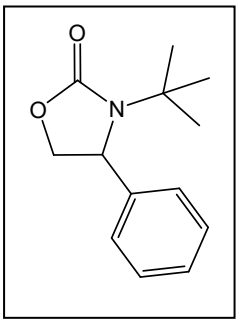

3-(tert-butyl)-5-phenyloxazolidin-2-one (9f): ^{1}H NMR ($CDCl_3$) δ (ppm) = 1.24 (s, 9H, CH_3), 4.28 (dd, 1H, CH_2, J = 7.9, 8.6 Hz), 4.73 (t, 1H, J = 8.4 Hz), 5.61 (t, 1H, CH_2, J = 8.0 Hz), 7.29-7.31 (m, 2Harom), 7.36-7.39 (m, 3Harom). ^{13}C{^{1}H} NMR ($CDCl_3$) δ (ppm) = 28.8, 49.5, 50.0, 70.3, 125.0, 128.4, 128.9, 134.9, 153.9.

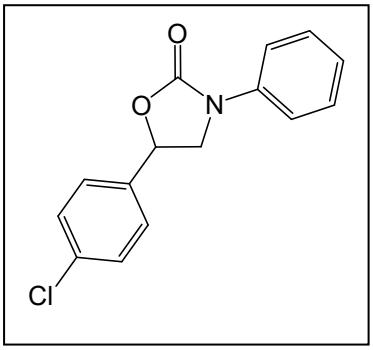

5-(4-chlorophenyl)-3-phenyloxazolidin-2-one (8f): ^{1}H NMR ($CDCl_3$) δ (ppm) = 3.92 (dd, 1H, CH_2, J = 7.5, 8.9 Hz), 4.39 (t, 1H, J = 8.8 Hz), 5.60-5.63 (m, 1H, CH_2), 7.14-7.18 (m, 1Harom), 7.36-7.42 (m, 6Harom), 7.53-7.55 (m, 2Harom). ^{13}C{^{1}H} NMR ($CDCl_3$) δ (ppm) = 52.8, 73.5, 118.5, 124.5, 127.2, 129.3, 129.4, 135.2, 136.7, 138.1, 154.6.

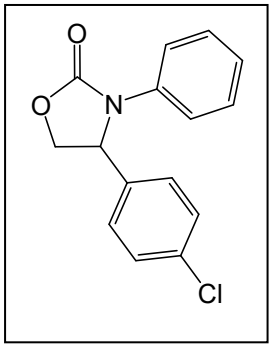

4-(4-chlorophenyl)-3-phenyloxazolidin-2-one (9g): ^{1}H NMR ($CDCl_3$) δ (ppm) = 4.20 (dd, 1H, CH_2, *J* = 6.0, 8.7 Hz), 4.81 (t, 1H, *J* = 8.7 Hz), 5.42 (dd, 1H, CH_2, *J* = 6.0, 8.7 Hz), 7.11-7.14 (m, 1Harom), 7.27-7.32 (m, 2Harom), 7.36-7.40 (m, 6Harom). ^{13}C{^{1}H} NMR ($CDCl_3$) δ (ppm) = 60.3, 69.7, 121.0, 125.1, 127.8, 129.2, 129.5, 129.8, 134.9, 136.9.

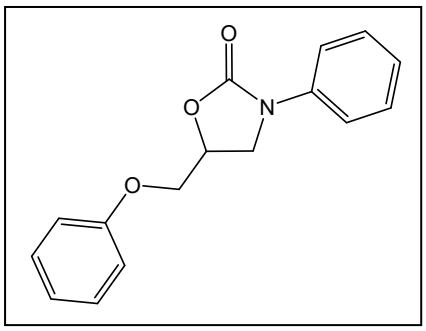

5-(phenoxymethyl)-3-phenyloxazolidin-2-one (8g): ^{1}H NMR ($CDCl_3$) δ (ppm) = 4.08 (dd, 1H, CH_2, *J* = 5.9, 8.9 Hz), 4.19-4.24 (m, 3H, CH, CH_2O), 4.96-5.02 (m, 1H, CH_2), 6.90-6.93 (m, 2Harom), 6.98-7.02 (m, 1Harom), 7.14-7.18 (m, 1Harom), 7.28-7.32 (m, 2Harom), 7.38-7.42 (m, 2Harom), 7.57-7.59 (m, 2Harom). ^{13}C{^{1}H} NMR ($CDCl_3$) δ (ppm) = 47.6, 67.9, 70.5, 114.7, 118.4, 121.9, 124.4, 129.3, 129.8, 138.3, 154.5, 158.1.

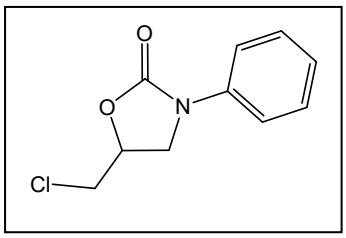

5-(chloromethyl)-3-phenyloxazolidin-2-one (8h): ^{1}H NMR ($CDCl_3$) δ (ppm) = 3.77 (qd, 2H, CH_2Cl, *J* = 5.4, 11.6 Hz), 3.97 (dd, 1H, CH_2, *J* = 5.7, 9.2 Hz), 4.17 (t, 1H, CH, *J* = 9.0 Hz), 4.87 (m, 1H, CH_2), 7.15-7.18 (m, 1Harom), 7.37-7.41 (m, 2Harom), 7.54-7.56 (m, 2Harom). ^{13}C{^{1}H} NMR ($CDCl_3$) δ (ppm) = 44.6, 48.3, 70.9, 118.5, 124.6, 129.3, 137.9, 154.0.

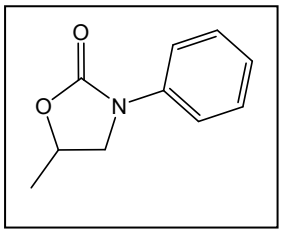

5-methyl-3-phenyloxazolidin-2-one (8i): ^{1}H NMR ($CDCl_3$) δ (ppm) = 1.53 (dd, 3H, CH_3, *J* = 0.9, 6.3 Hz), 3.60-3.64 (m, 1H, CH_2), 4.11 (td, 1H, CH, *J* = 0.9, 8.6 Hz), 4.78 (dtd, 1H, CH_2, *J* = 0.8, 7.1, 8.0 Hz), 7.11-7.15 (m, 1Harom), 7.35-7.39 (m, 2Harom), 7.52-7.54 (m, 2Harom). ^{13}C{^{1}H} NMR ($CDCl_3$) δ (ppm) = 20.8, 52.0, 69.7, 118.3, 124.1, 129.2, 138.5, 155.0.

Table S2. Reported catalysts for the coupling of isocyanates and epoxides.

Catalyst	mol%	t (h)	T (ºC)	Conversion (%)	TON	TOF (h^{-1})	Reference
Bu_3SnI / PPh_3	10	2	40	96	10	4.8	4a
LiBr / Ph_3PO	3	15	80	99	33	2.2	4b
Ph_4SbI	10	1	45	100	10	10.0	4c
YCl_3	10	3	25	99	10	3.3	4d
Bu_3PO / LiBr	5	32	110	96	19	0.6	4e
$SmCl_3 \cdot 6H_2O$	50	1	60	98	2	2.0	4f
$[Al(salen)]_2O$	5	24	80	100	20	0.8	4g
[Cr(salcen)]Cl / PPh_3O	3	2	60	90	30	15.0	4h
[V(salen)] / Bu_4NBr	2	5	80	90	45	9.0	4i
[Nd(O_3N ligand)]/Bu_4NI	0,5	18	80	98	196	10.9	4j
Al heteroscoropionate / Bu_4NBr	5	24	80	100	20	0.8	4k
[Cr(salphen)]Cl	1,5	4	80	90	60	15.0	4l
$Me(OH)PhPPh_3^+I^-$	2	24	100	98	49	2.0	4m
$[R_3R'Sb]^+$	10	18	40	62	6	0.3	4n
Heterocyclic carbene / LiCl	1	4	200	89	89	22.3	4o
(p-$MeOPh_4$)PI	2	24	80	93	47	1.9	4p
L-Ascorbic acid / Bu_4NI	4	24	65	96	24	1.0	4q
Et_3NI	10	1	100	83	8	8.3	4r
Scuaramide / Bu_4NI	5	24	100	99	20	0.8	4s
Urea bifunctional phase-transfer catalyst	2,5	12	100	92	37	3.1	4t
Hydroxypyridinium iodide	5	0,25	100	95	19	76.0	4u
Hydroxyimidazolium iodide	3	14	90	100	33	2.4	4v
Aminocyclopropenium chloride	2	8	80	92	46	5.8	4w
Catalyst 1	**2**	**24**	**100**	**95**	**48**	**2.0**	**This work**

7. NMR spectra

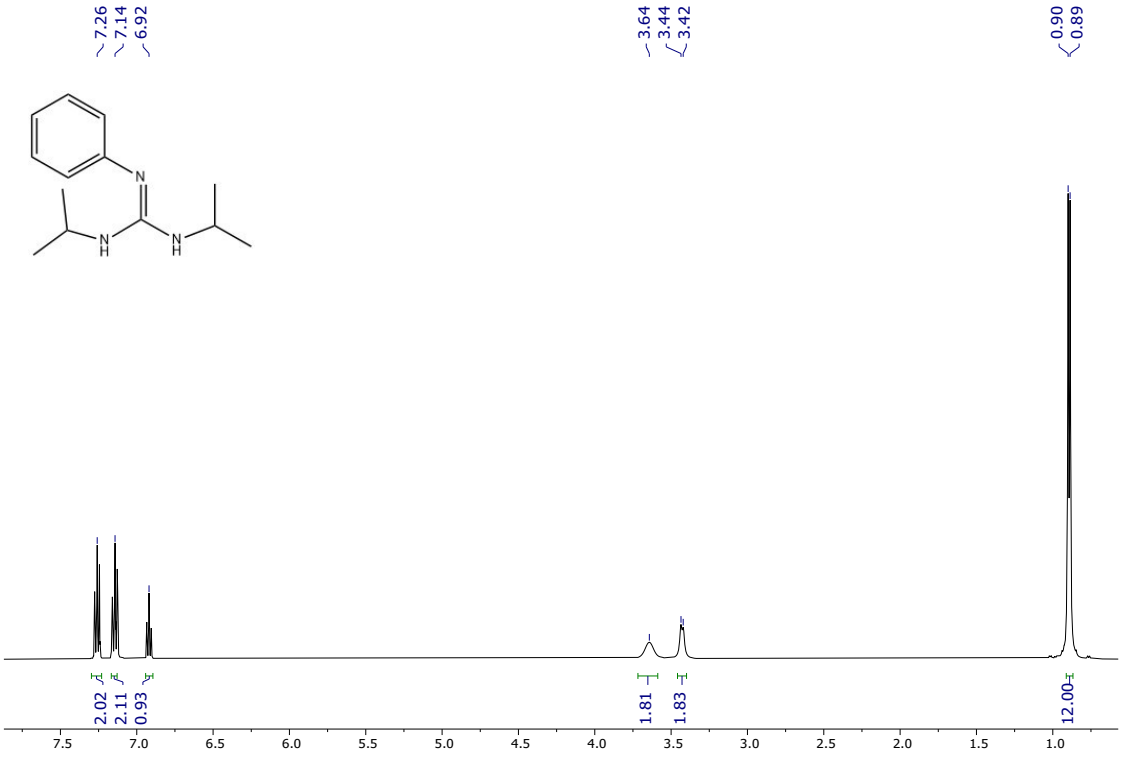

Figure S1. ^{1}H-NMR for **L^{1}H** in C_6D_6.

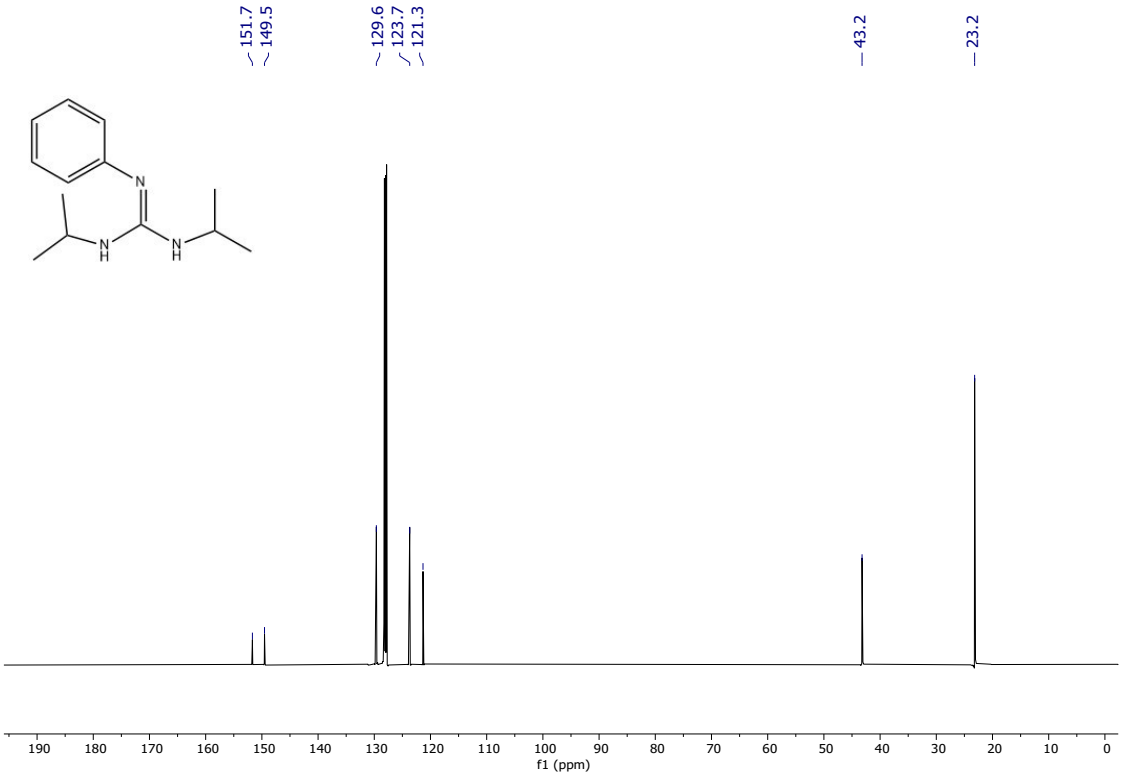

Figure S2. ^{13}C{^{1}H}-NMR for **L^{1}H** in C_6D_6.

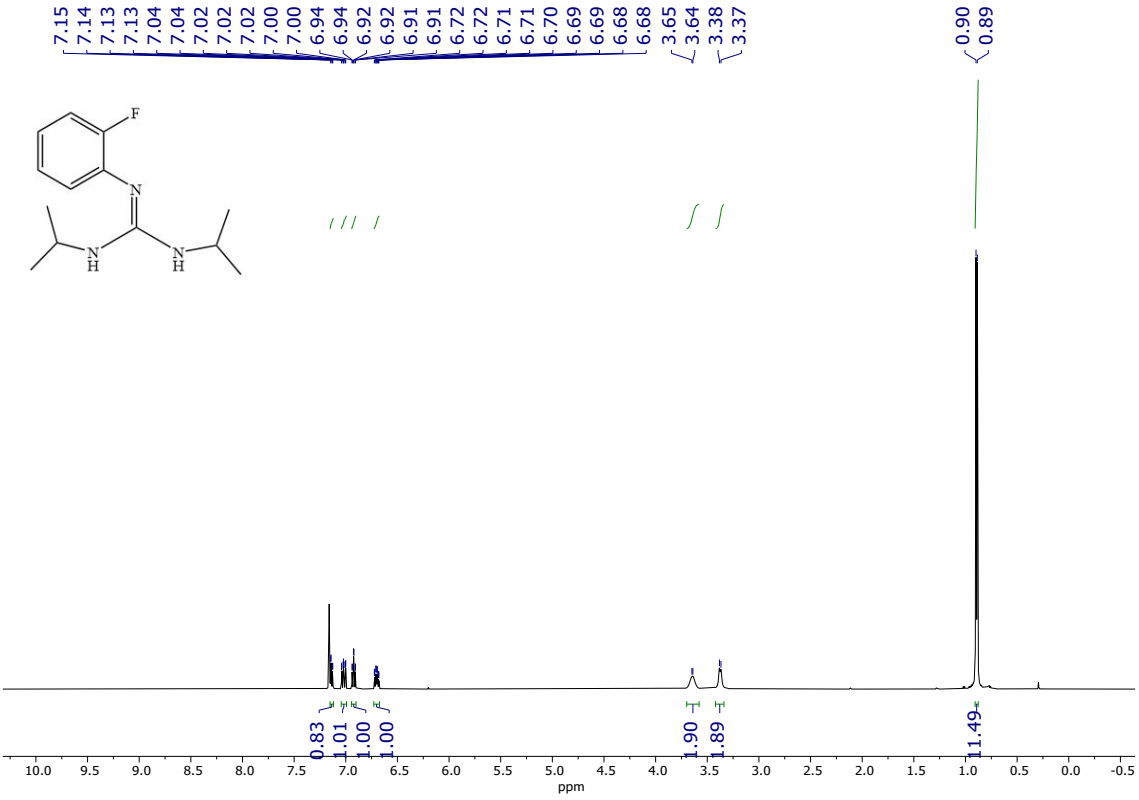

Figure S3. ^{1}H-NMR for **L^{4}H** C_6D_6.

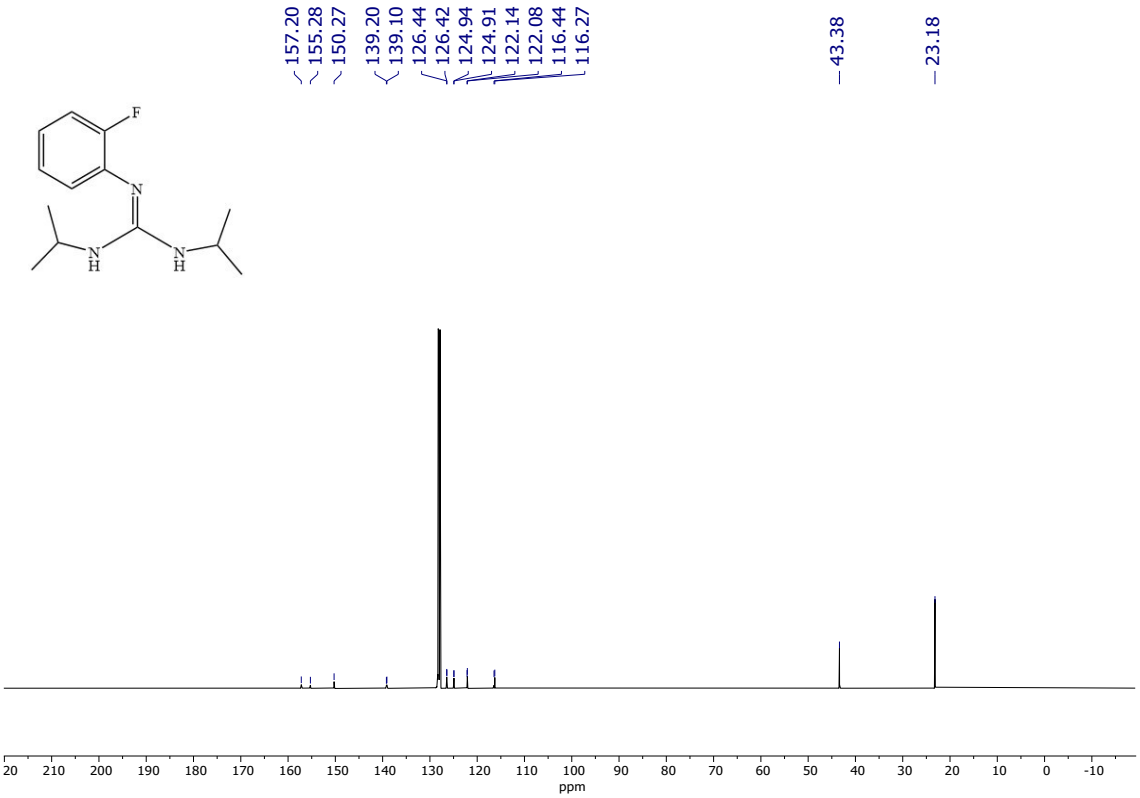

Figure S4. ^{13}C{^{1}H}-NMR for **L^{3}H** in C_6D_6.

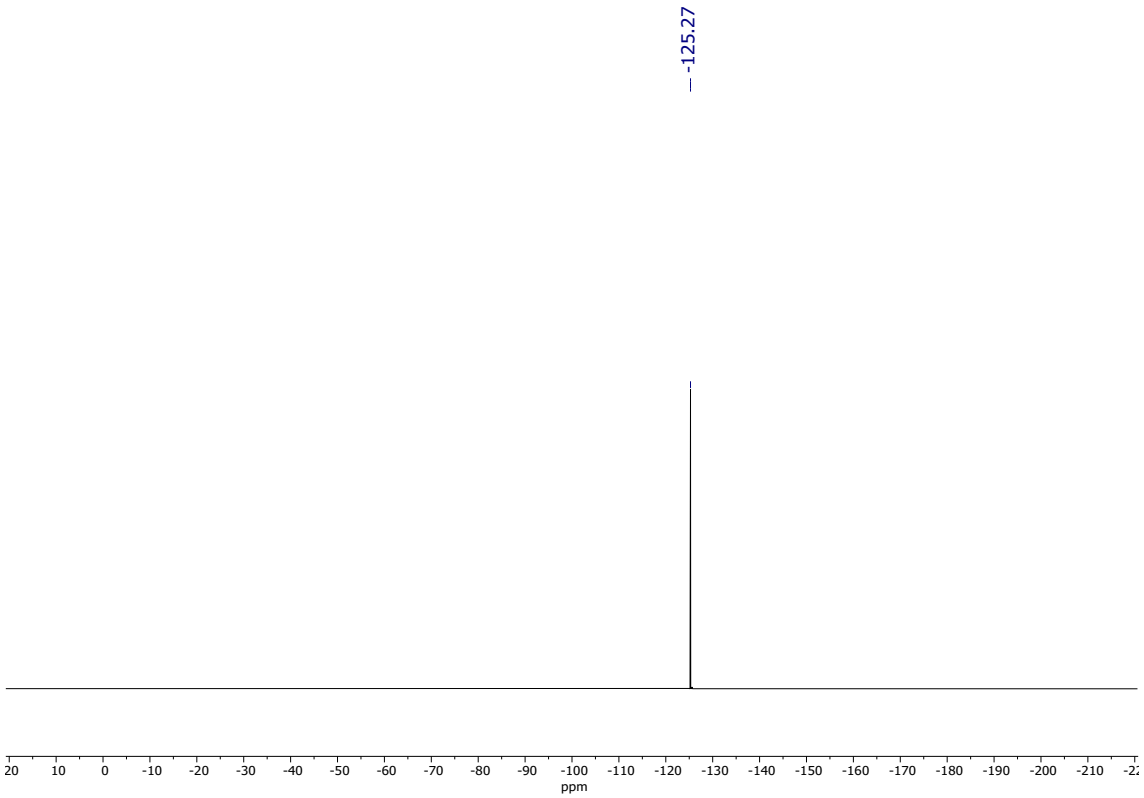

Figure S5. $^{19}F\{^{1}H\}$-NMR for **L^{3}H** in C_6D_6.

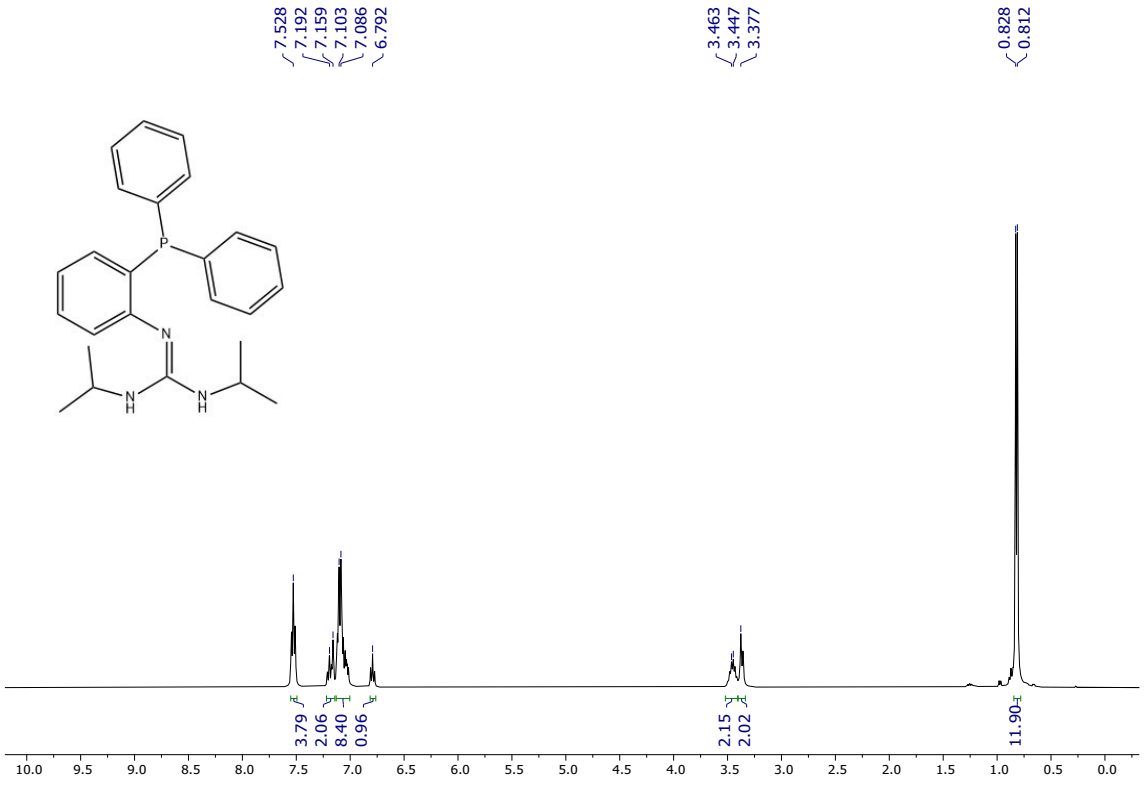

Figure S6. ^{1}H-NMR for **L^{3}H** in C_6D_6.

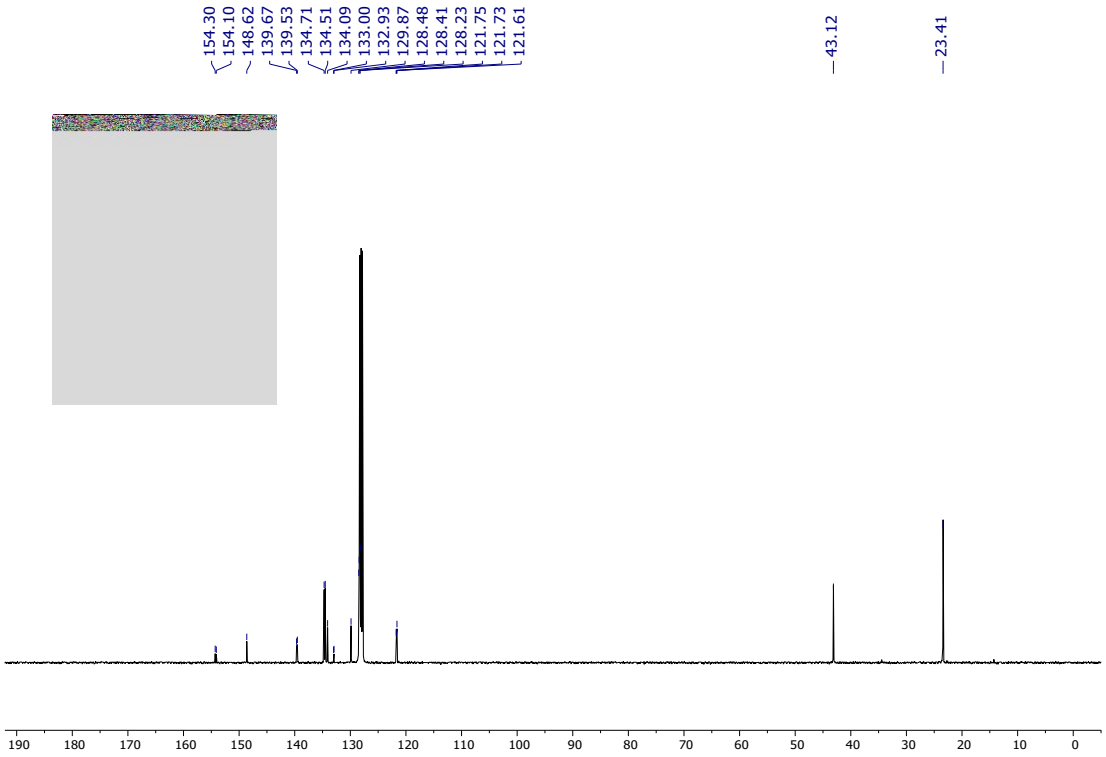

Figure S7. ^{13}C{^{1}H}-NMR for **L^{3}H** in C_6D_6.

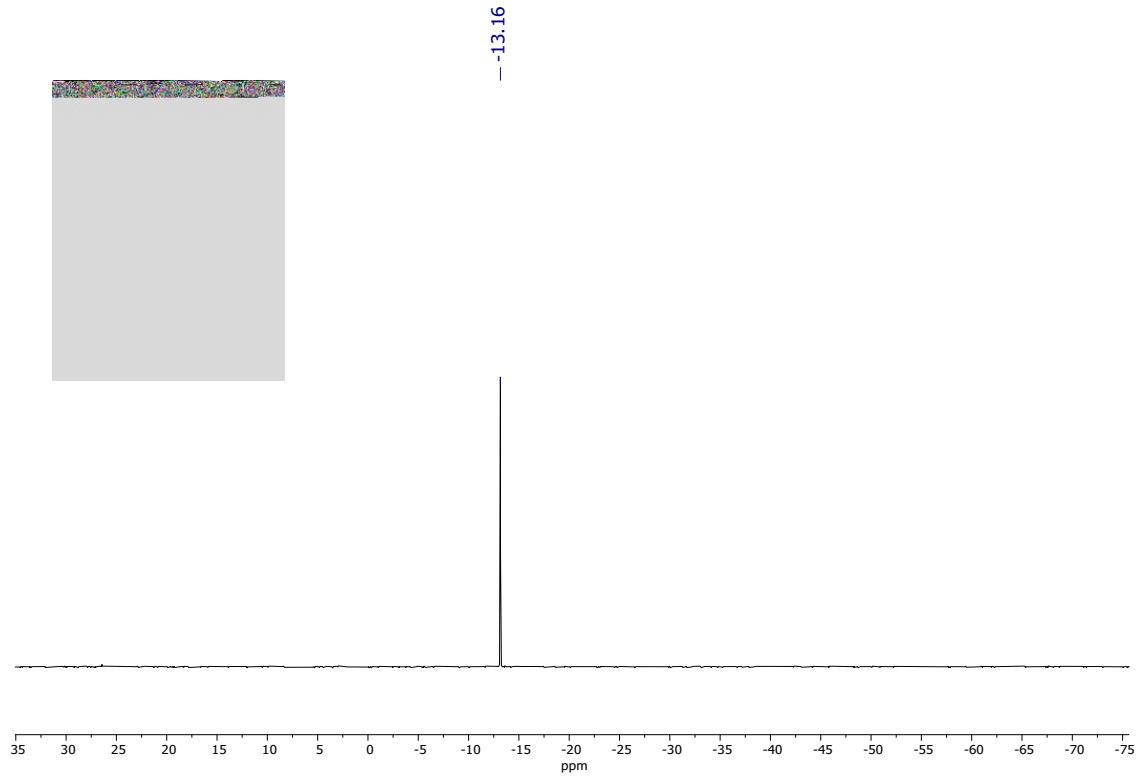

Figure S8. ^{31}P{^{1}H}-NMR for **L^{3}H** C_6D_6.

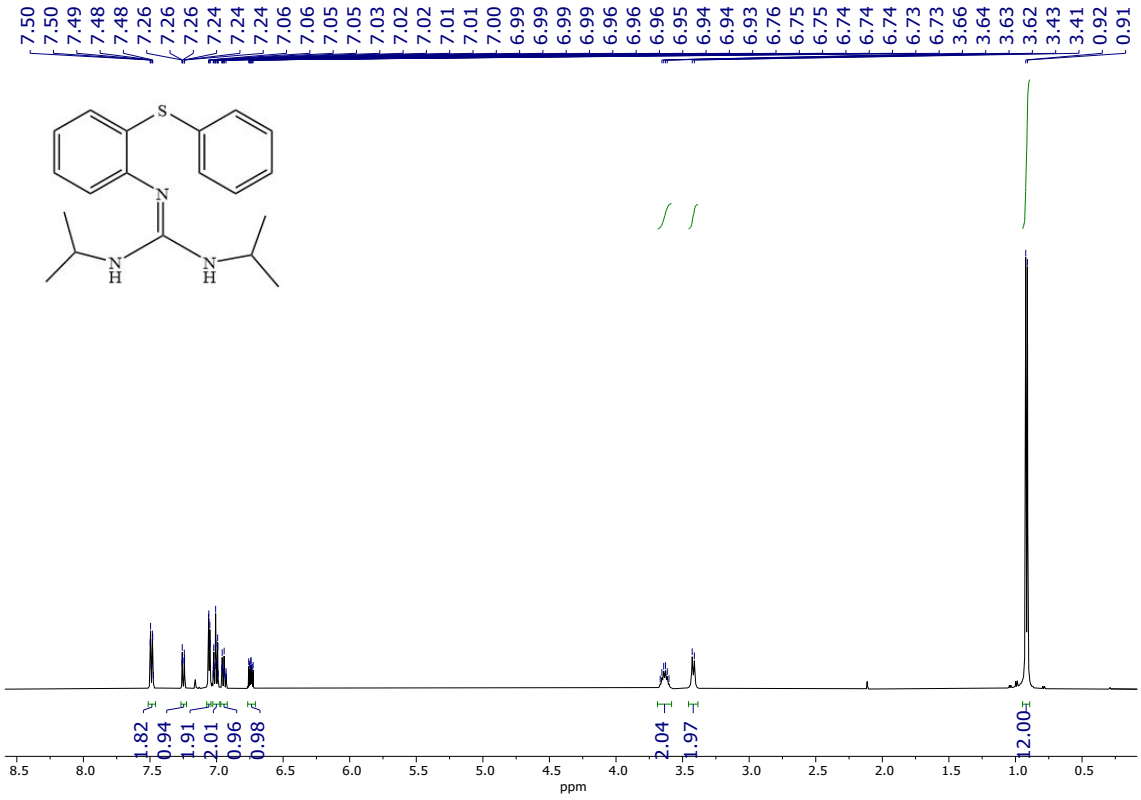

Figure S9. ^{1}H-NMR for **L^{4}H** in C_6D_6.

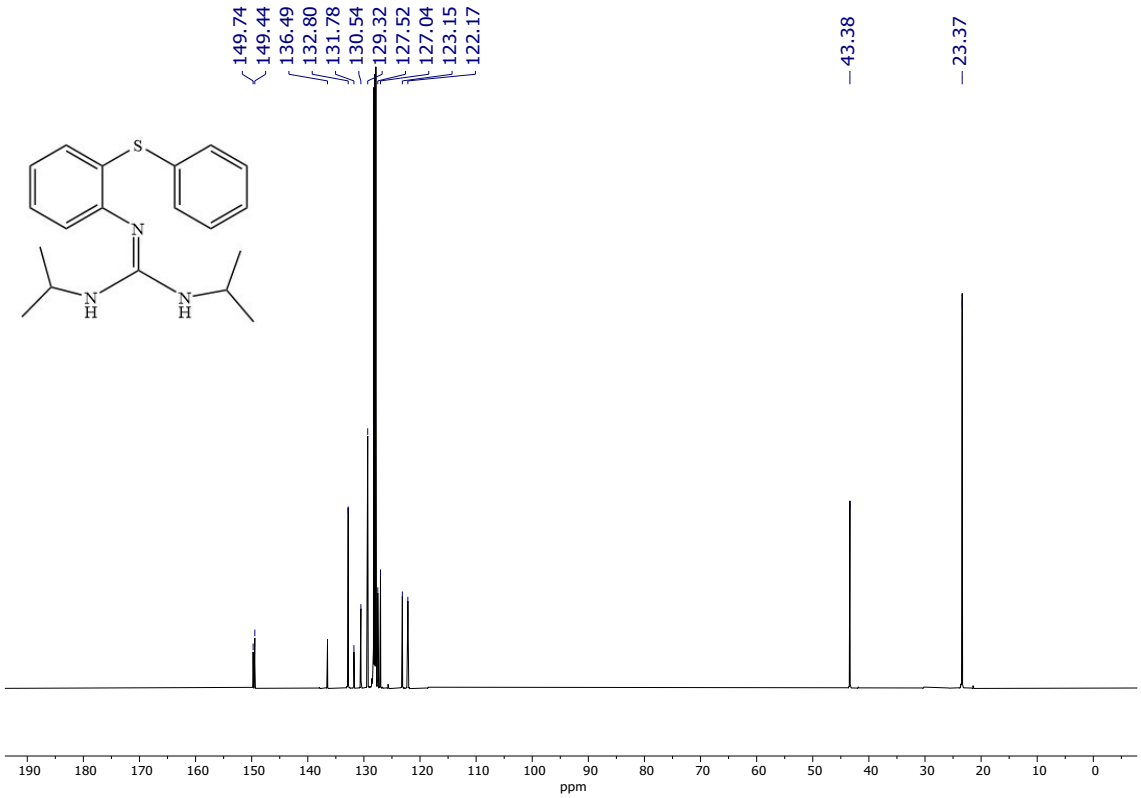

Figure S10. ^{13}C{^{1}H}-NMR for **L^{4}H** in C_6D_6.

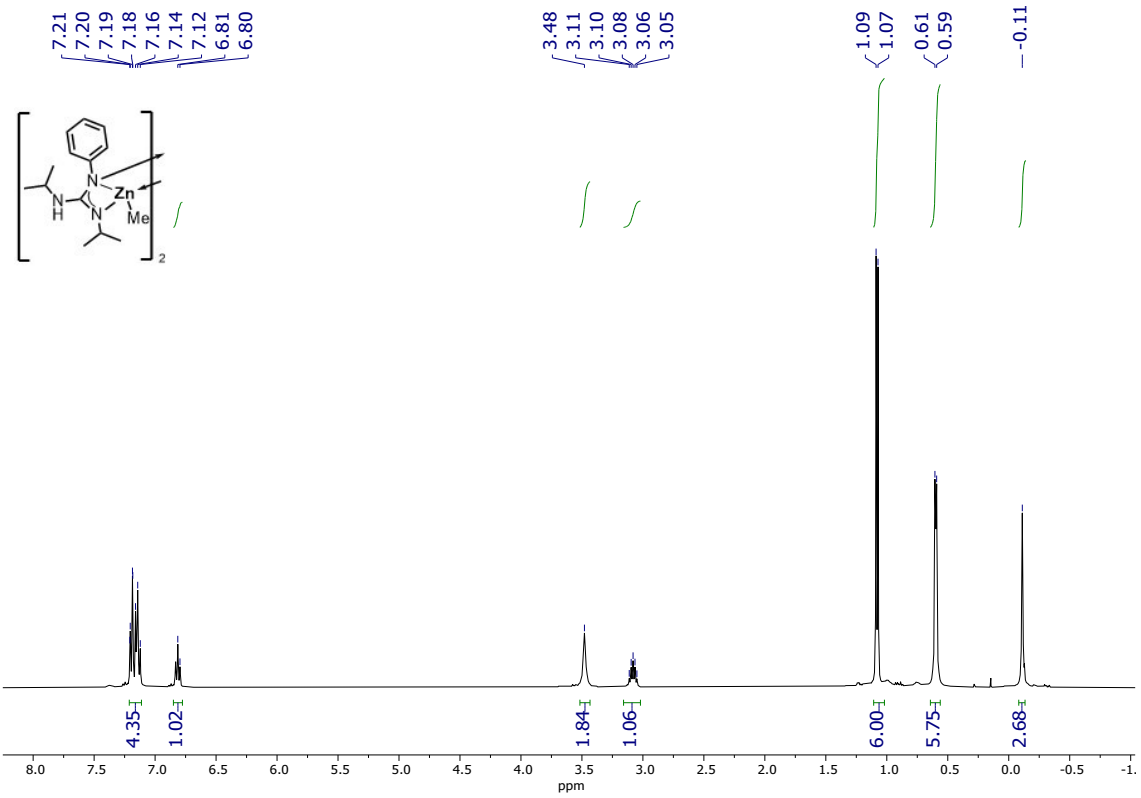

Figure S11. ^{1}H-NMR for **complex 1** in C_6D_6.

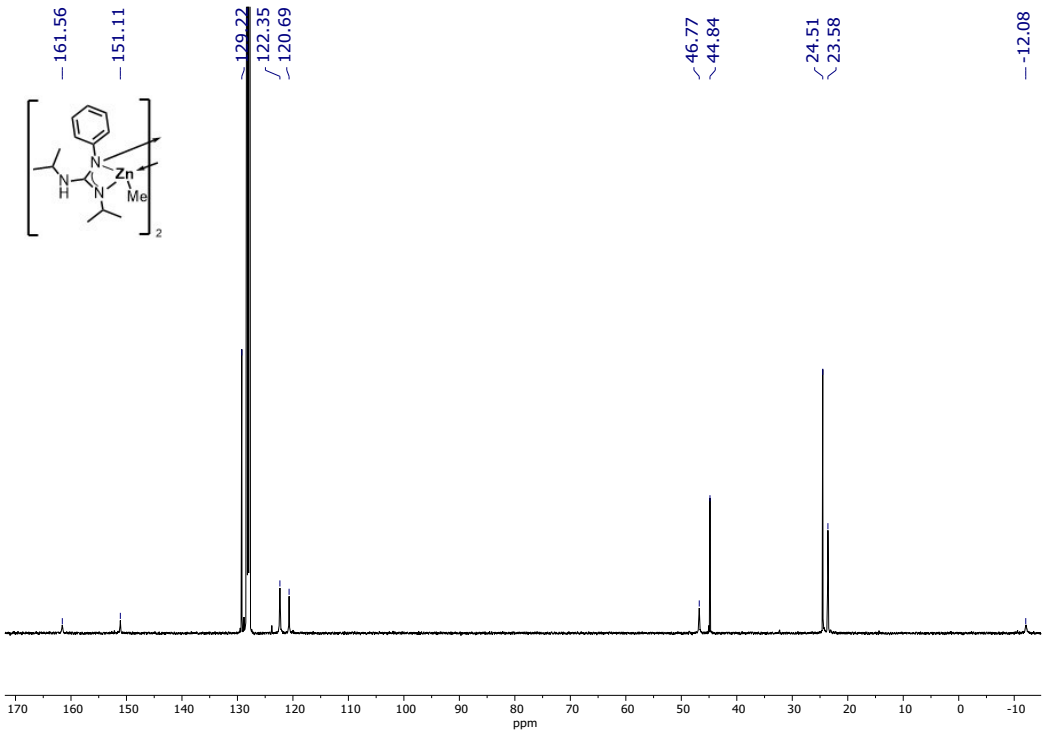

Figure S12. ^{13}C{^{1}H}-NMR for **complex 1** in C_6D_6.

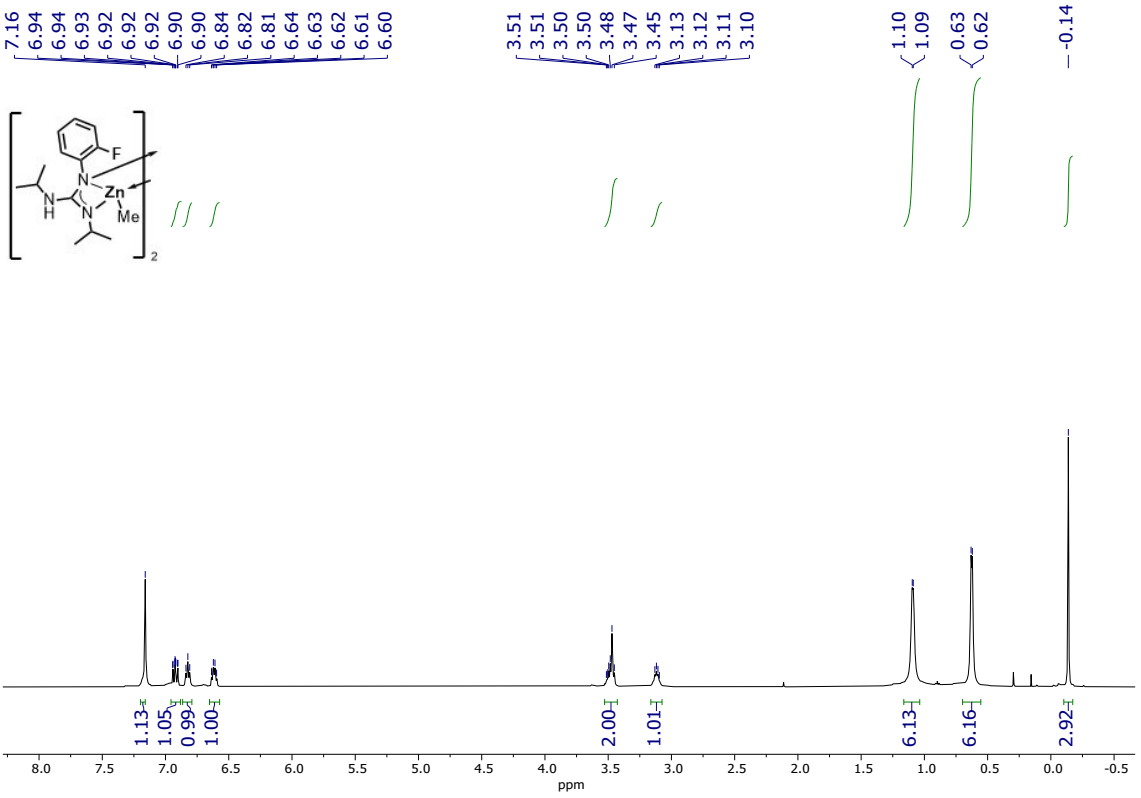

Figure S13. ^{1}H-NMR for **complex 2** in C_6D_6.

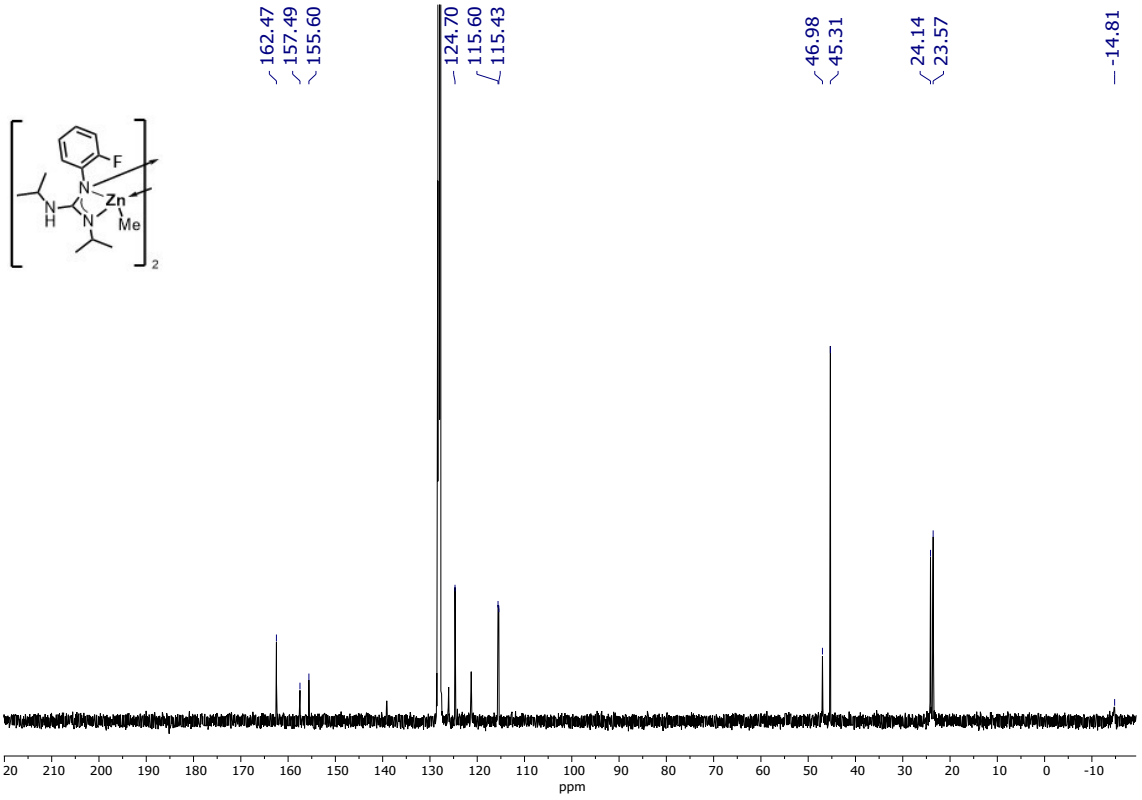

Figure S14. ^{13}C{^{1}H}-NMR for **complex 2** in C_6D_6.

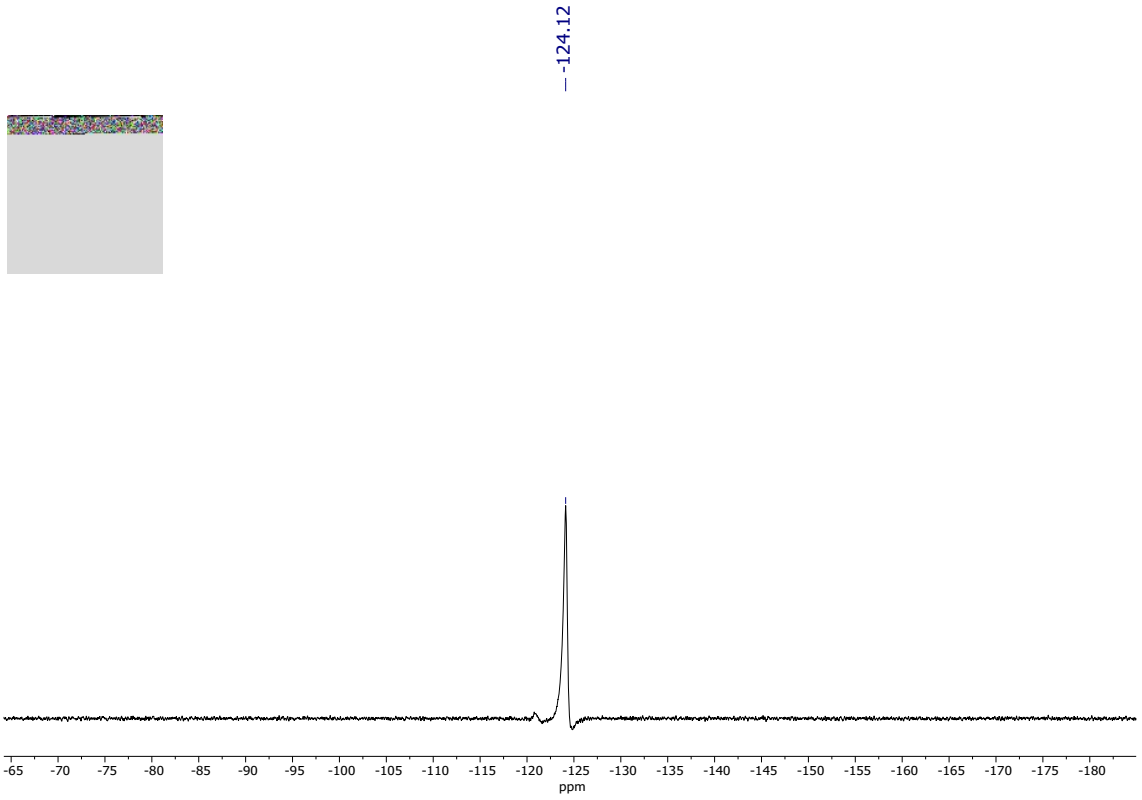

Figure S15. $^{19}F\{^{1}H\}$-NMR for **complex 2** in C_6D_6.

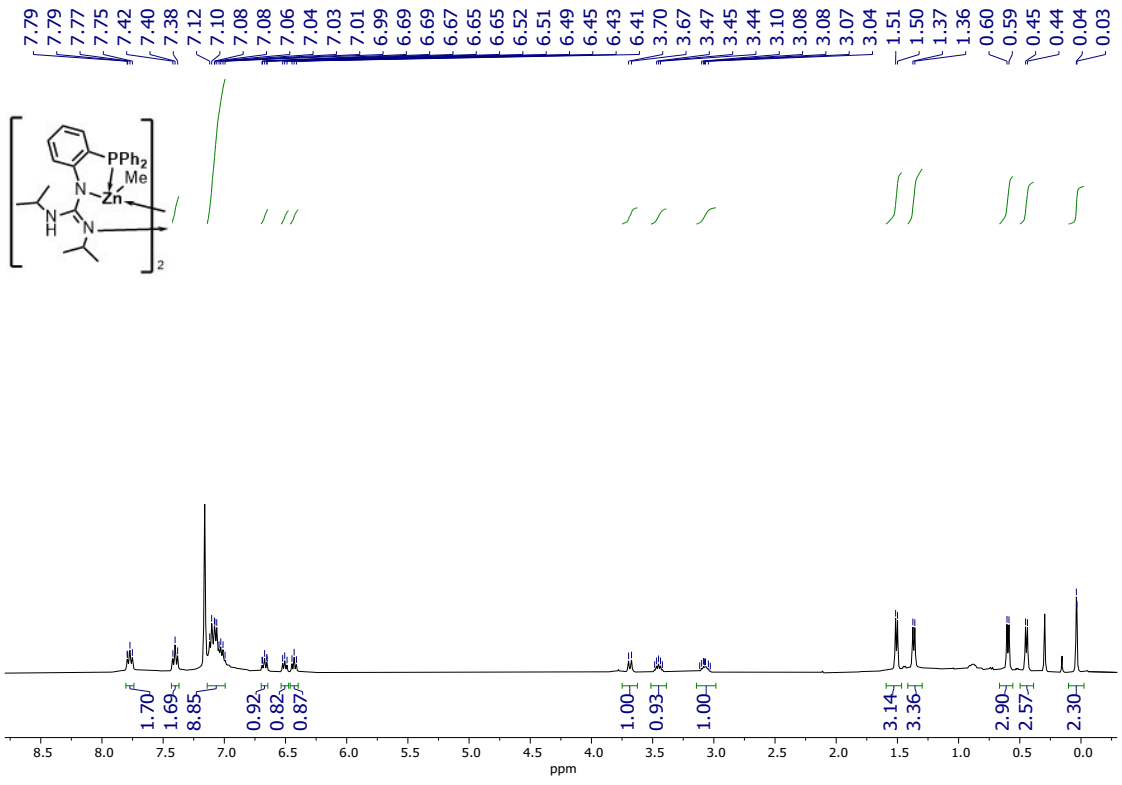

Figure 16. ^{1}H-NMR for **complex 3** in C_6D_6.

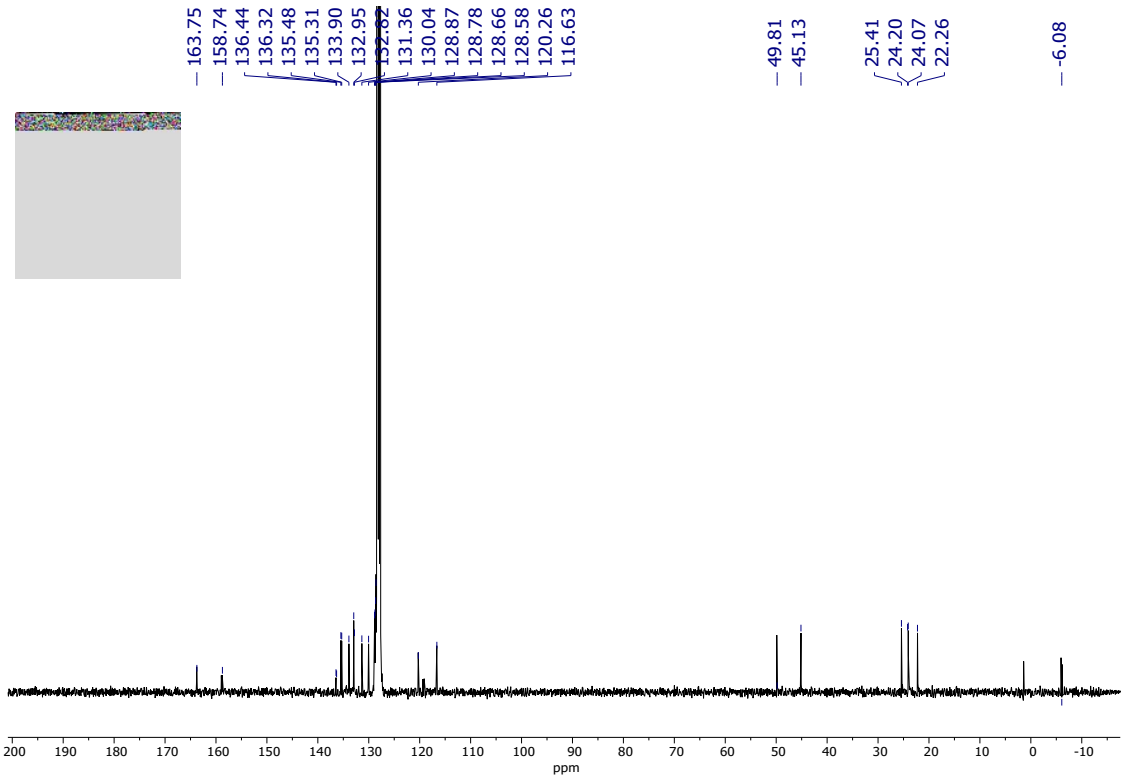

Figure S17. $^{13}C\{^{1}H\}$-NMR for **complex 3** in C_6D_6.

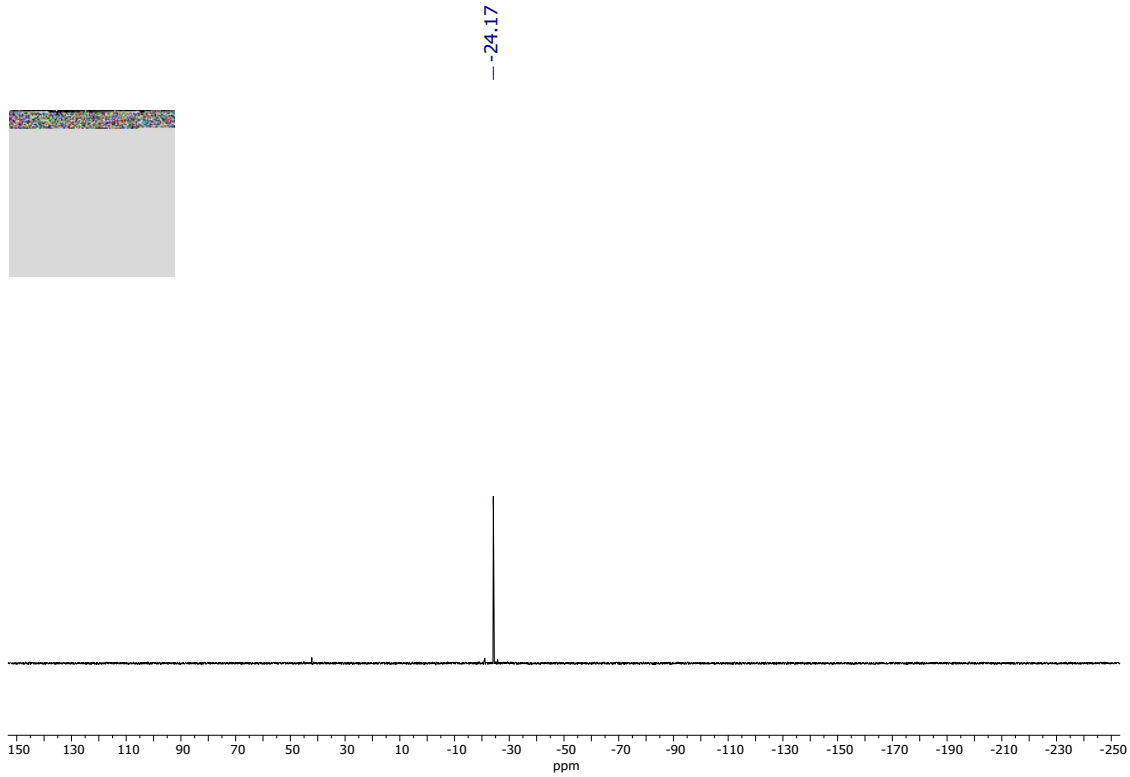

Figure S18. $^{31}P\{^{1}H\}$-NMR for **complex 3** in C_6D_6.

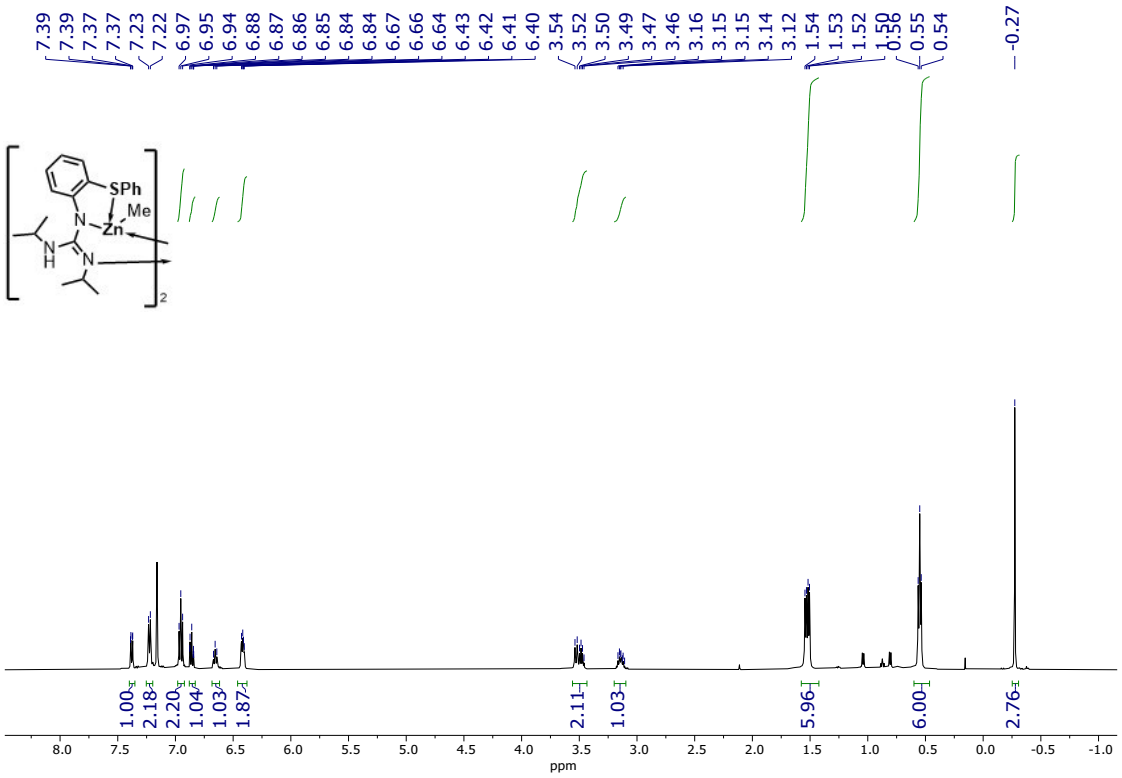

Figure S19. ^{1}H-NMR for **complex 4** in C_6D_6.

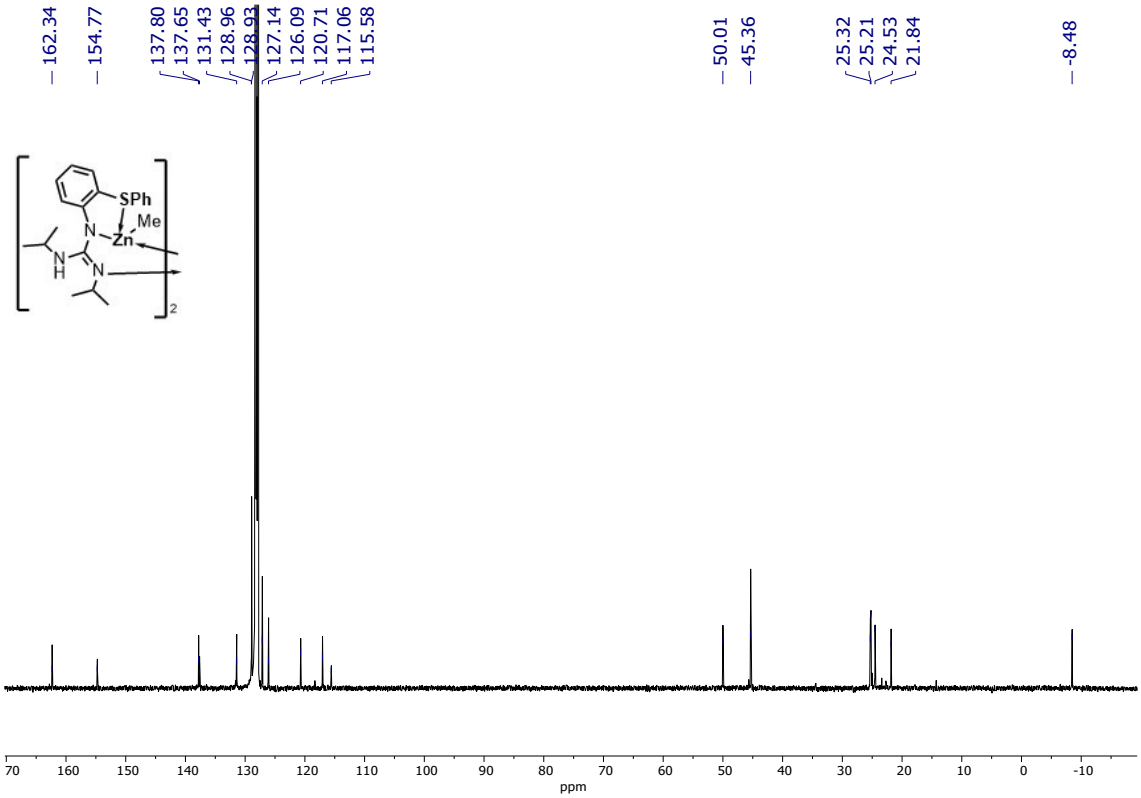

Figure S20. ^{13}C{^{1}H}-NMR for **complex 4** in C_6D_6.

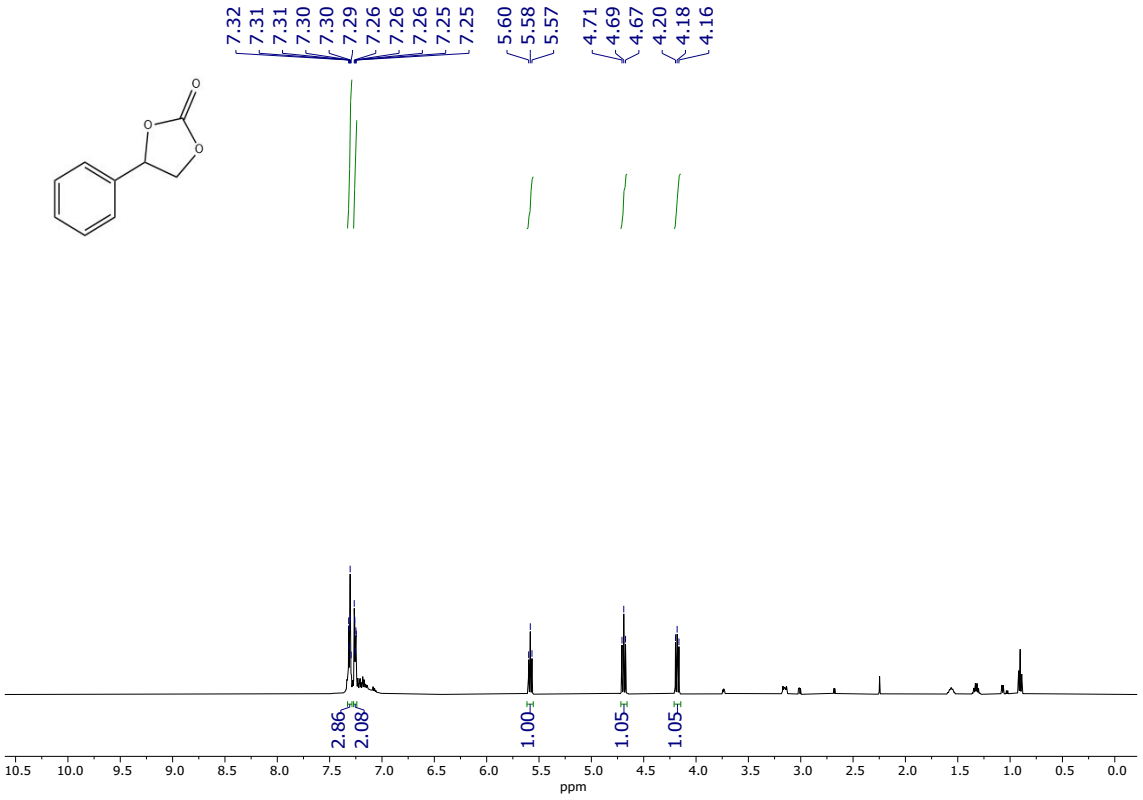

Figure S21. ^{1}H-NMR from reaction crude for the synthesis of compound **6a** in $CDCl_3$.

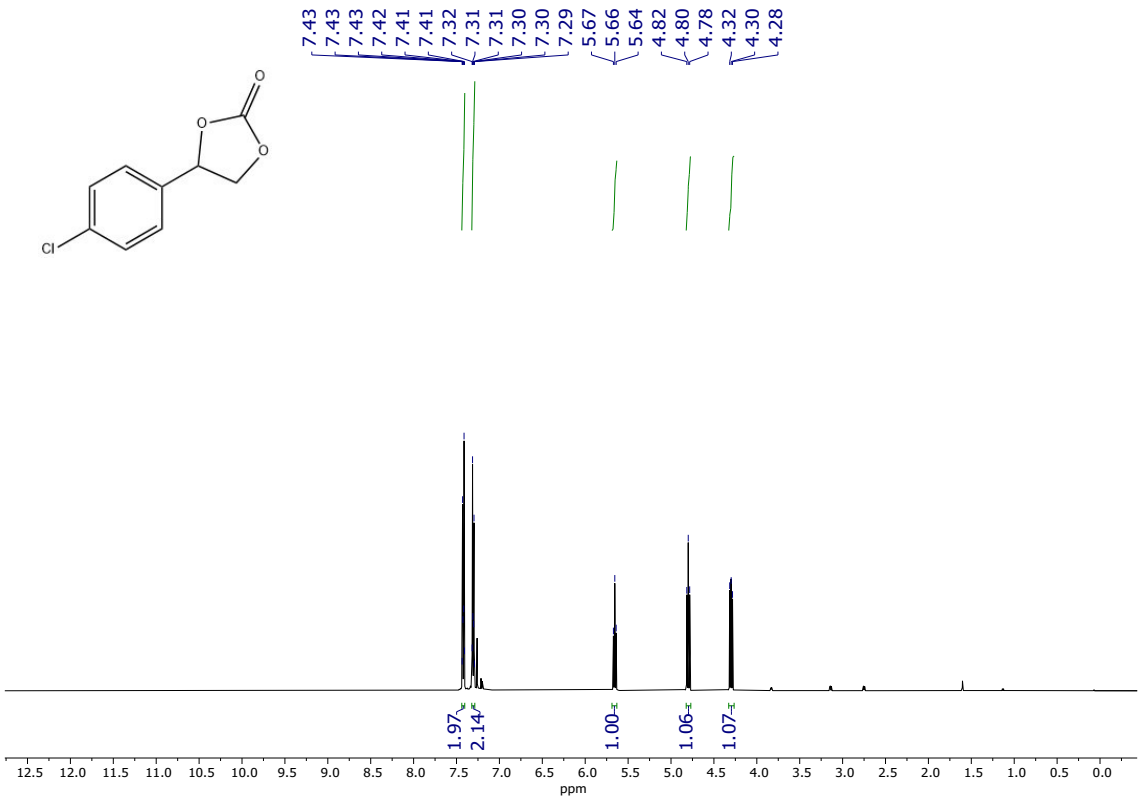

Figure S22. ^{1}H-NMR from reaction crude for the synthesis of compound **6b** in $CDCl_3$.

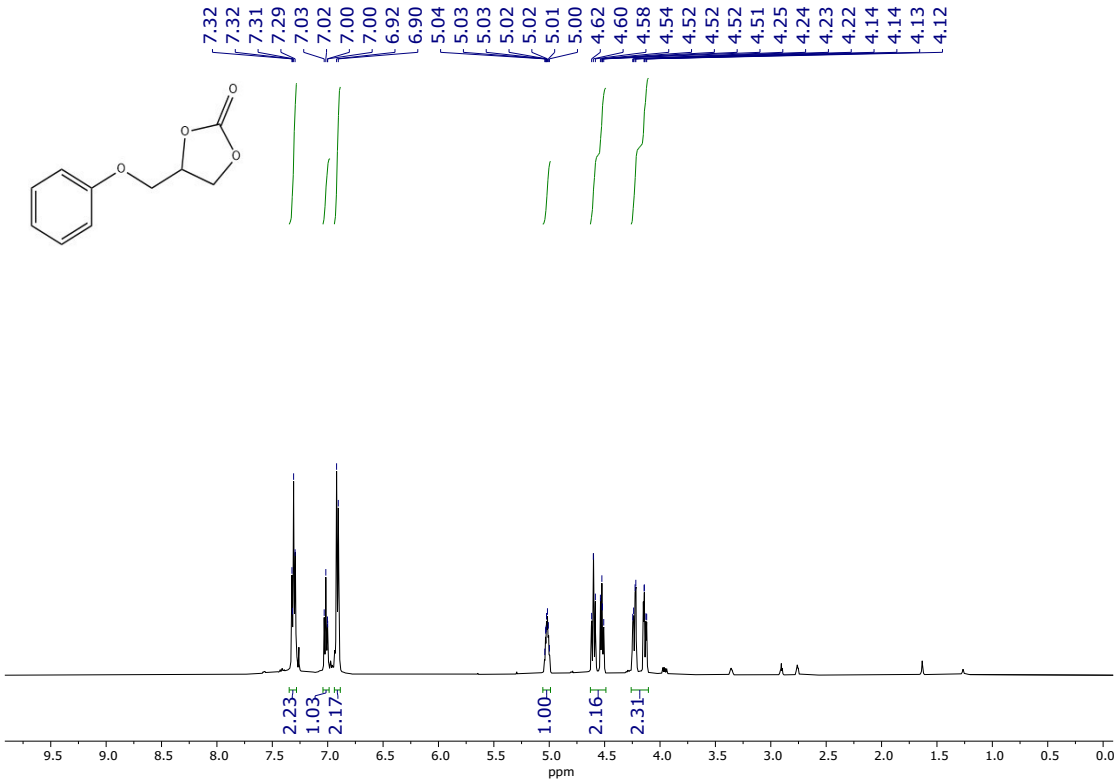

Figure S23. ^{1}H-NMR from reaction crude for the synthesis of compound **6c** in $CDCl_3$.

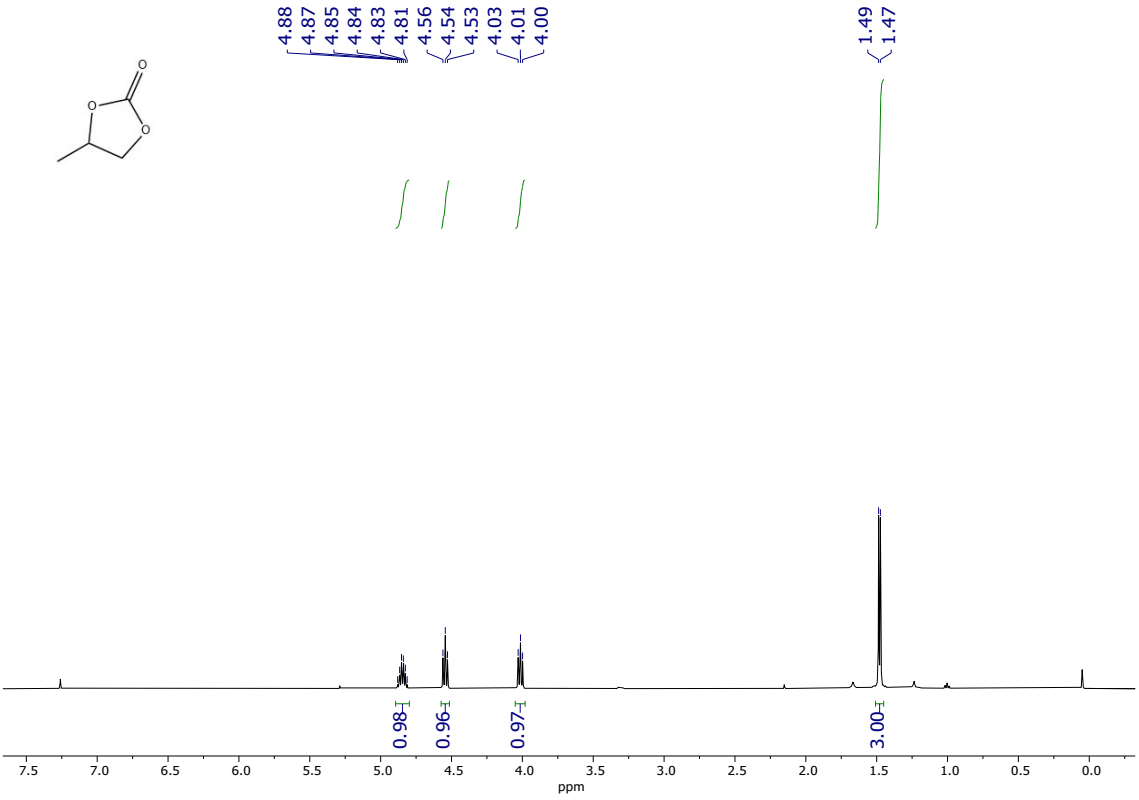

Figure S24. ^{1}H-NMR from reaction crude for the synthesis of compound **6d** in $CDCl_3$.

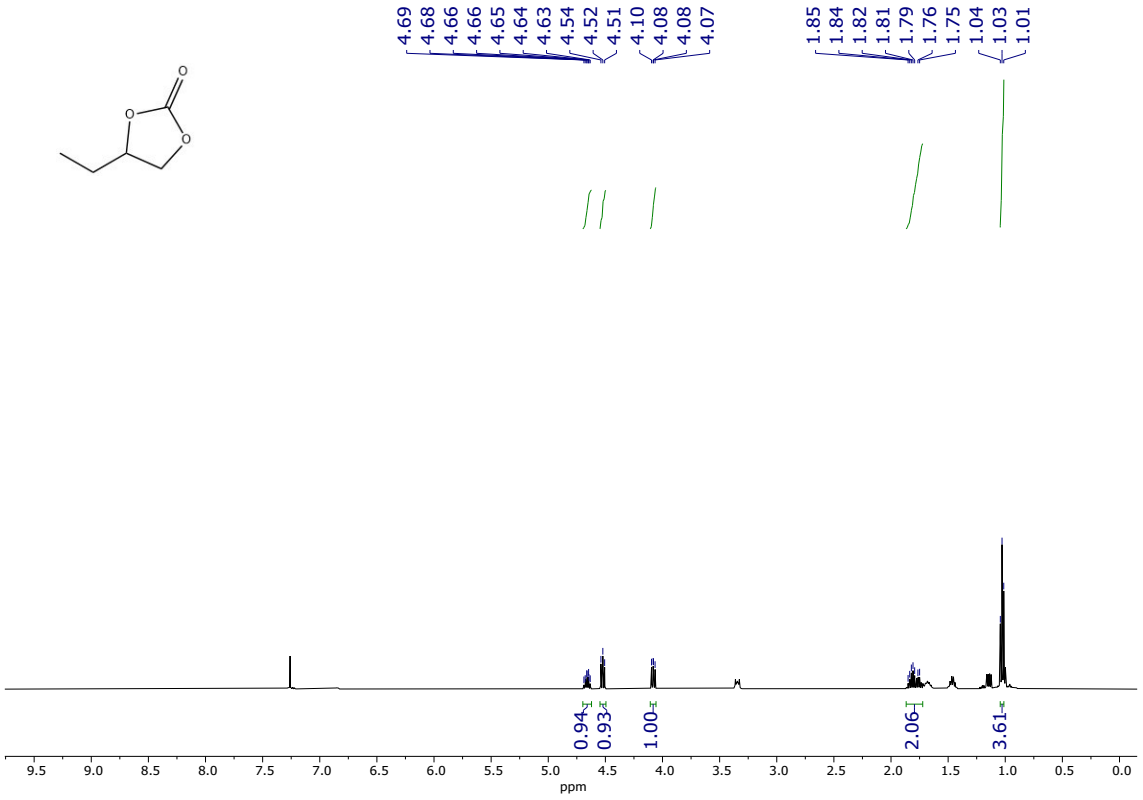

Figure S25. ^{1}H-NMR from reaction crude for the synthesis of compound **6e** in $CDCl_3$.

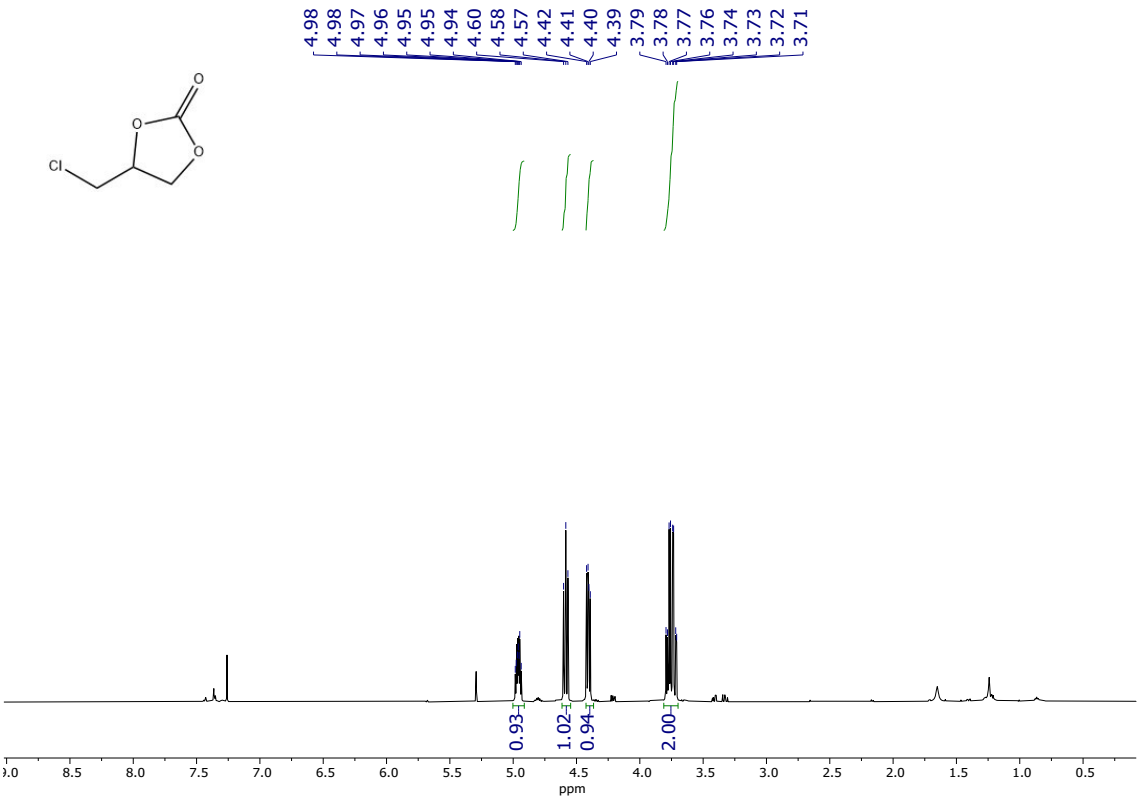

Figure S26. ^{1}H-NMR from reaction crude for the synthesis of compound **6f** in $CDCl_3$.

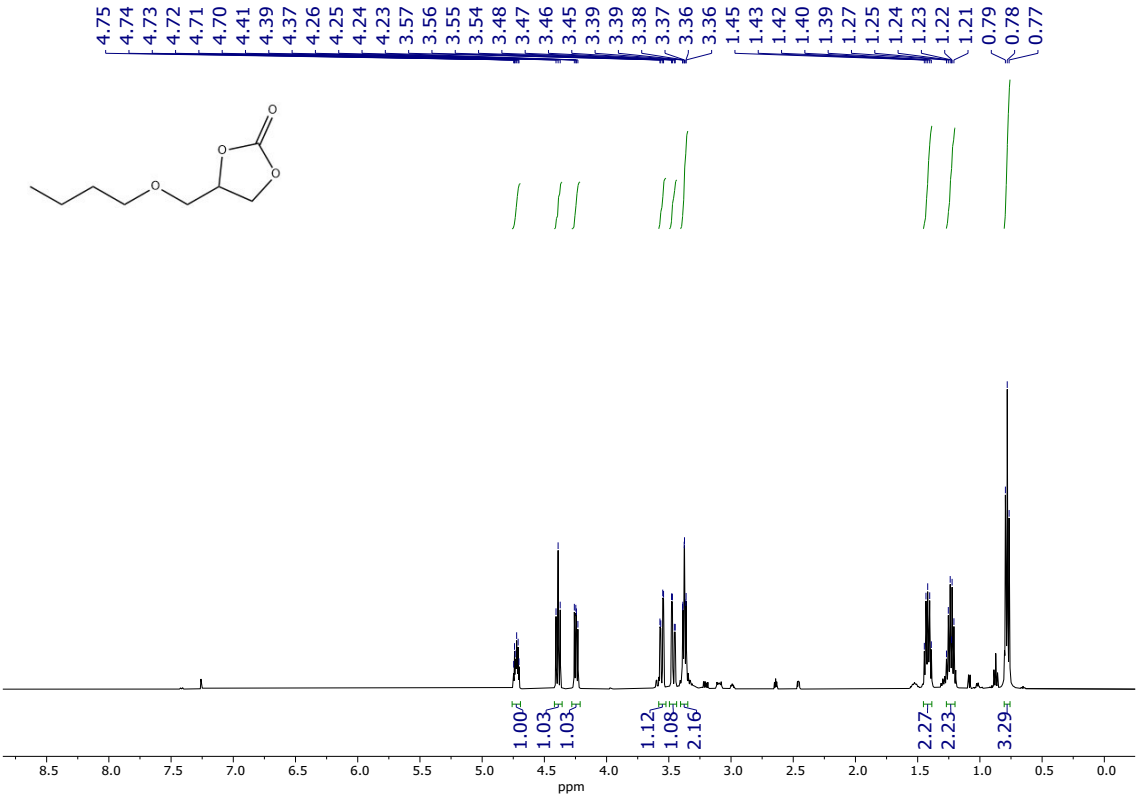

Figure S27. ^{1}H-NMR from reaction crude for the synthesis of compound **6g** in $CDCl_3$.

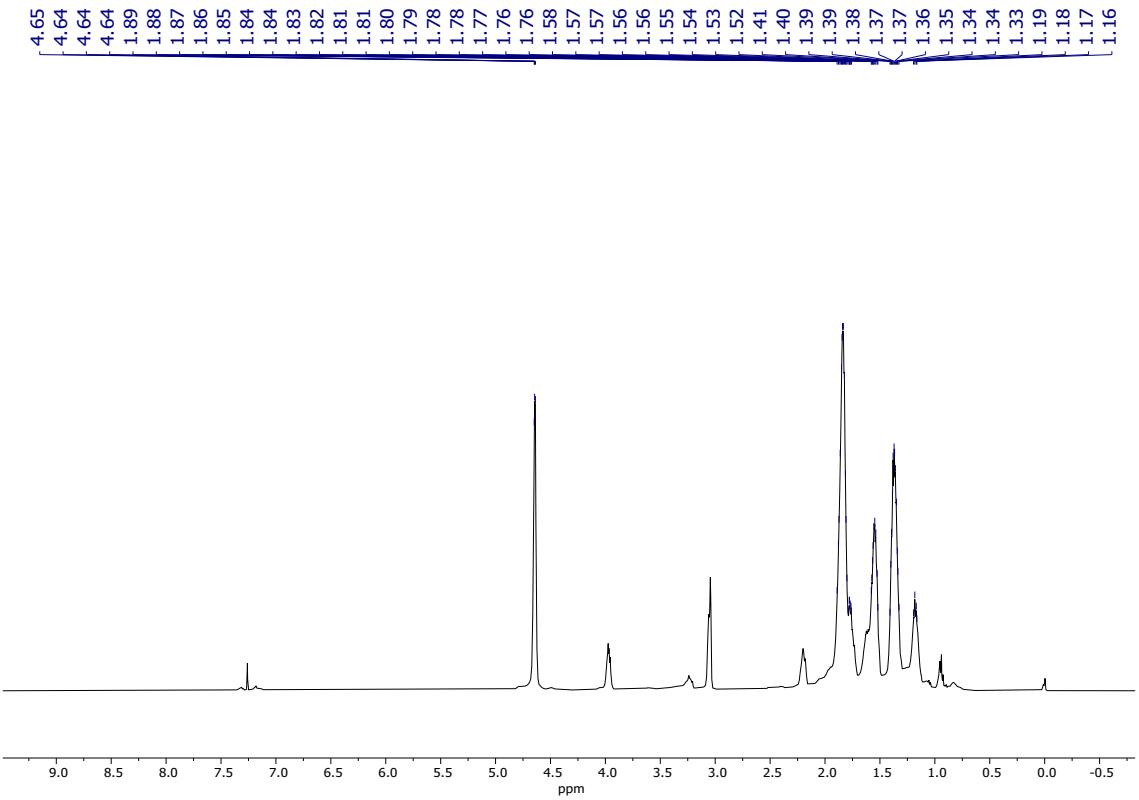

Figure S28. ^{1}H-NMR of the crude product of the reaction of cyclohexene oxide and CO_2 in $CDCl_3$.

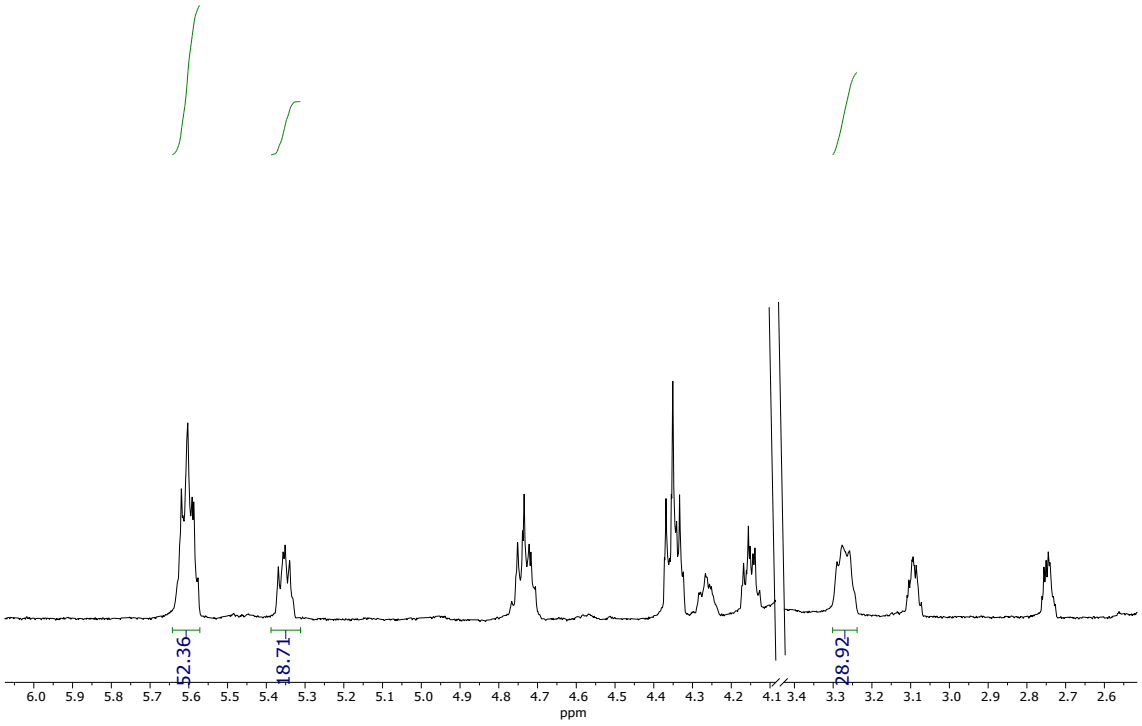

Figure S29. ^{1}H-NMR from reaction crude for the synthesis of compounds **8a** and **9a** in $CDCl_3$.

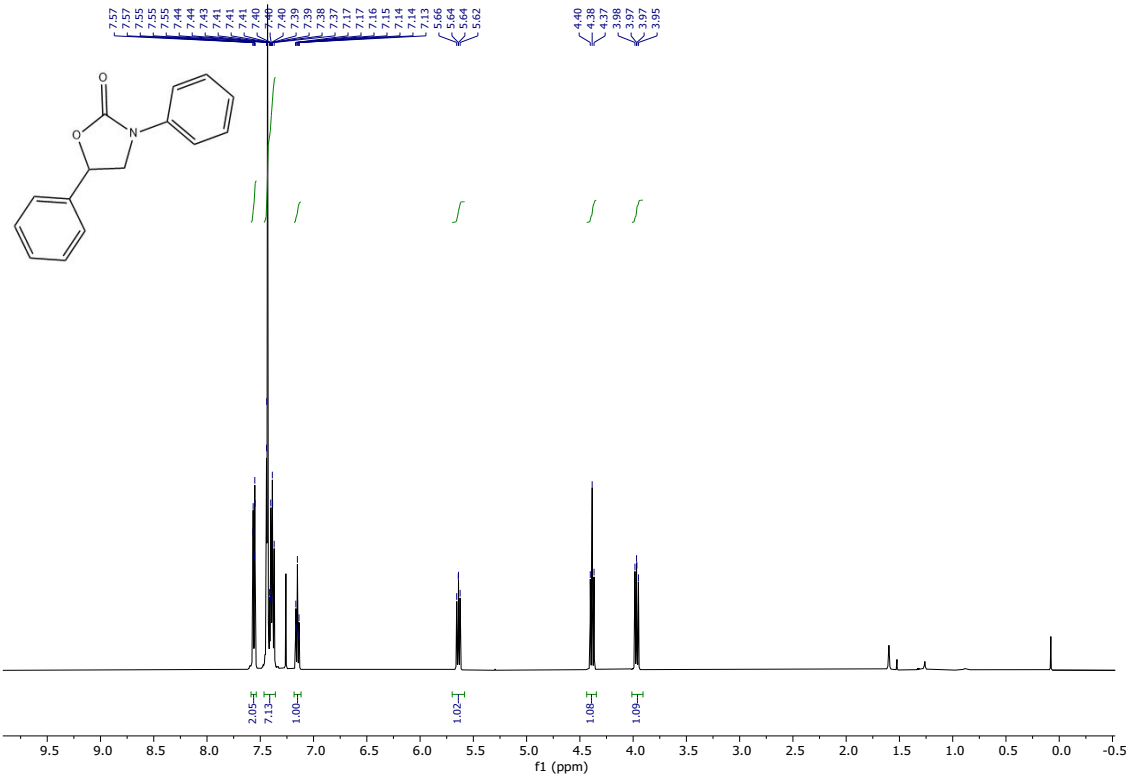

Figure S30. ^{1}H-NMR full chart for compound **8a** in $CDCl_3$.

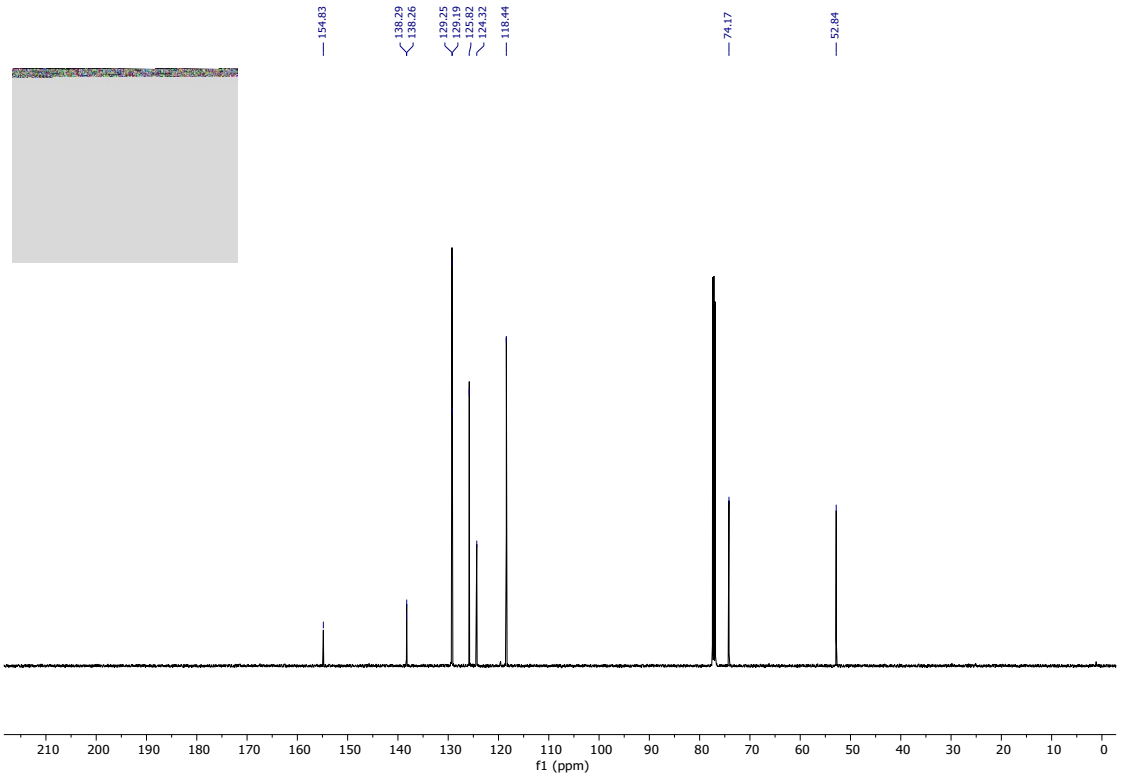

Figure S31. $^{13}C\{^{1}H\}$-NMR full chart for compound **8a** in $CDCl_3$.

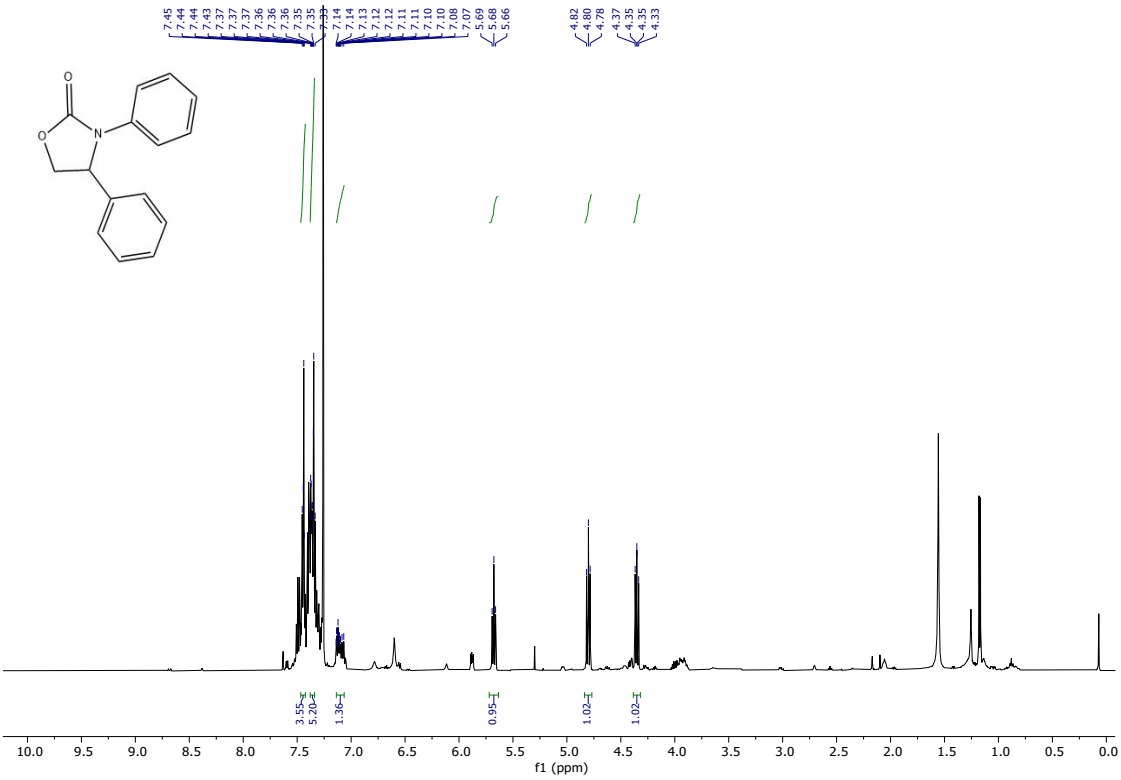

Figure S32. ^{1}H-NMR full chart for compound **9a** in $CDCl_3$.

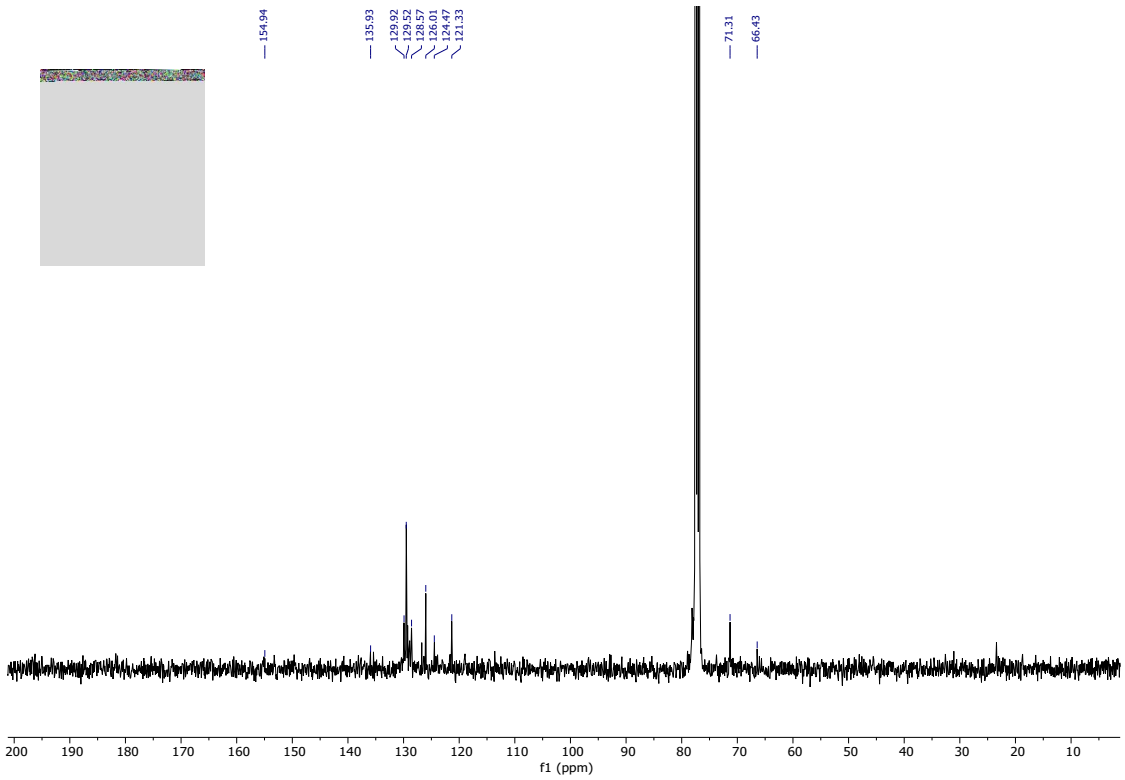

Figure S33. $^{13}C\{^{1}H\}$-NMR full chart for compound **9a** in $CDCl_3$.

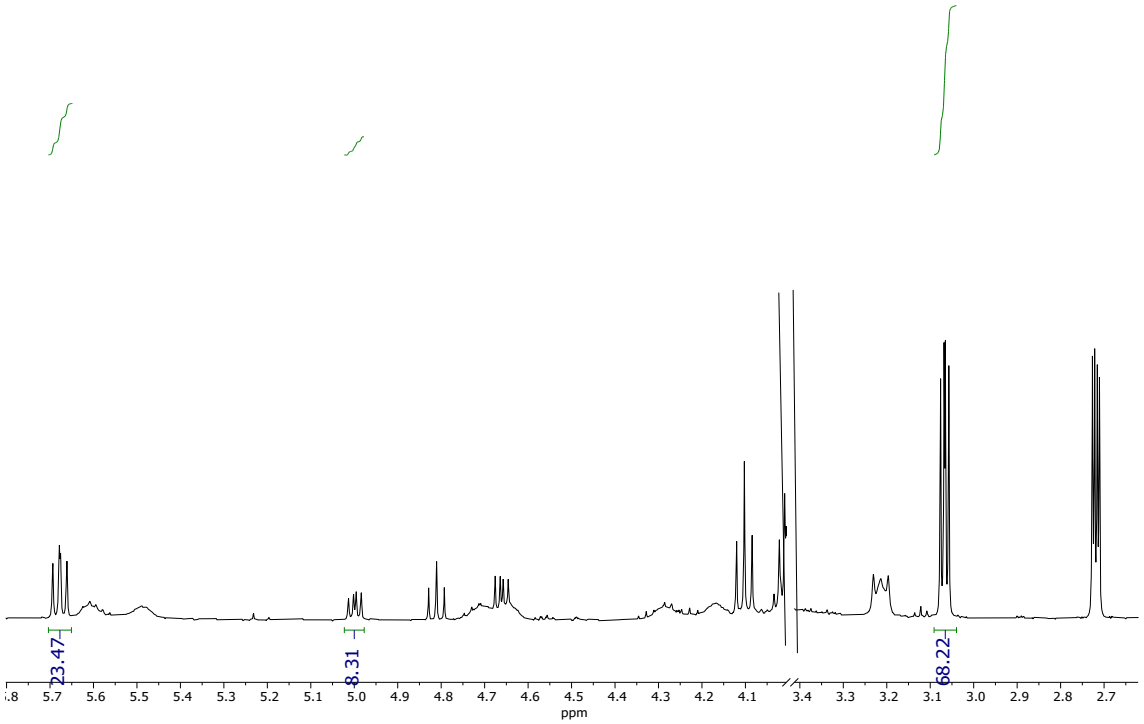

Figure S34. ^{1}H-NMR from reaction crude for the synthesis of compounds **8b** and **9b** in $CDCl_3$.

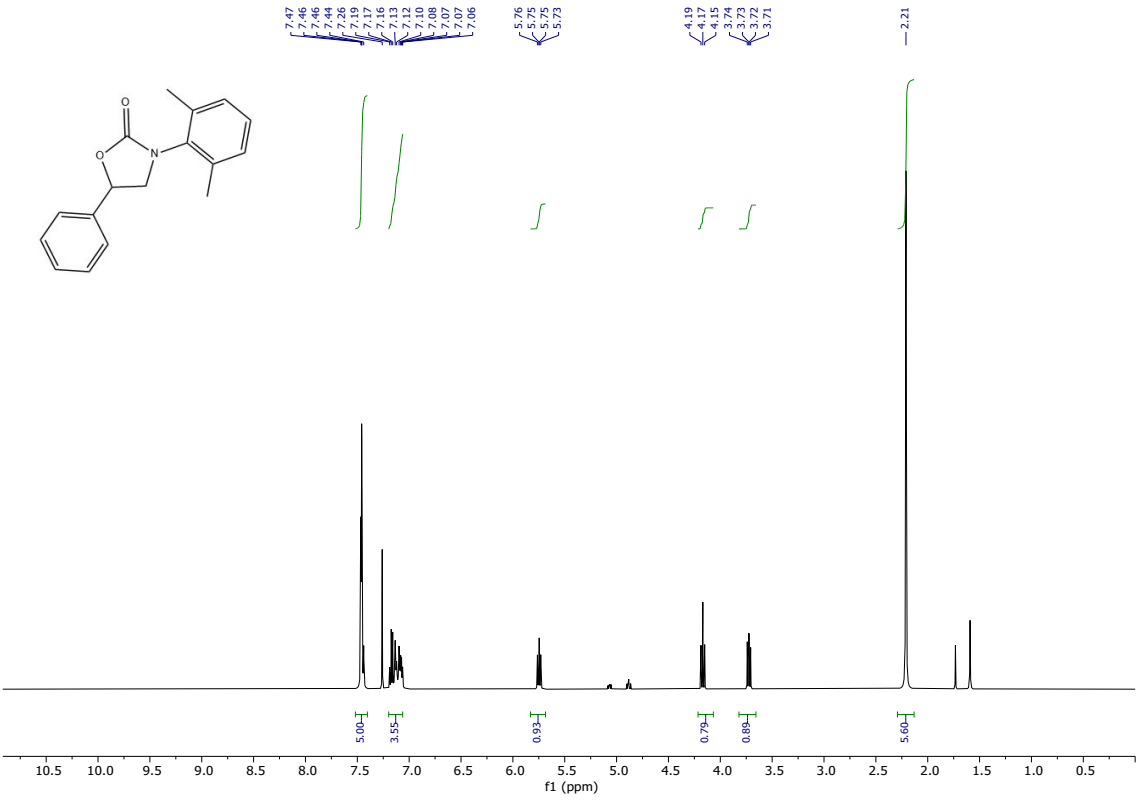

Figure 35. ^{1}H-NMR full chart for compound **8b** in $CDCl_3$.

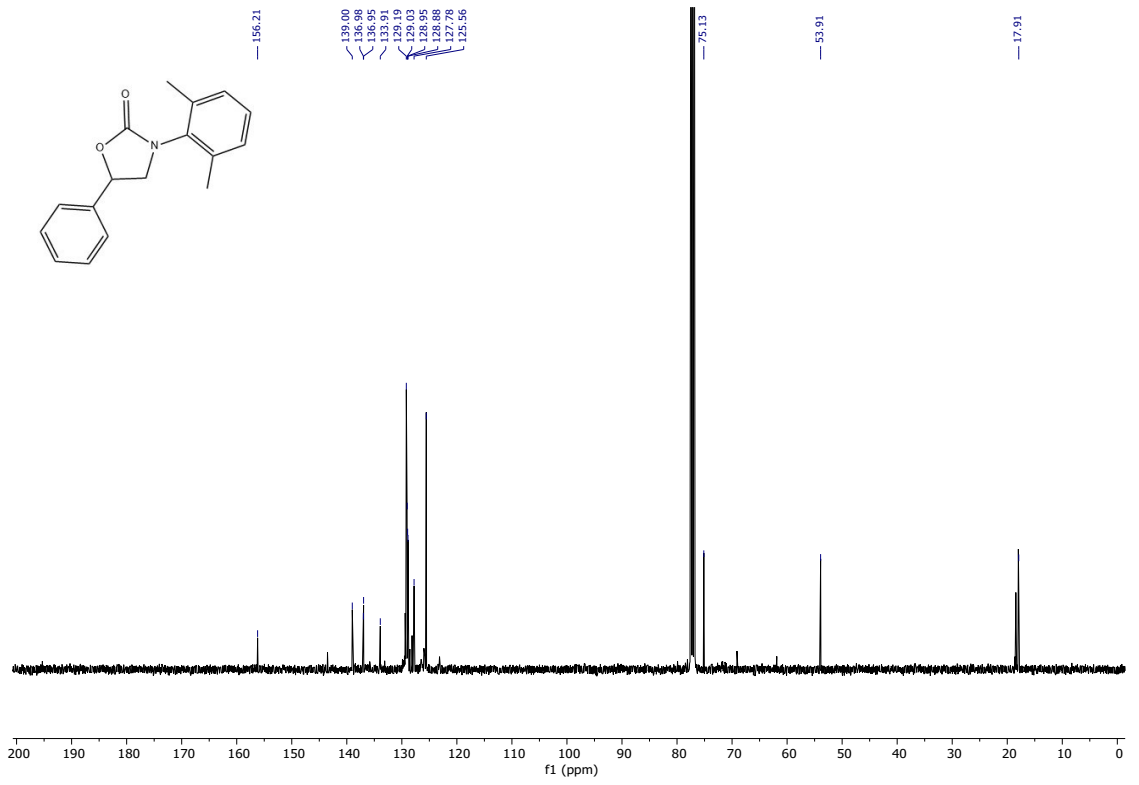

Figure S36. ^{13}C{^{1}H}-NMR full chart for compound **8b** in $CDCl_3$.

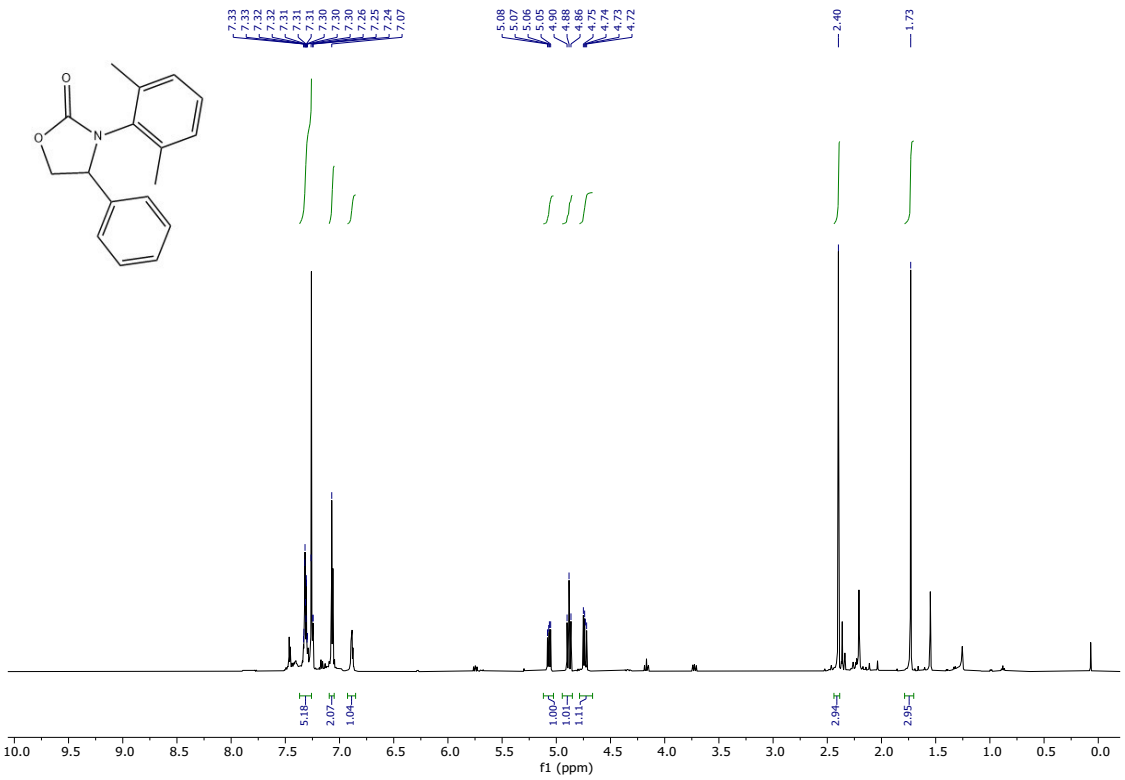

Figure S37. ^{1}H-NMR full chart for compound **9b** in $CDCl_3$.

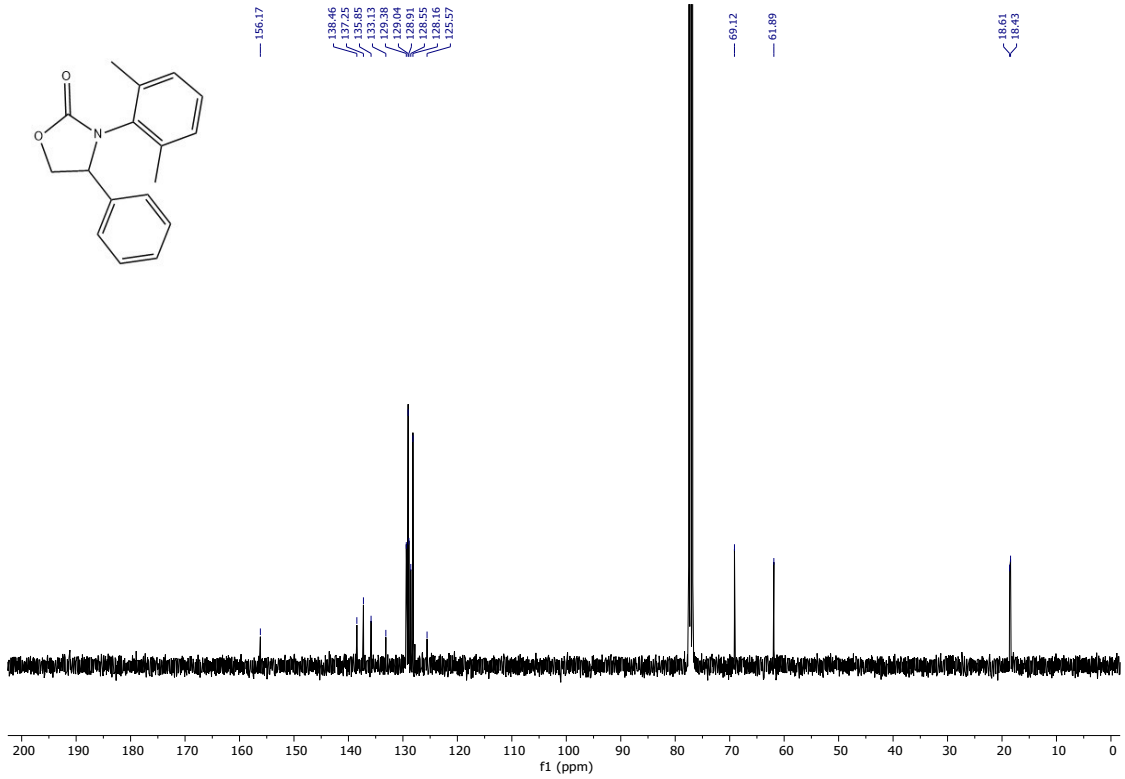

Figure S38. ^{13}C{^{1}H}-NMR full chart for compound **9b** in $CDCl_3$.

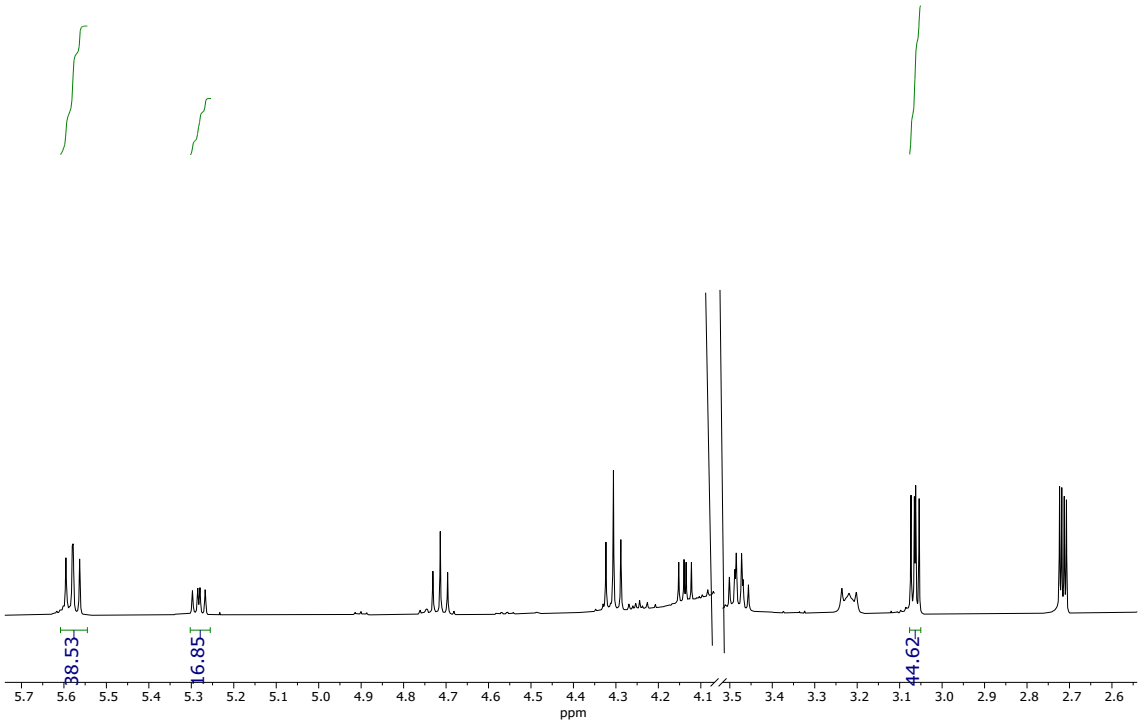

Figure S39. ^{1}H-NMR from reaction crude for the synthesis of compounds **8c** and **9c** in $CDCl_3$.

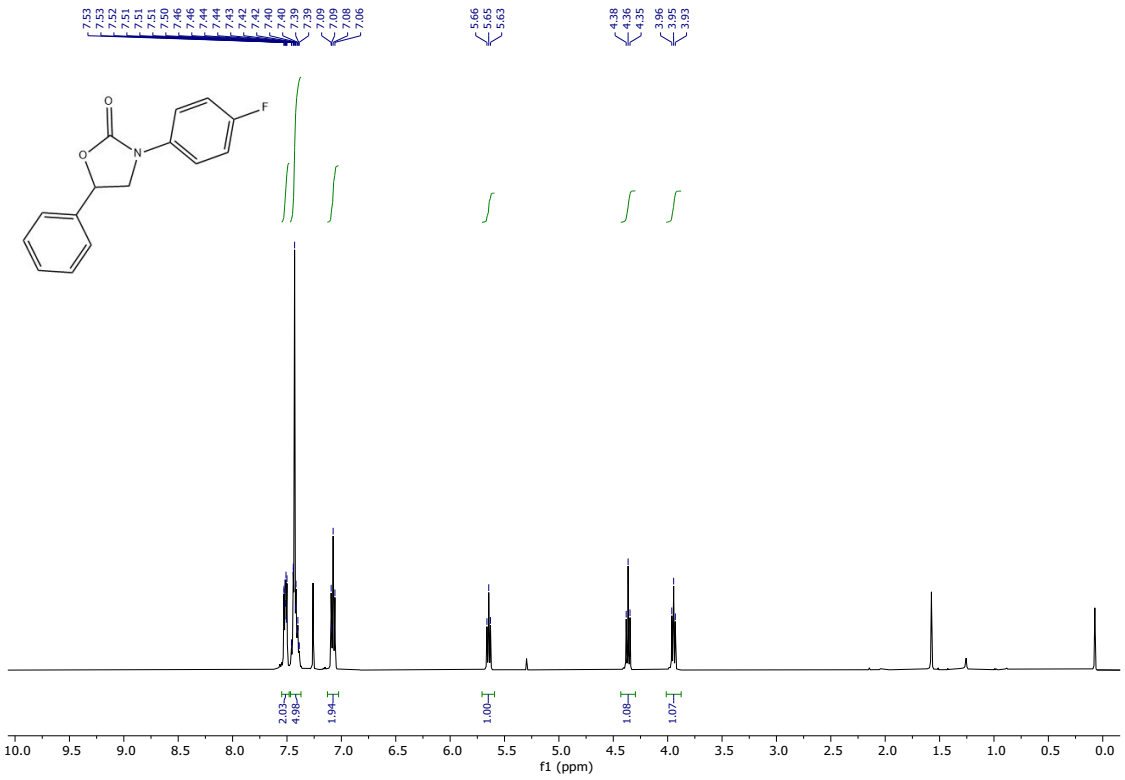

Figure S40. ^{1}H-NMR full chart for compound **8c** in $CDCl_3$.

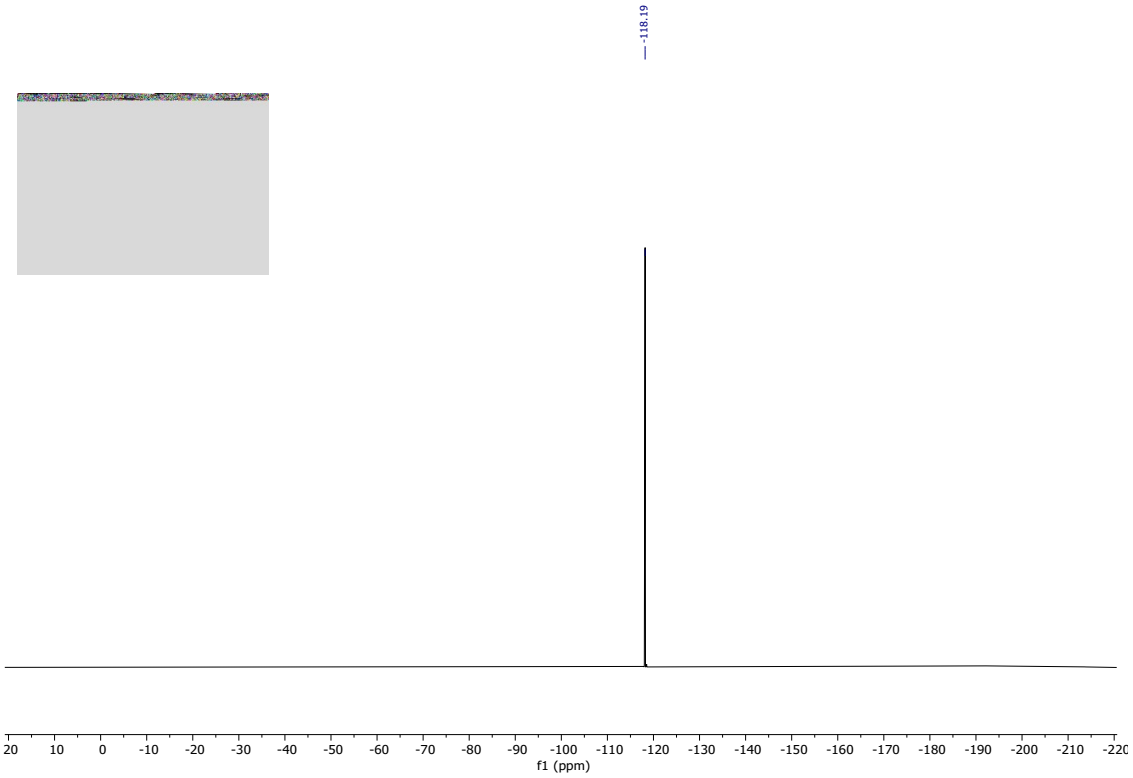

Figure S41. $^{19}F\{^{1}H\}$-NMR full chart for compound **8c** in $CDCl_3$.

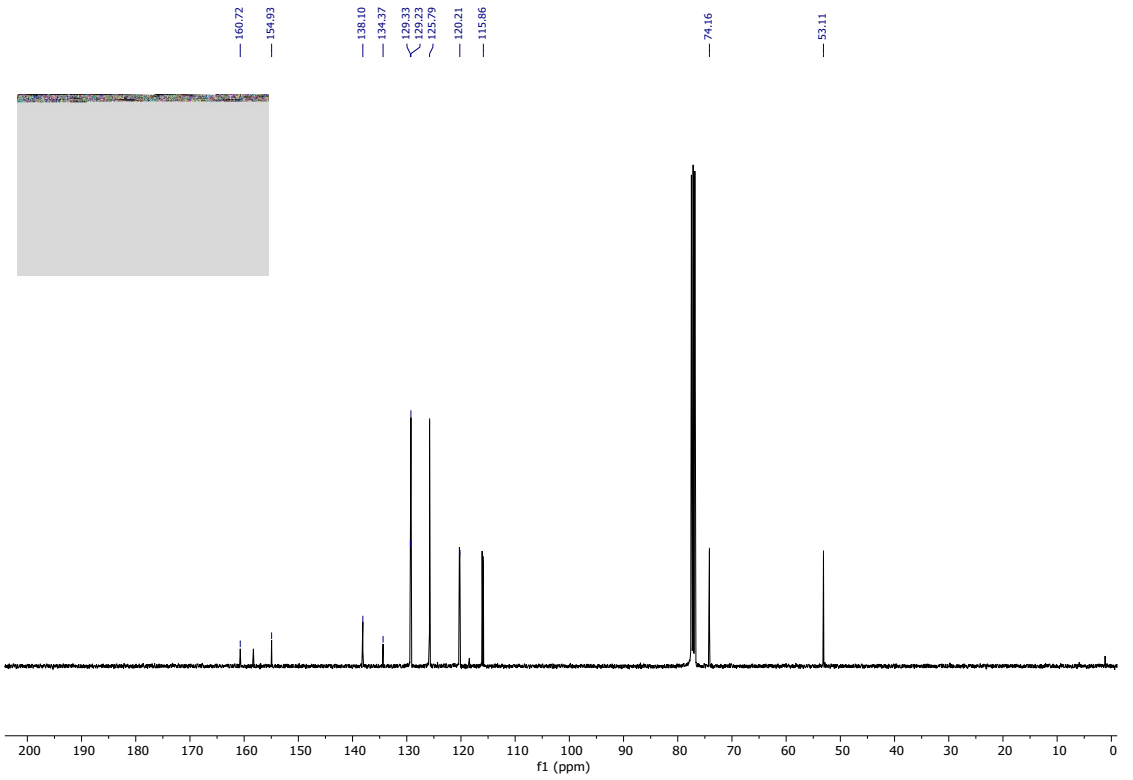

Figure 42. $^{13}C\{^{1}H\}$-NMR full chart for compound **8c** in $CDCl_3$.

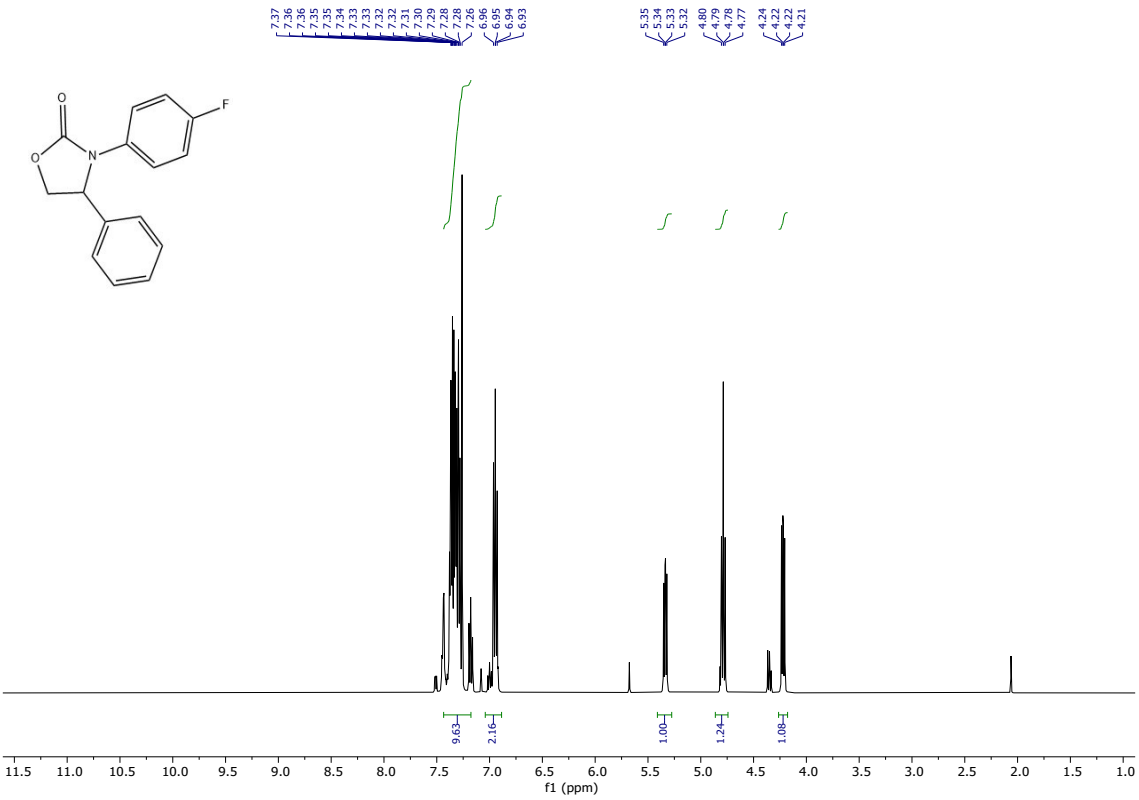

Figure S43. ^{1}H-NMR full chart for compound **9c** in $CDCl_3$.

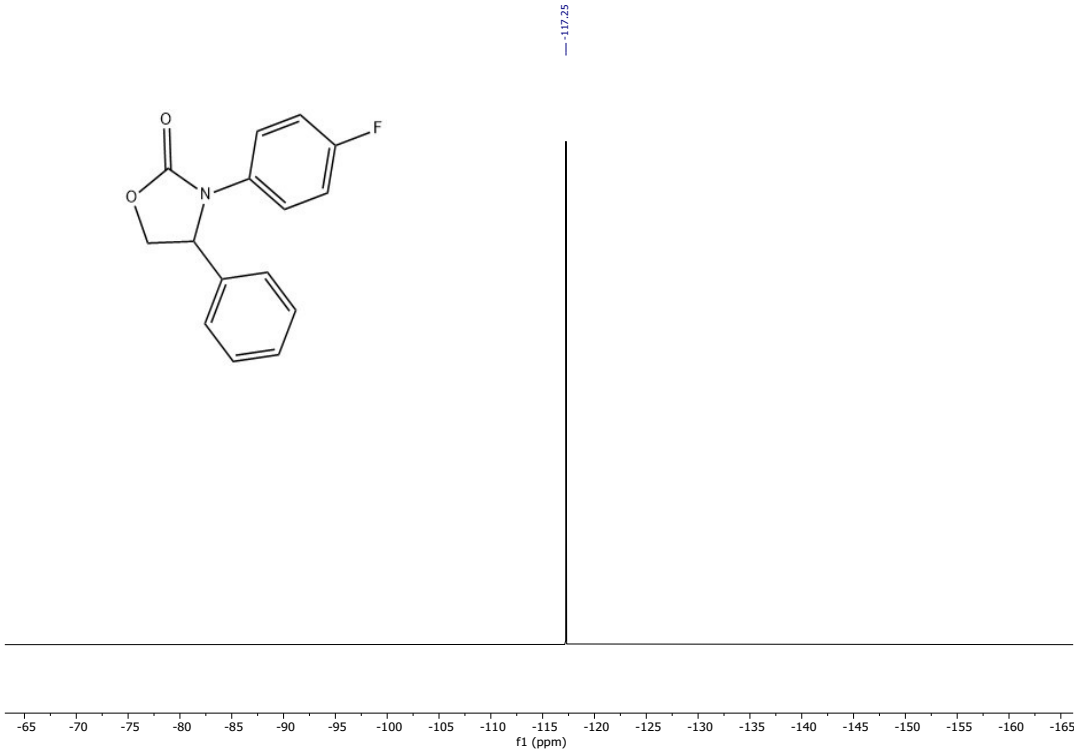

Figure S44. ^{19}F{^{1}H}-NMR full chart for compound **9c** in $CDCl_3$.

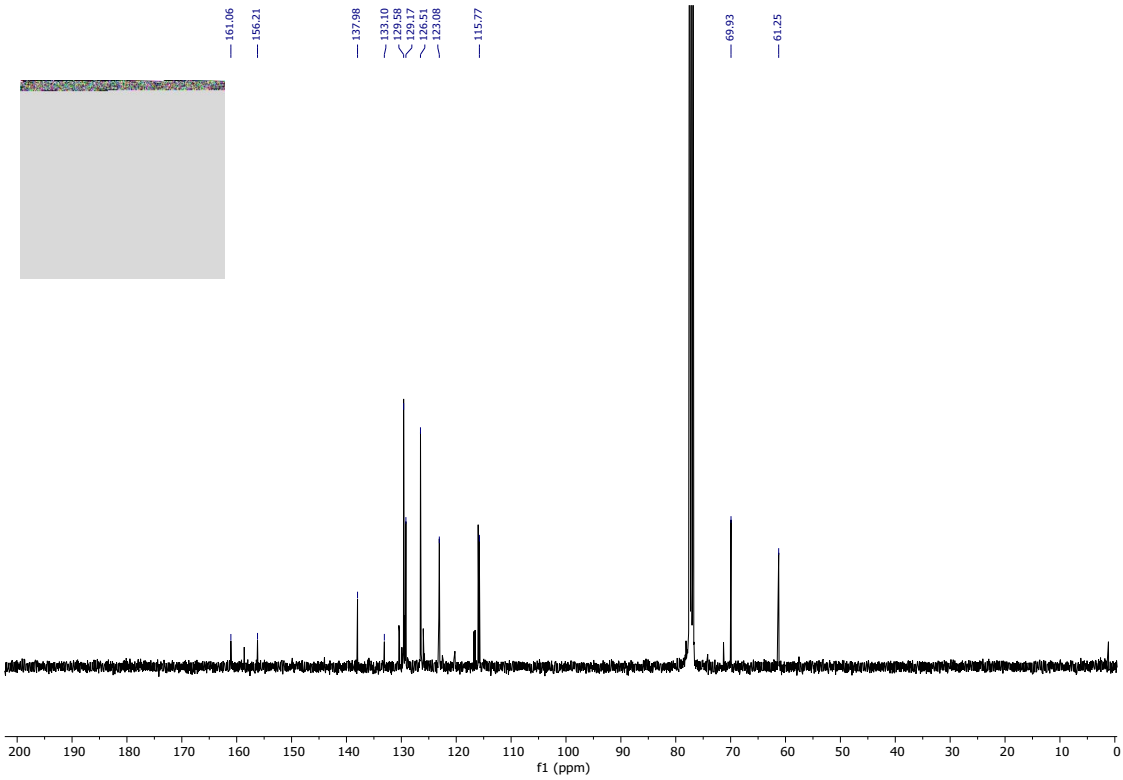

Figure S45. $^{13}C\{^{1}H\}$-NMR full chart for compound **9c** in $CDCl_3$.

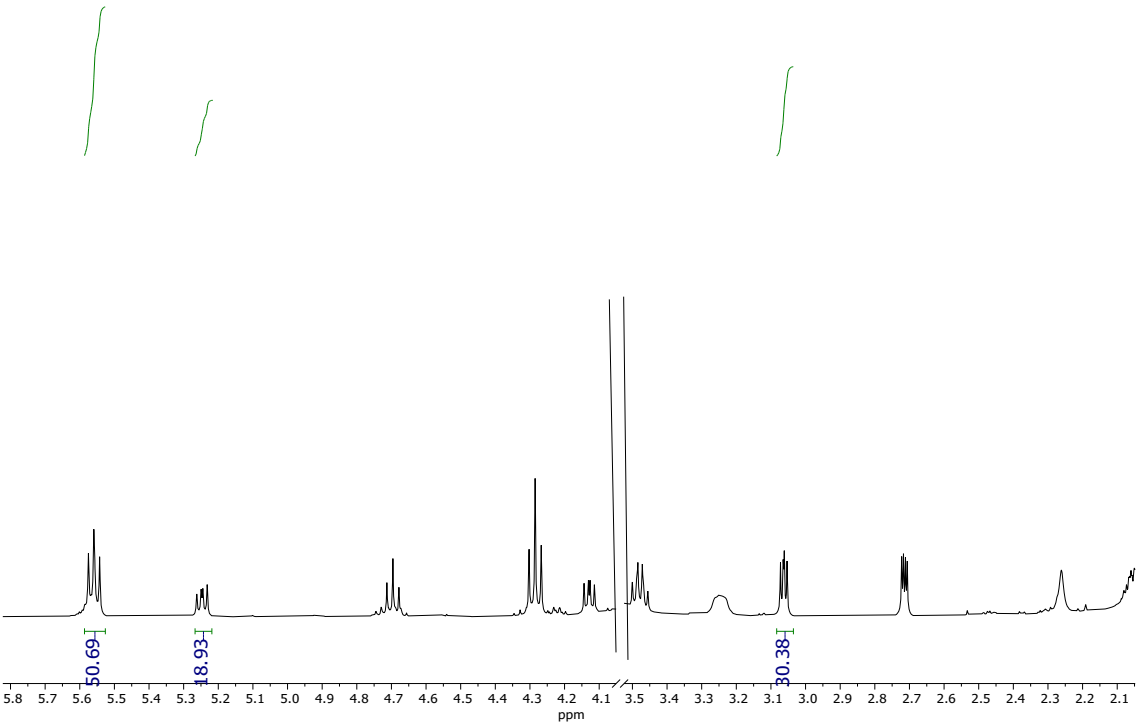

Figure S46. ^{1}H-NMR from reaction crude for the synthesis of compounds **8d** and **9d** in $CDCl_3$.

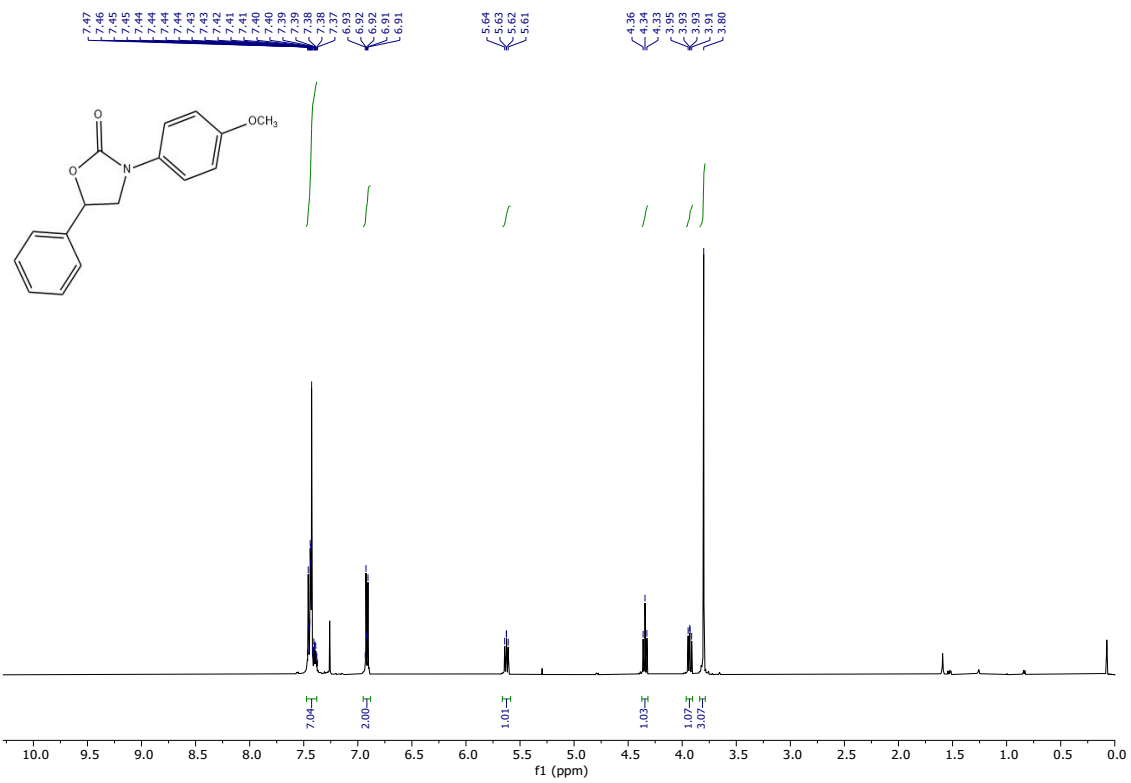

Figure S47. ^{1}H-NMR full chart for compound **8d** in $CDCl_3$.

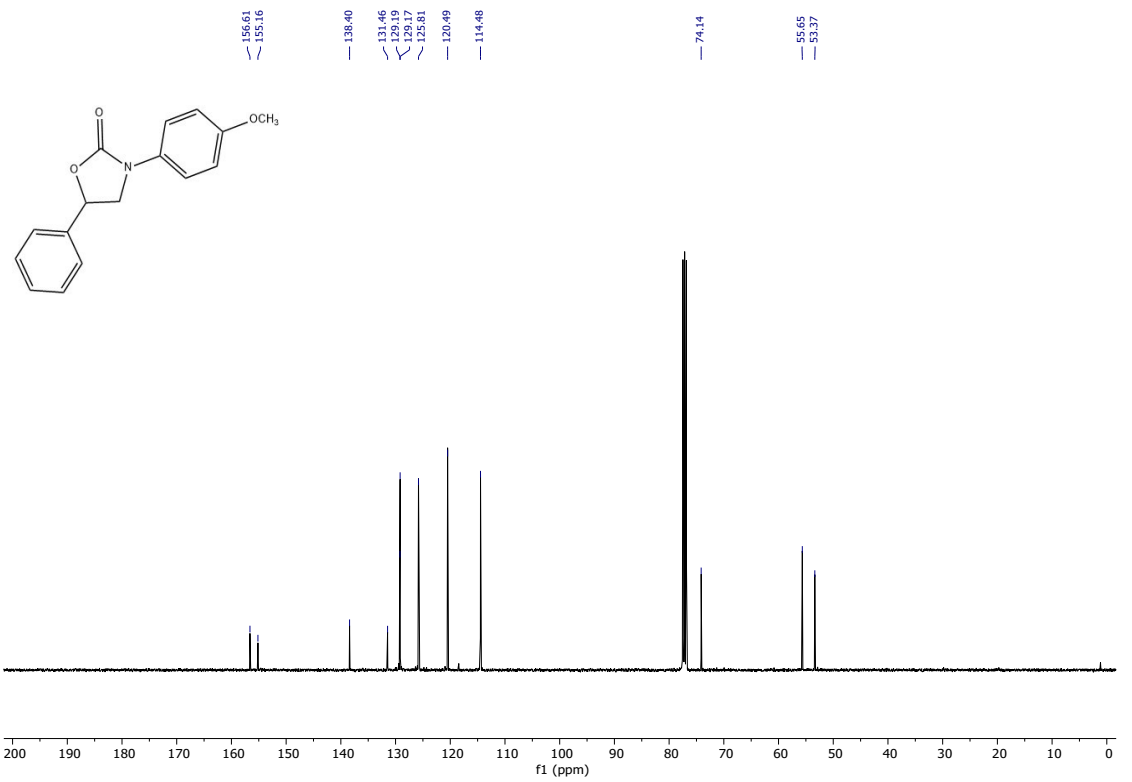

Figure S48. ^{13}C{^{1}H}-NMR full chart for compound **8d** in $CDCl_3$.

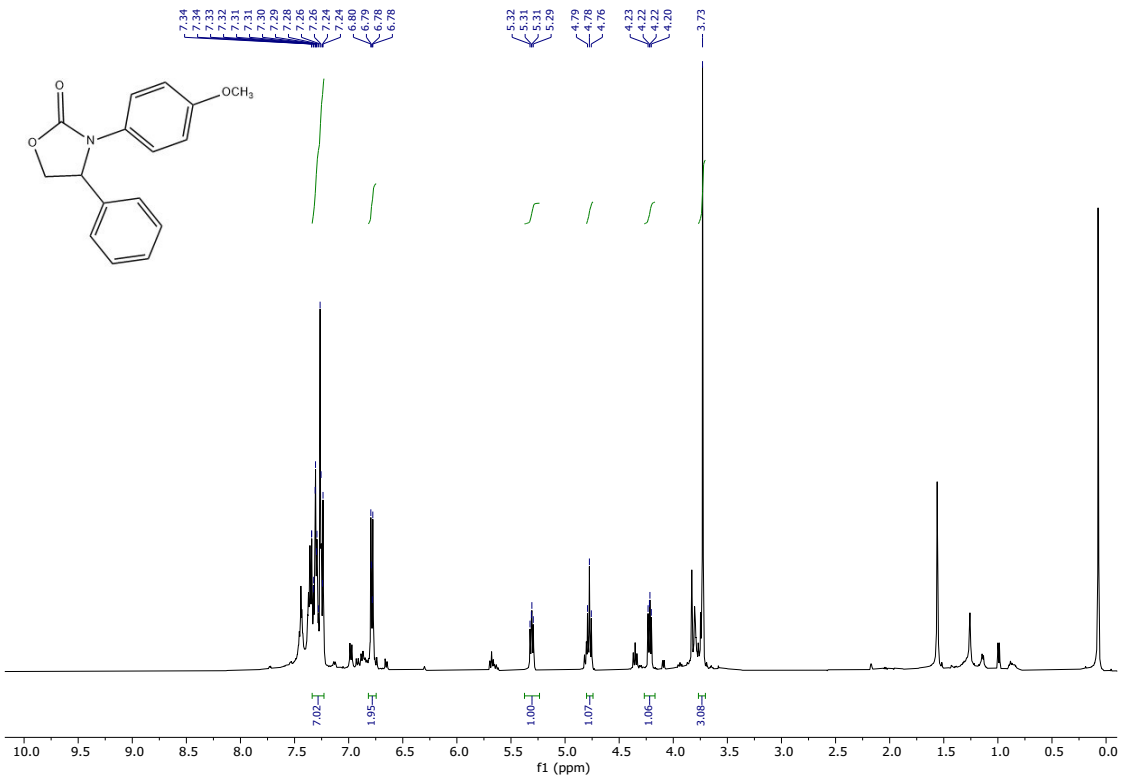

Figure S49. ^{1}H-NMR full chart for compound **9d** in $CDCl_3$.

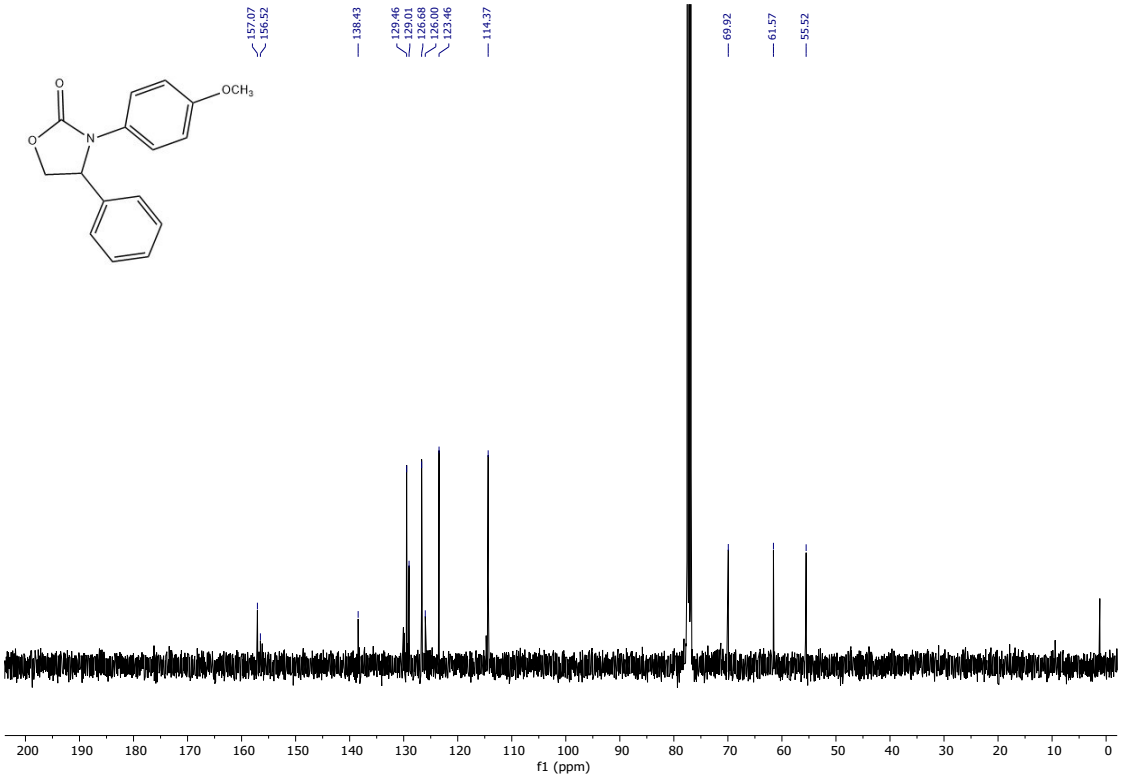

Figure S50. ^{13}C{^{1}H}-NMR full chart for compound **9d** in $CDCl_3$.

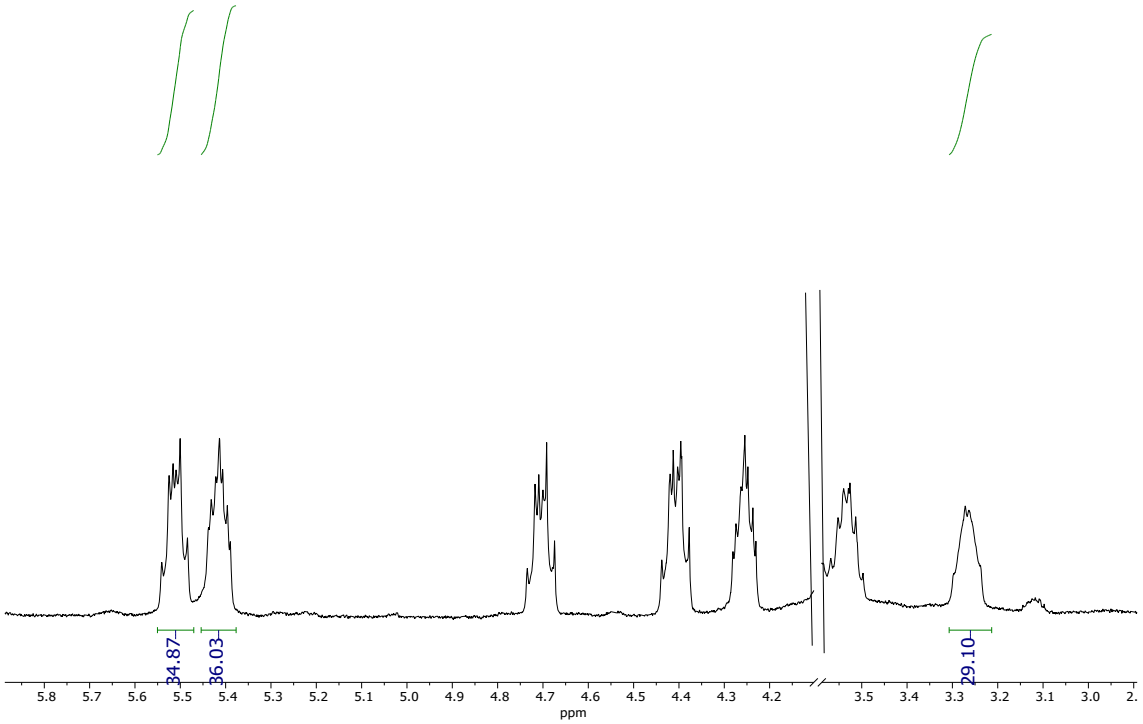

Figure S51. ^{1}H-NMR from reaction crude for the synthesis of compounds **8e** and **9e** in $CDCl_3$.

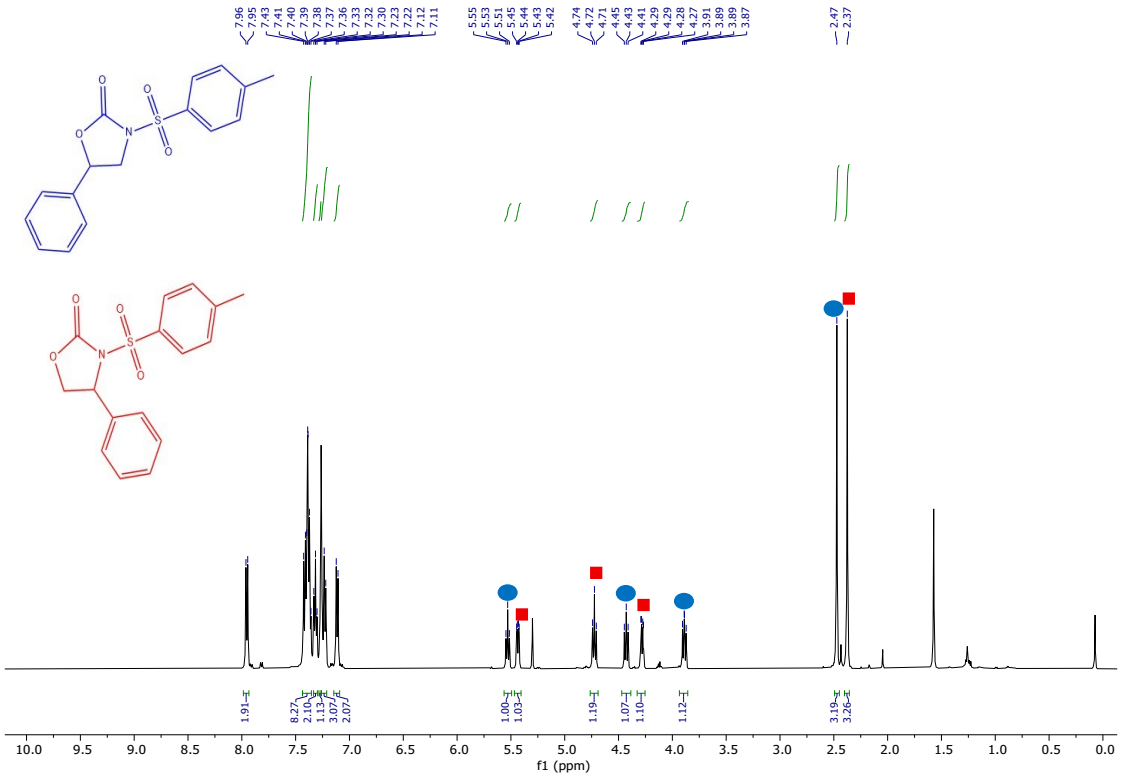

Figure S52. ^{1}H-NMR full chart for compounds **8e** and **9e** in $CDCl_3$.

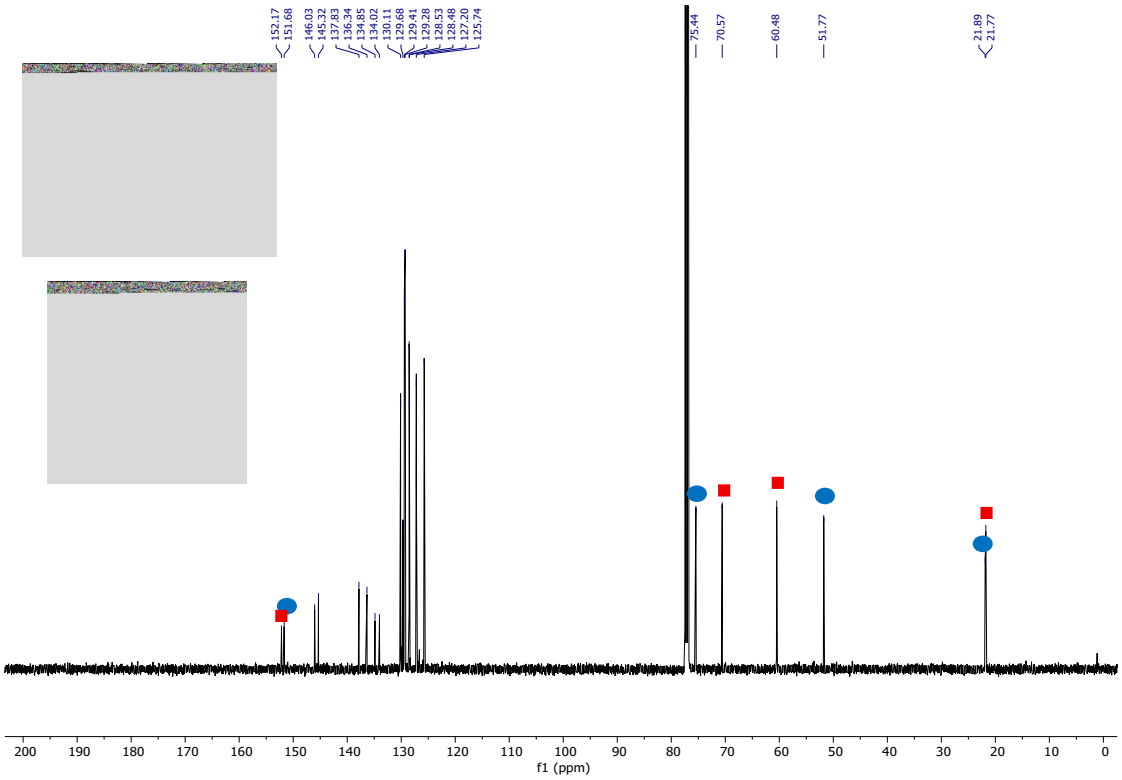

Figure S53. ^{13}C{^{1}H}-NMR full chart for compound **8e** and **9e** in $CDCl_3$.

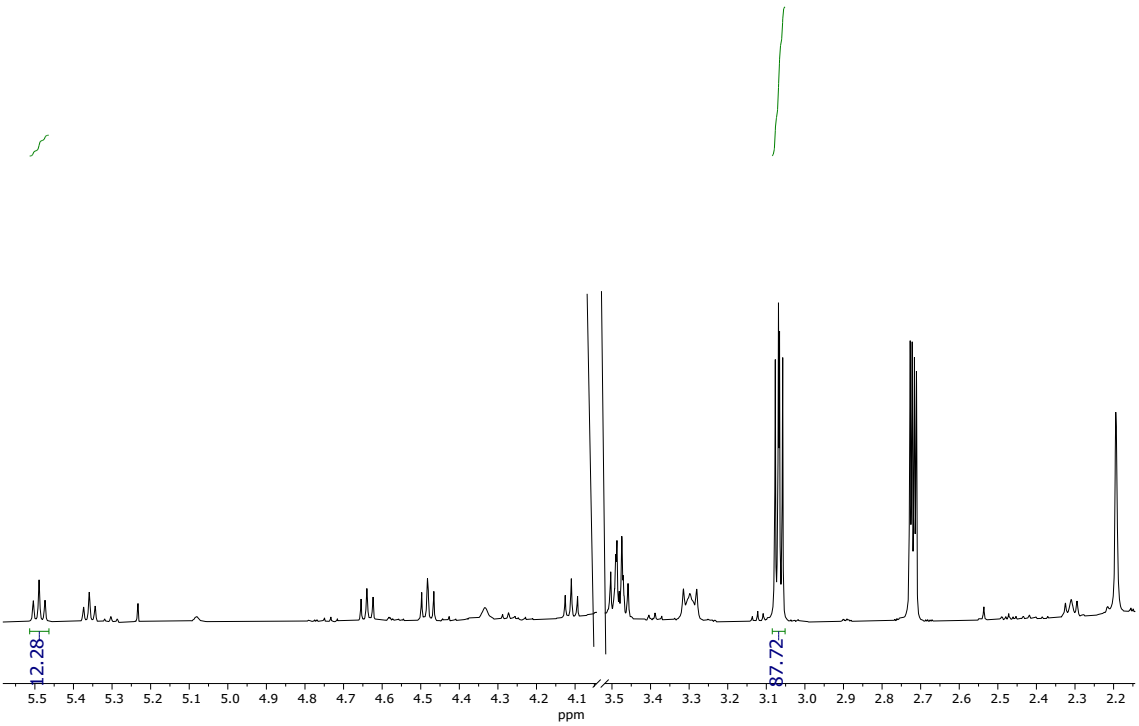

Figure S54. ^{1}H-NMR from reaction crude for the synthesis of product **9f** in $CDCL_3$.

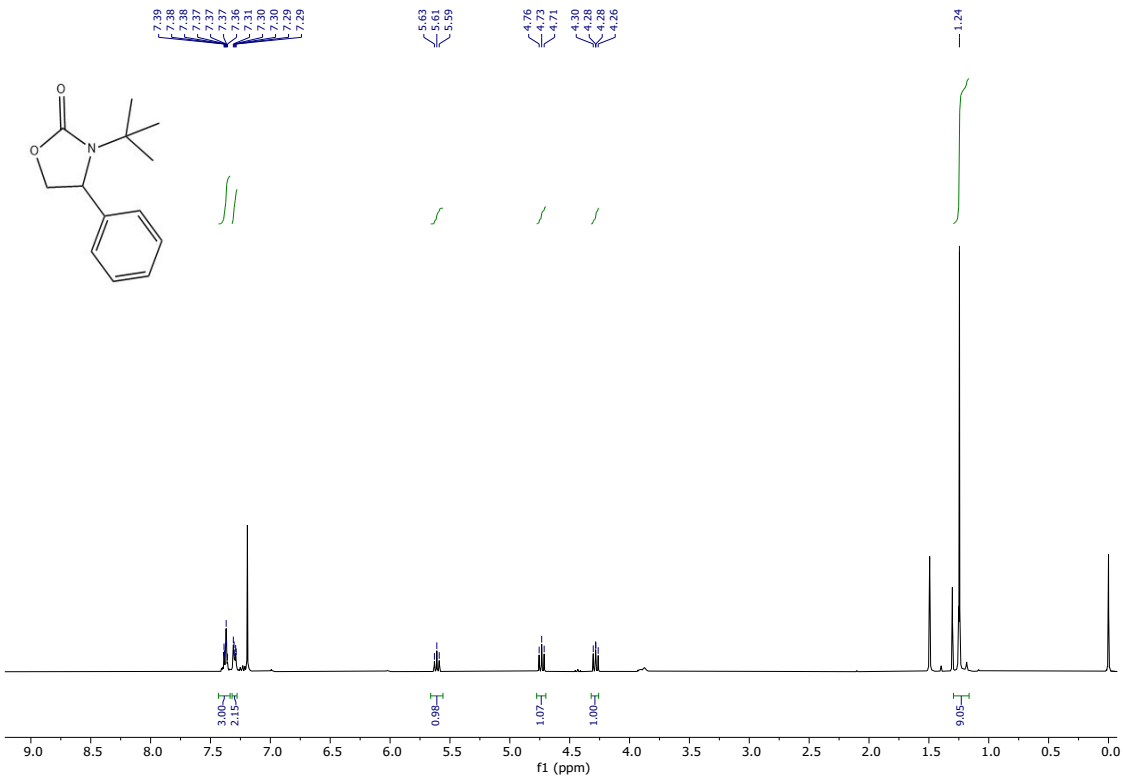

Figure S55. ^{1}H-NMR full chart for compound **9f** in $CDCl_3$.

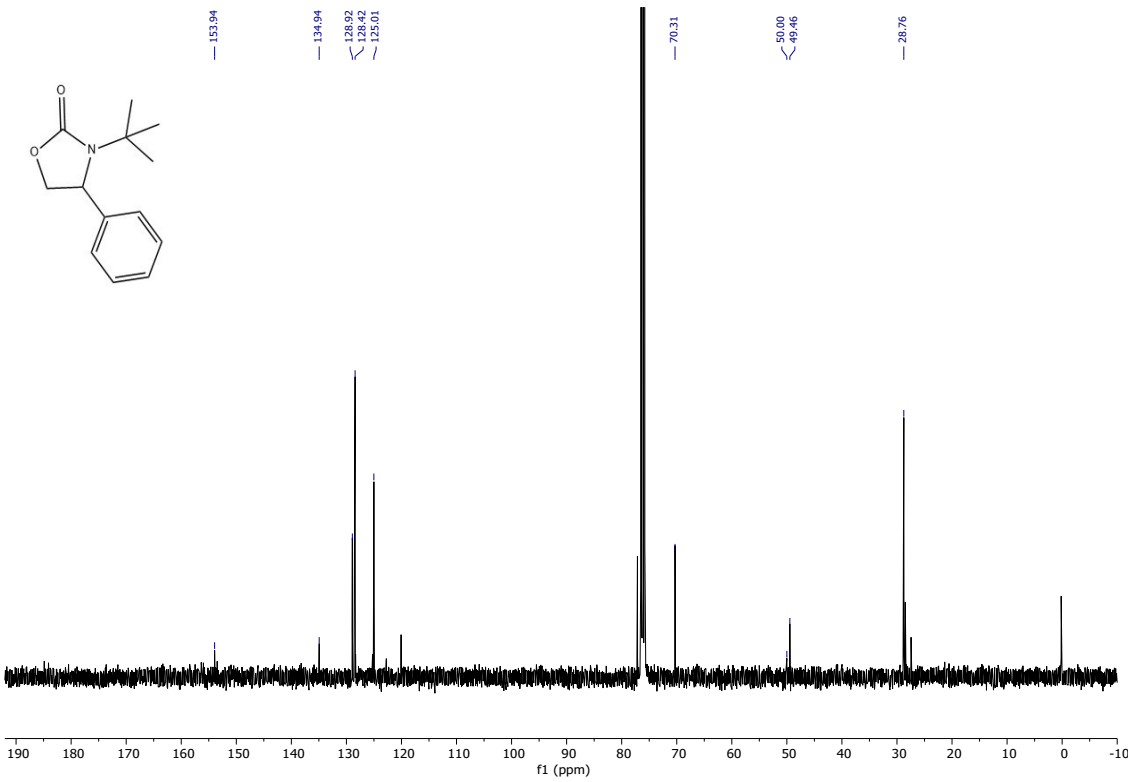

Figure S56. ^{13}C{^{1}H}-NMR full chart for compound **9f** in $CDCl_3$.

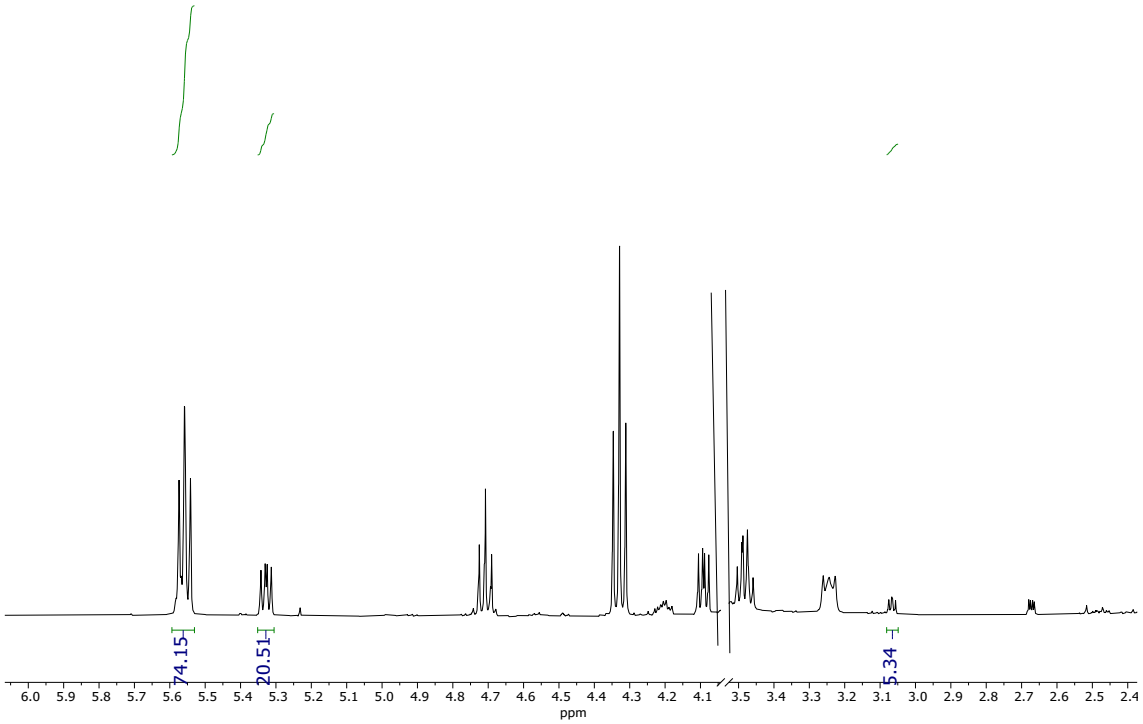

Figure S57. ^{1}H-NMR from reaction crude for the synthesis of compounds **8f** and **9g** in $CDCl_3$.

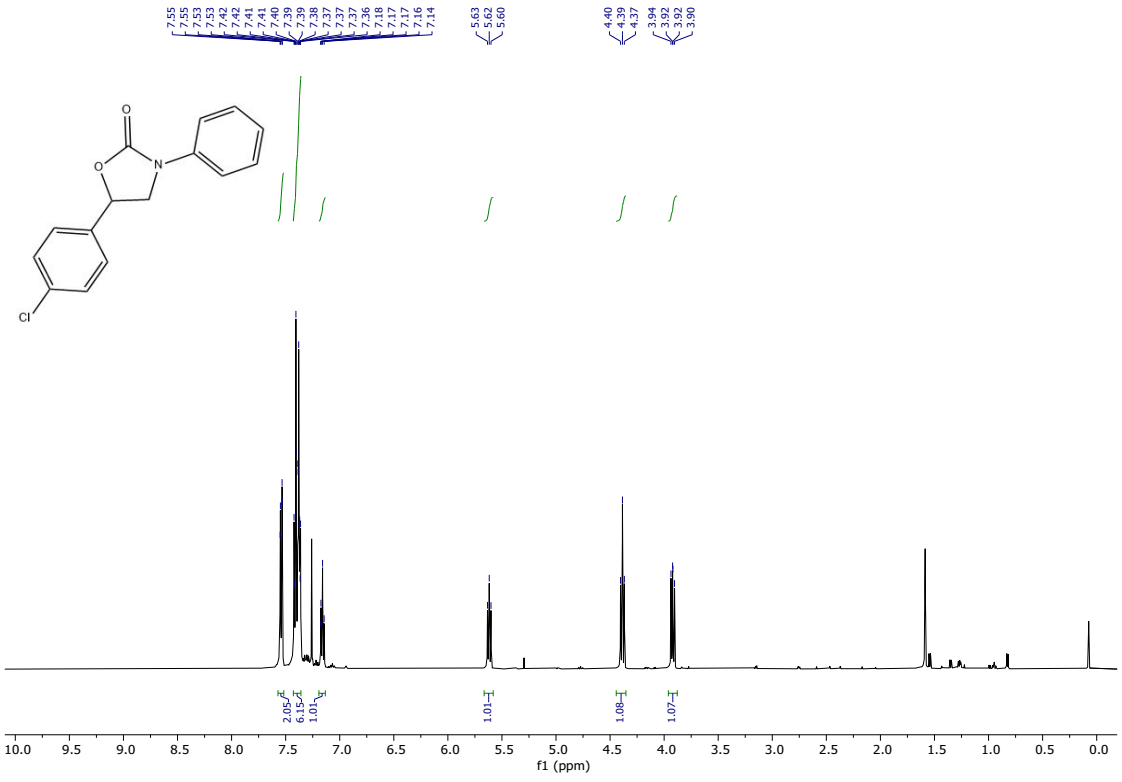

Figure S58. ^{1}H-NMR full chart for compound **8f** in $CDCl_3$.

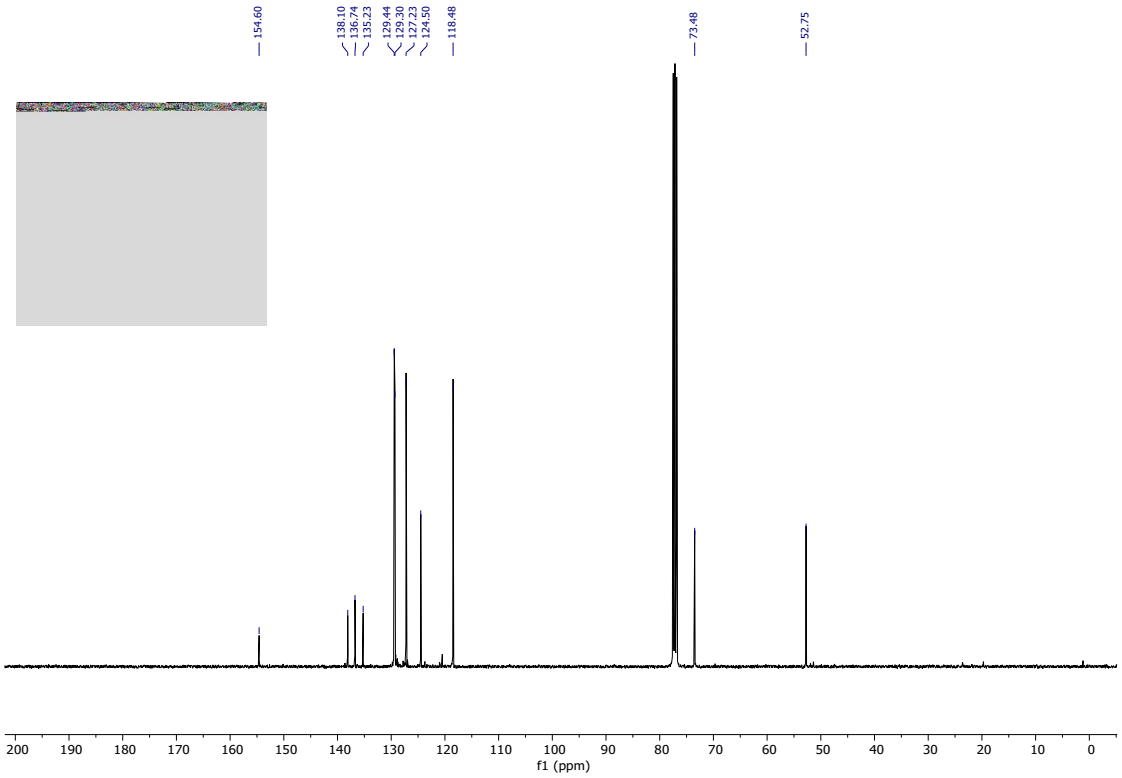

Figure S59. $^{13}C\{^{1}H\}$-NMR full chart for compound **8f** in $CDCl_3$.

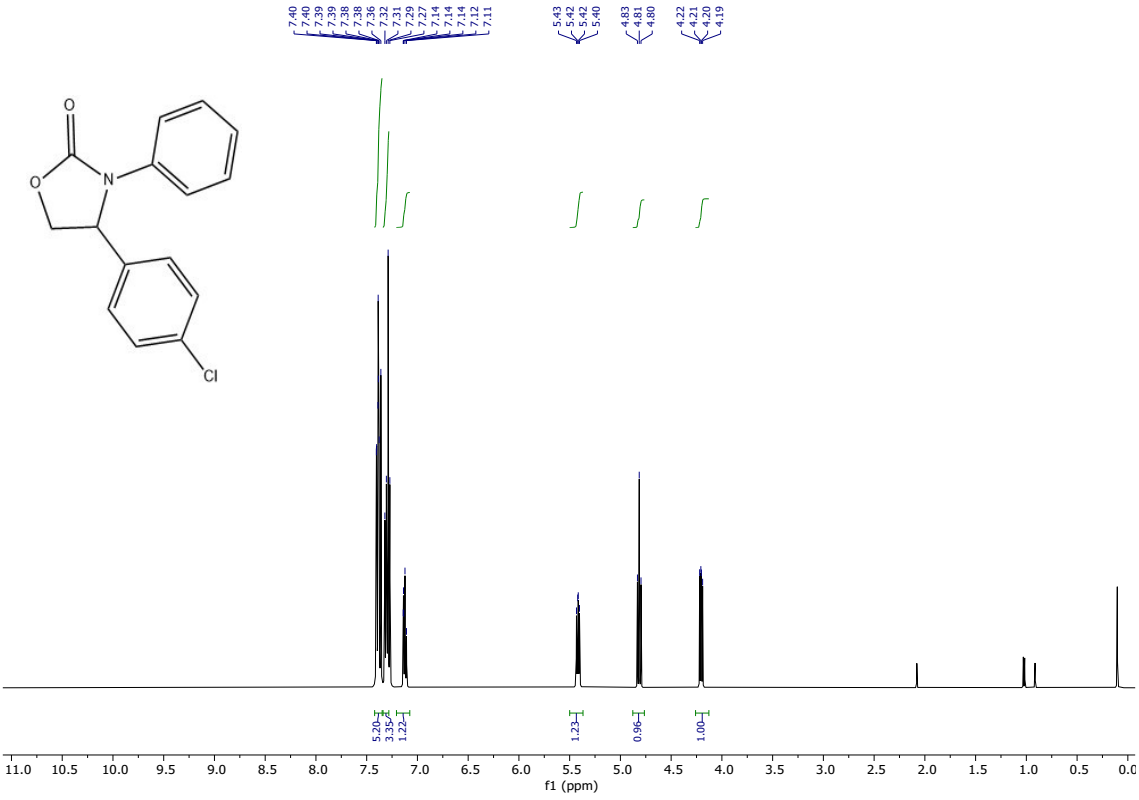

Figure S60. ^{1}H-NMR full chart for compound **9g** in $CDCl_3$.

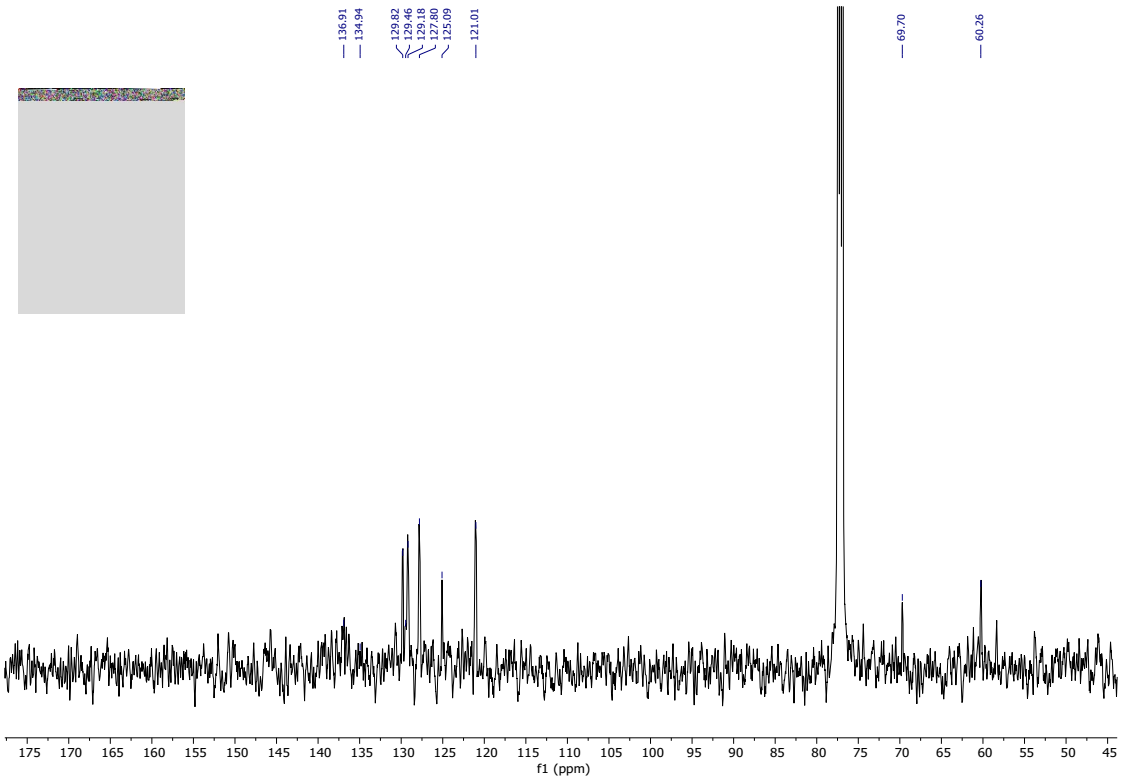

Figure S61. ^{13}C{^{1}H}-NMR full chart for compound **9g** in $CDCl_3$.

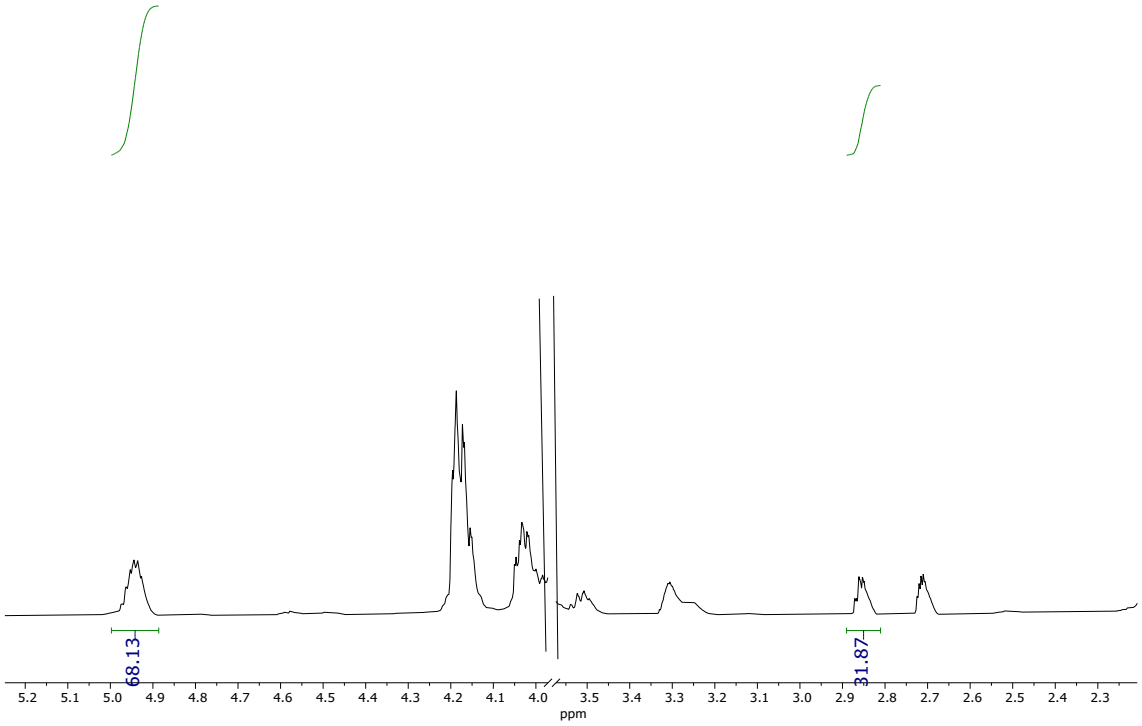

Figure S62. ^{1}H-NMR from reaction crude for the synthesis of product **8g** in $CDCl_3$.

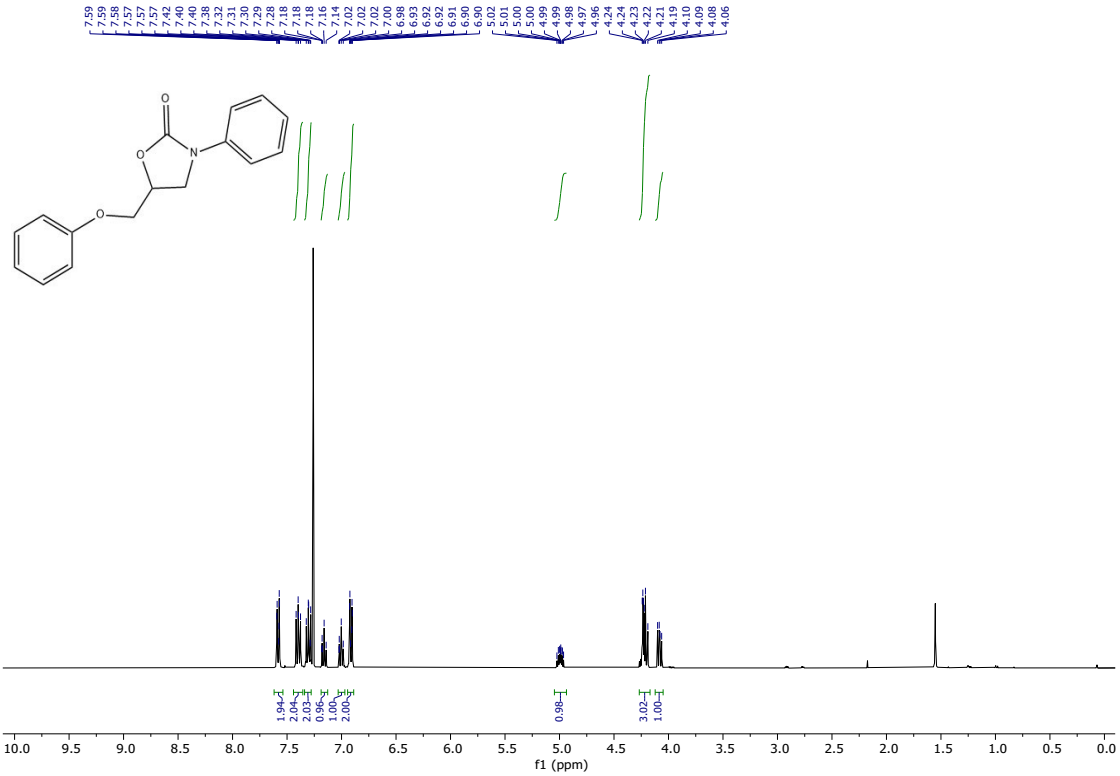

Figure S63. ^{1}H-NMR full chart for compound **8g** in $CDCl_3$.

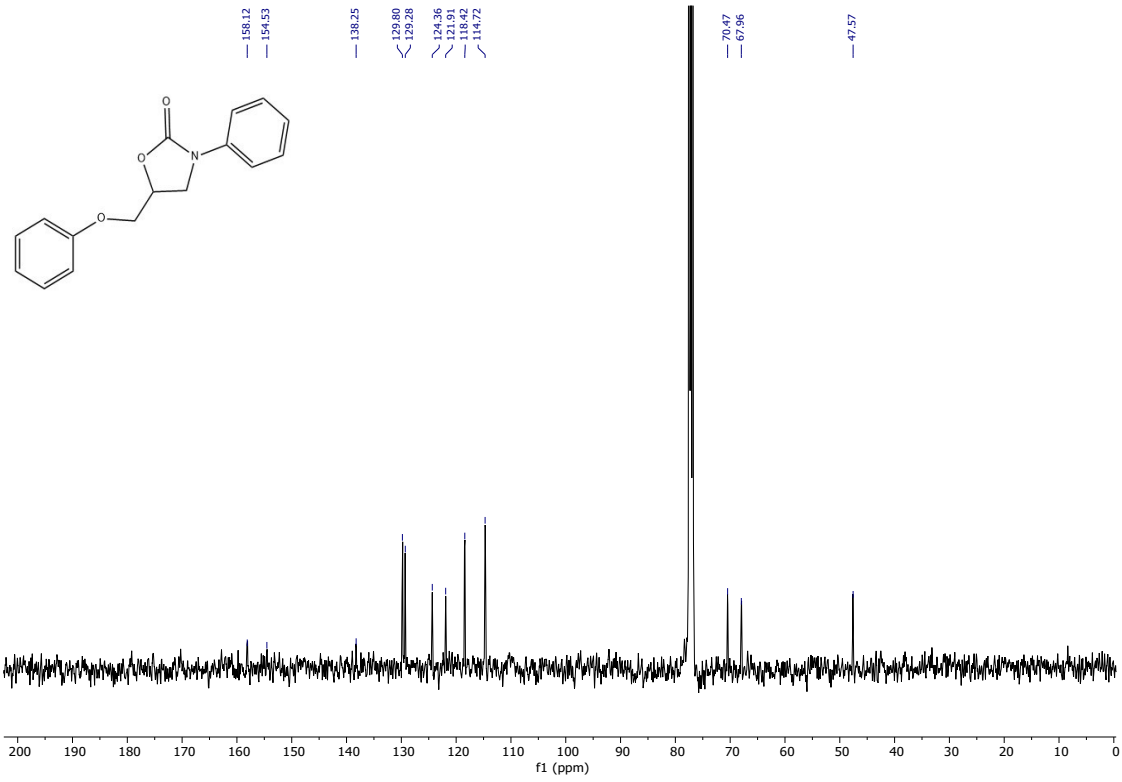

Figure S64. $^{13}C\{^{1}H\}$-NMR full chart for compound **8g** in $CDCl_3$.

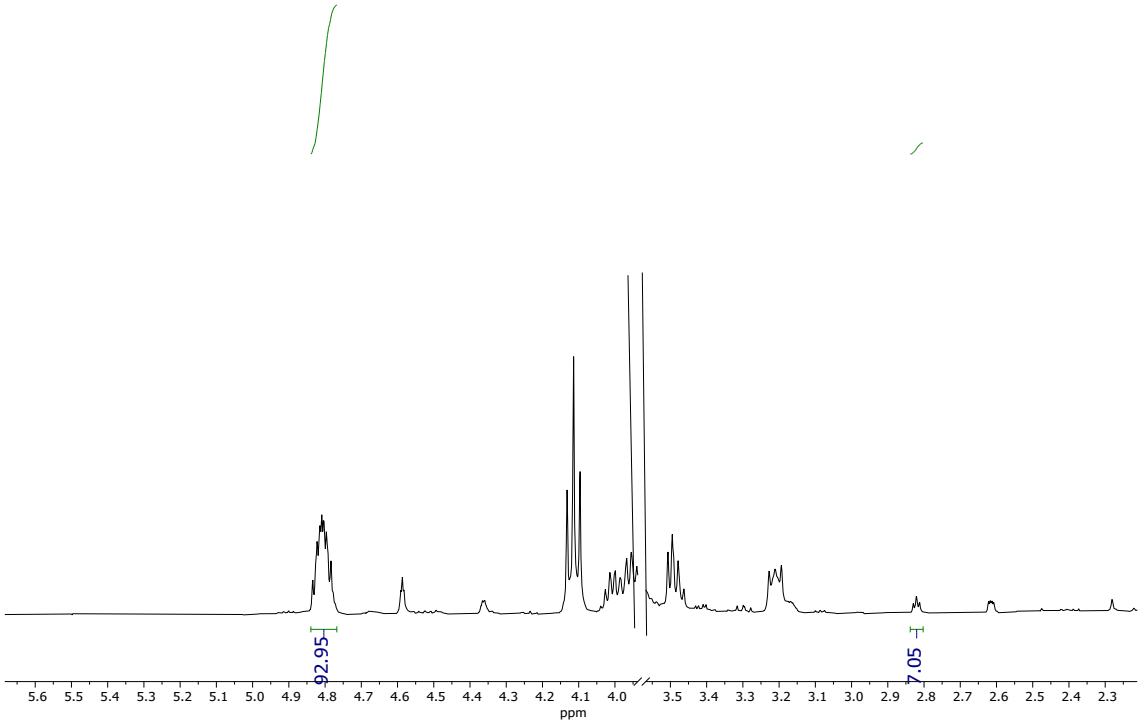

Figure S65. ^{1}H-NMR from reaction crude for the synthesis of product **8h** in $CDCl_3$.

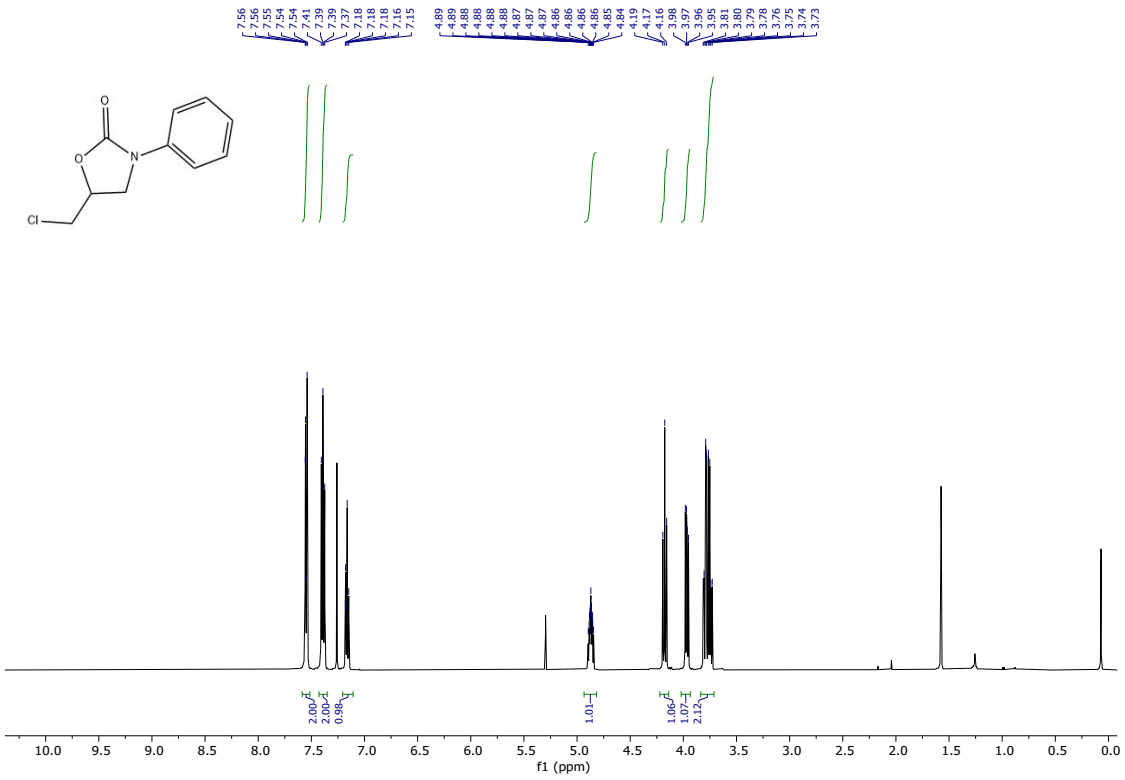

Figure S66. ^{1}H-NMR full chart for compound **8h** in $CDCl_3$.

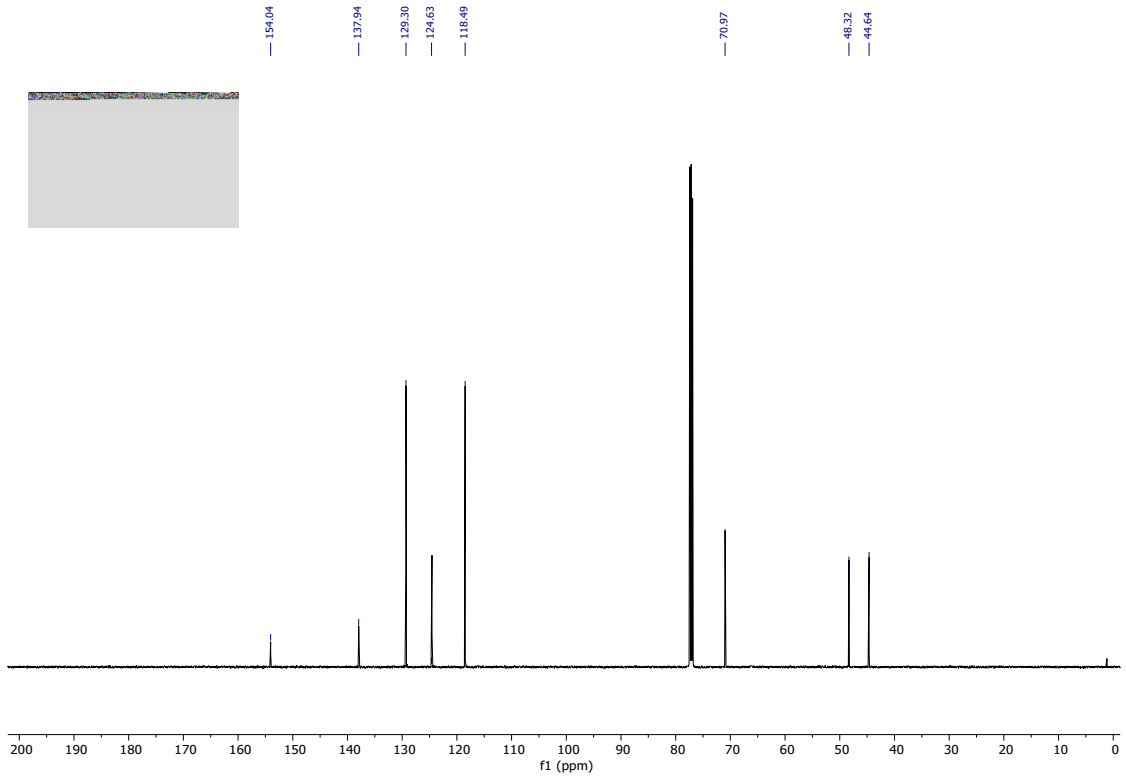

Figure S67. $^{13}C\{^{1}H\}$-NMR full chart for compound **8h** in $CDCl_3$.

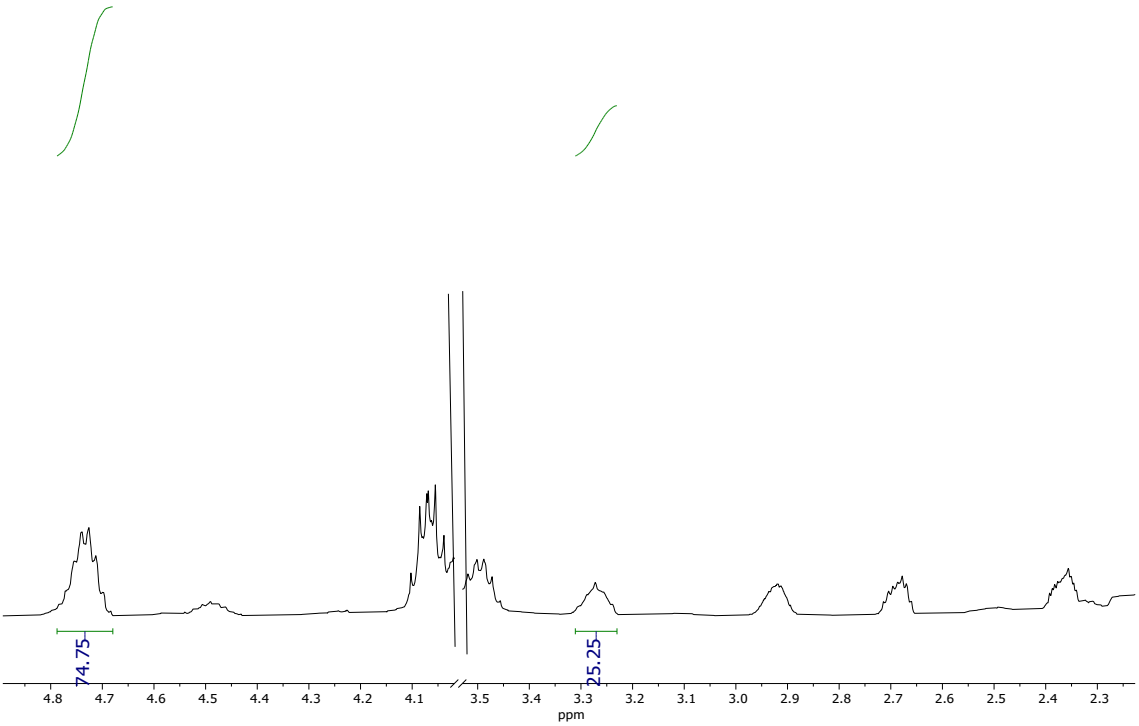

Figure S68. ^{1}H-NMR from reaction crude for the synthesis of product **8i** in $CDCl_3$.

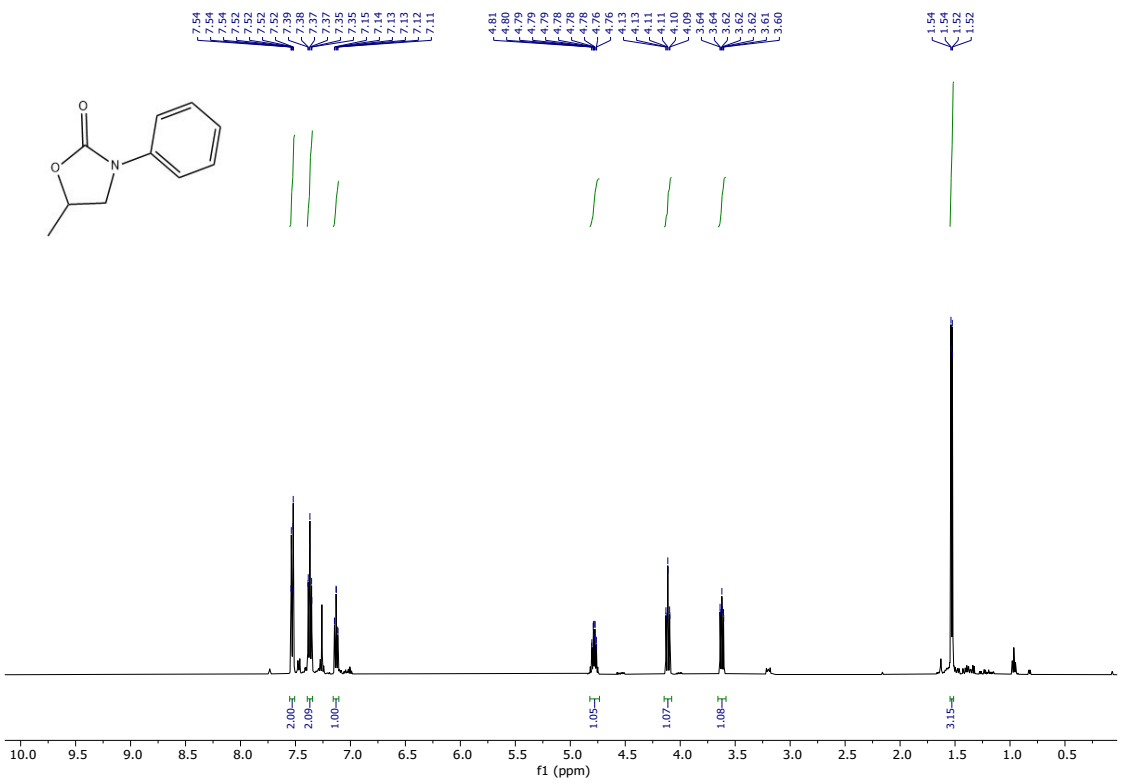

Figure S69. ^{1}H-NMR full chart for compound **8i** in $CDCl_3$.

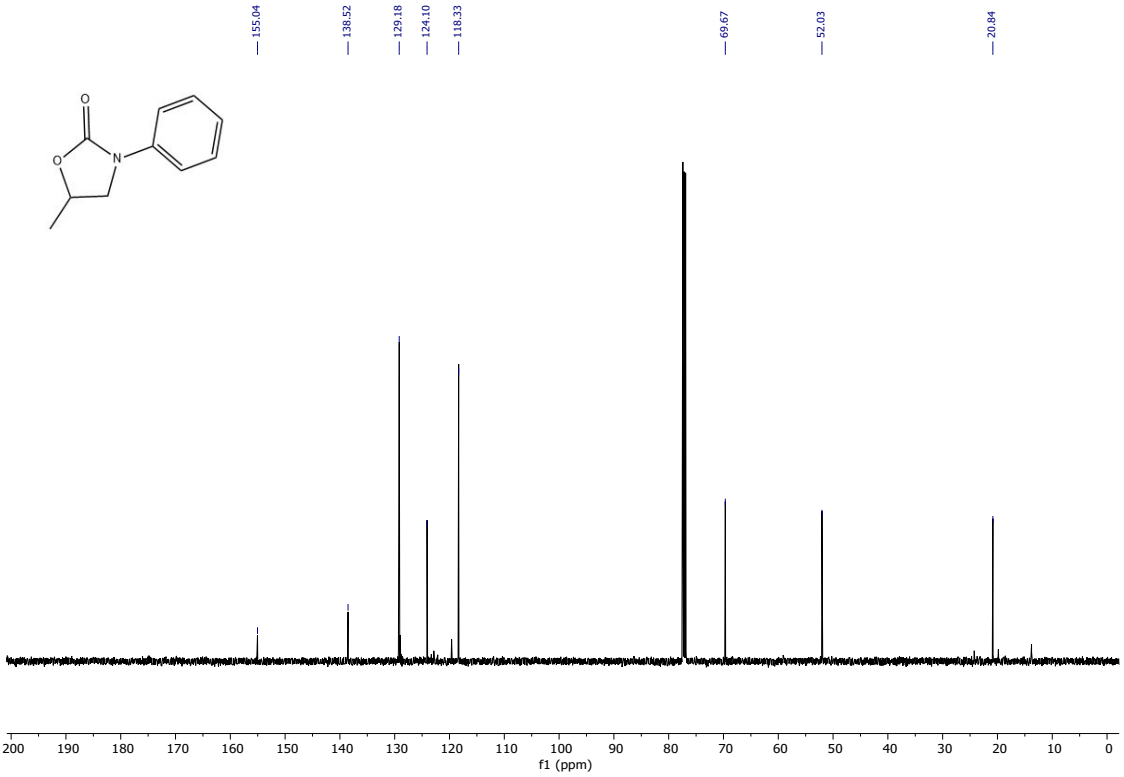

Figure S70. ^{13}C{^{1}H}-NMR full chart for compound **8i** in $CDCl_3$.

8. NMR diffusion studies

The diffusion coefficients were measured by ^{1}H DOSY NMR experiments in a Bruker AV400 using the ledbpgp2s pulse sequence, at room temperature in C_6D_6. We estimate the molecular weight from DOSY NMR results (diffusion coefficients) of the analyte (complex **1**) and the reference (Tetramethylsilane), using the method and software described by Stalke *et al.* [5] In this way, a coefficient of $\log D_{1,norm}$ = -9.1572 g/mol was measured and a molecular weight of 572 g/mol was estimated for compound **1**.

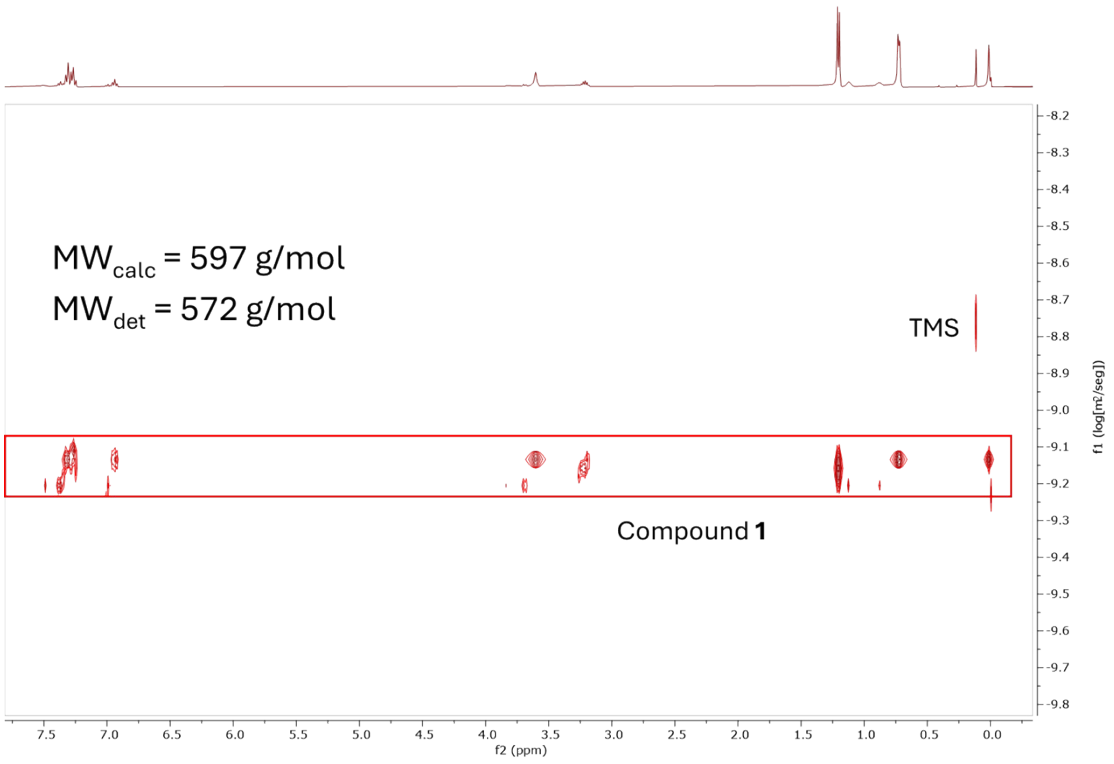

Figure S71. The ^{1}H DOSY NMR spectrum of complex **1**.

9. X-ray structural analyses

Crystal of compounds **1´**, **3** and **4** were mounted on a glass fibre and cooled to the 250 K for compounds **1´** and **4** and 200 K for compound **3**. Data for compound **3** were collected on a Bruker APEX II CCD-based diffractometer equipped with a graphite monochromated MoKα radiation source (λ=0.71073 Å). Intensities were integrated in SAINT[6] and absorption corrections based on equivalent reflections were applied using SADABS.[7] Data for compounds **1´** and **4** were collected on a Rigaku Oxford Diffraction XtaLAB Synergy diffractometer equipped with CuKα radiation

source. Data collection strategy was calculated with the program CrysAlis Pro CCD,[8] and data reduction and cell refinement were performed with the program CrysAlis Pro RED.[8] An empirical absorption correction was applied using the SCALE3 ABSPACK algorithm as implemented in the program CrysAlis Pro RED. Structures were solved using ShelXT,[9] all of the structures were refined by full matrix least squares against F2 in ShelXL[10,11] using Olex2.[12] All of the non-hydrogen atoms were refined anisotropically, while all of the hydrogen atoms were located geometrically and refined using a riding model. Compound **3** shows some disordered fragments and the occupancies of the disordered group were refined with their sum set to equal 1 and subsequently fixed at the refined values. Restraints were applied to maintain sensible thermal and geometric parameters. The X-ray crystallographic coordinates for the structures reported in this study have been deposited at the Cambridge Crystallographic Data Centre (CCDC) under deposition numbers 2520689-2520691. These data can be obtained free of charge via http://www.ccdc.cam.ac.uk/data_request/cif

Table S3. Crystal data and structure refinement for **1´**, **3** and **4**.

Identification code	**1´**	**3**	**4**
Empirical formula	$C_{28}H_{46}N_6O_2Zn_2$	$C_{118}H_{144}N_{12}P_4Zn_4$	$C_{40}H_{54}N_6S_2Zn_2$
Formula weight	629.45	2115.80	813.75
Temperature/K	250.00(10)	200.0	250.15
Crystal system	monoclinic	triclinic	monoclinic
Space group	$P2_1/n$	P-1	$P2_1/c$
a/Å	9.50200(10)	11.8289(5)	12.0842(5)
b/Å	10.97330(10)	11.9812(5)	34.2298(10)
c/Å	15.7972(2)	20.7760(9)	11.1316(4)
α/°	90	100.505(2)	90
β/°	104.7640(10)	99.090(2)	116.101(5)
γ/°	90	100.839(2)	90
Volume/Å^3	1592.76(3)	2786.5(2)	4134.9(3)
Z	2	1	4

ρ_{calc}g/cm^3	1.312	1.261	1.307
μ/mm^{-1}	2.106	0.960	1.296
F(000)	664.0	1116.0	1712.0
Crystal size/mm^3	0.142 × 0.133 × 0.05	0.167 × 0.135 × 0.038	0.35 × 0.3 × 0.1
Radiation	Cu Kα (λ = 1.54184)	MoKα (λ = 0.71073)	MoKα (λ = 0.71073)
2Θ range for data collection/°	9.888 to 136.692	3.546 to 52.934	4.244 to 62.084
Index ranges	-11 ≤ h ≤ 11, -13 ≤ k ≤ 13, -18 ≤ l ≤ 19	-14 ≤ h ≤ 14, -14 ≤ k ≤ 14, -25 ≤ l ≤ 26	-16 ≤ h ≤ 16, -48 ≤ k ≤ 47, -13 ≤ l ≤ 15
Reflections collected	28765	53749	48378
Independent reflections	2921 [R_{int} = 0.0217, R_{sigma} = 0.0094]	11427 [R_{int} = 0.0667, R_{sigma} = 0.0634]	10900 [R_{int} = 0.0301, R_{sigma} = 0.0252]
Data/restraints/parameters	2921/0/177	11427/199/674	10900/187/531
Goodness-of-fit on F^2	1.067	1.066	1.115
Final R indexes [I>=2σ (I)]	R_1 = 0.0228, wR_2 = 0.0639	R_1 = 0.0477, wR_2 = 0.1304	R_1 = 0.0571, wR_2 = 0.1435
Final R indexes [all data]	R_1 = 0.0238, wR_2 = 0.0646	R_1 = 0.0920, wR_2 = 0.1745	R_1 = 0.0709, wR_2 = 0.1486
Largest diff. peak/hole / e Å^{-3}	0.27/-0.25	0.78/-1.12	0.77/-0.65

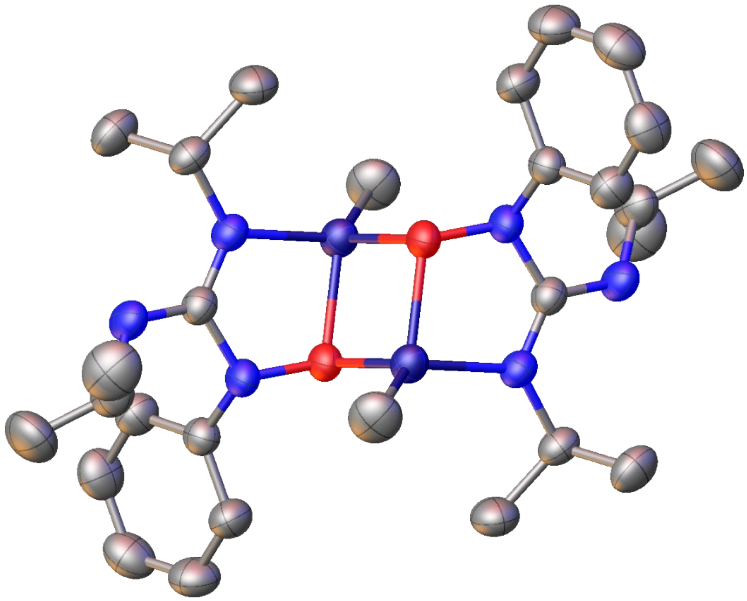

Figure S72. Molecular structures of compound **1´**. H atoms are omitted for clarity.

10. Computational methods

All DFT calculations were carried out using the GAUSSIAN16 package,[13] with the ωB97XD functional.[14] A pruned numerical integration grid (99,590) was used for all the calculations via keyword Int=Ultrafine. All elements were described using the 6-311+G(d,p) basis.[15] Geometry optimizations were performed without symmetry restrictions, using analytical gradient techniques, and starting from initial coordinates derived from X-ray data of related complexes or suitably modified versions of them. Transition States were searched for, either by using Synchronous Transit-Guided Quasi-Newton (STQN) methodologies (keywords QST2 or QST3), or by the "distinguished reaction coordination procedure" by choosing an internal coordinate (typically a distance) as reaction coordinate and running an energy scan calculation along it, with the maxima of this plot being then used as starting point for a conventional transition state optimization. Frequency analysis was performed for all the stationary points to ensure that either, a minimum structure with no imaginary frequencies, or a saddle point with only one negative frequency along the reaction coordinate, were achieved. This calculation also provides thermochemical information about the reaction pathways at 298.15 K and 1 atm using the harmonic approximation. The connectivity of the optimized transition states was corroborated in the forward and backward direction via IRC calculations or by manual displacement of the geometrical parameters along the negative frequency and further optimization of the resulting geometries. Additional .xyz file is provided with the Cartesian coordinates for all the optimized structures.

10.1 DFT calculated structure of compound **1**.

The dimeric structure of compound **1** was fully optimized using the X-ray data of [Zn(Et){(4-t-BuC$_6$H$_4$)NC(NiPr)(NHiPr)}]$_2$ as starting point,[2] and the optimized structure is shown in Figure S73. In order to evaluate the feasibility of a potential deaggregation of the dimer into monomeric species, we also optimized the hypothetical structure of a monomer (Figure S73). However, the calculated Gibbs free energy for the reaction: dimer → 2·monomer, was calculated to be ΔG_r= +15.8 kcal·mol^{-1}, indicating a significantly higher stability of the dimeric motif.

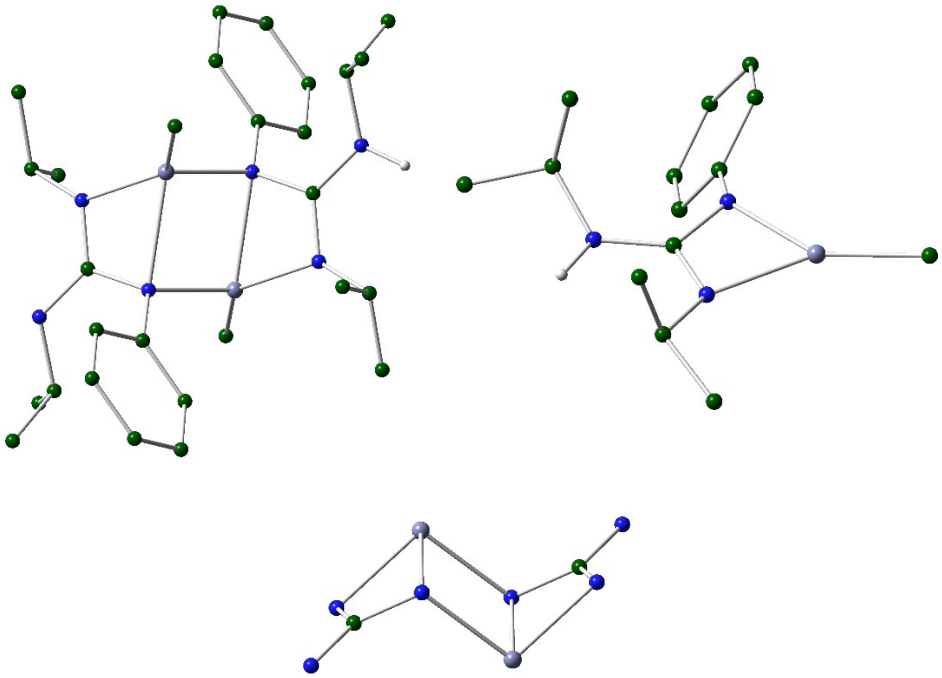

Figure S73. Optimized structures for compound **1** (left) and its monomeric form (right) with a view of the central core in the dimer (bottom). Hydrogen atoms, except those directly bonded to N, omitted for clarity.

11. References

1. C. Ginés, B. Parra-Cadenas, R. Fernández-Galán, D. García-Vivó, D. Elorriaga, A. Ramos, F. Carrillo-Hermosilla, Magnesium and Calcium Bisguanidinates: Catalytic Activity in the Hydroboration of Unsaturated Molecules, *Adv. Synth. Catal.*, 2025, 367, e202400843, 1–12.

2. C. Alonso-Moreno, F. Carrillo-Hermosilla, A. Garcés, A. Otero, I. López-Solera, A. M. Rodriguez, A. Antiñolo, Simple, Versatile, and Efficient Catalysts for Guanylation of Amines, *Organometallics*, 2010, 29(12), 2789–2795.

3. a) H. Vignesh Babu, K. Muralidharan, Y. Yang, Y. Hayashi, Y. Fujii, T. Nagano, Y. Kita, T. Ohshima, J. Okuda, K. Mashima, Efficient cyclic carbonate synthesis catalyzed by zinc cluster systems under mild conditions, Catal. Sci. Technol., 2012, 2(3), 509–513. b) H. Vignesh Babu, K. Muralidharan, Zn(II), Cd(II) and Cu(II) complexes of 2,5-bis{N-(2,6-diisopropylphenyl)iminomethyl}pyrrole: synthesis, structures and their high catalytic activity for efficient cyclic carbonate synthesis, Dalton Trans., 2013, 42(4), 1238–1248. c) X.-D. Lang, Y.-C. Yu, L.-N. He, Zn-salen complexes with multiple hydrogen bonding donor and protic ammonium bromide: Bifunctional catalysts for CO_2 fixation with epoxides at atmospheric pressure, J. Mol. Catal. A: Chem., 2016, 420, 208–215.d) L. Cuesta-Aluja, A. Campos-Carrasco, J. Castilla, M. Reguero, A. M. Masdeu-Bultó, A. Aghmiz, Highly active and selective Zn(II)-NN'O Schiff base catalysts for the cycloaddition of CO_2 to epoxides, J. CO_2 Util., 2016, 14, 10–22. e) S. He, F. Wang, W.-L. Tong, S.-M. Yiu, M. C. W. Chan, Topologically diverse shape-persistent bis-(Zn–salphen) catalysts: efficient cyclic carbonate formation under mild conditions, Chem. Commun., 2016, 52(7), 1017–1020. f) C. Maeda, J. Shimonishi, R. Miyazaki, J. Hasegawa, T. Ema, Highly active and robust metalloporphyrin catalysts for the synthesis of cyclic carbonates from a broad range of epoxides and carbon dioxide, Chem. Eur. J., 2016, 22(19), 6556–6563. g) Y. Ge, G. Cheng, N. Xu, W. Wang, H. Ke, Zinc 2-N-methyl N-confused porphyrin: an efficient catalyst for the conversion of CO_2 into cyclic carbonates, Catal. Sci. Technol., 2019, 9, 4255–4261. h) S. Zhang, F. Han, S. Yan, M. He, C. Miao, L.-N. He, Efficient catalysts in situ generated from zinc, amide and benzyl bromide for epoxide/CO_2 coupling reaction at atmospheric pressure, Eur. J. Org. Chem., 2019, 6, 1311–1316. i) J.-J. Chen, Y.-C. Xu, Z.-L. Gan, X. Peng, X.-Y. Yi, Zinc complexes with tridentate pyridyl–pyrrole ligands and their use as catalysts in CO_2 fixation into cyclic carbonates, Eur. J. Inorg. Chem., 2019(13), 1733–1739. j) S. Sobrino, M. Navarro, J. Fernández-Baeza, L. F. Sánchez-Barba, A. Garcés, A. Lara-Sánchez, J. A. Castro-Osma, Efficient CO_2 fixation into cyclic carbonates catalyzed by NNO-

scorpionate zinc complexes, Dalton Trans., 2019, 48(28), 10733–10742. k) G. Chen, J. Zhang, X. Cheng, X. Tan, J. Shi, D. Tan, B. Zhang, Q. Wan, F. Zhang, L. Liu, B. Han, G. Yang, Metal Ionic Liquids for the Rapid Chemical Fixation of CO_2 under Ambient Conditions, ChemCatChem, 2020, 12(7), 1963–1967. l) F. M. Al-Qaisi, A. K. Qaroush, A. H. Smadi, F. Alsoubani, K. I. Assaf, T. Repo, A. F. Eftaiha, CO_2 coupling with epoxides catalysed by using one-pot synthesised, in situ activated zinc ascorbate under ambient conditions, Dalton Trans., 2020, 49, 7673–7679. m) R. Kumar, S. C. Sahoo, P. K. Nanda, A μ_4-Oxo Bridged Tetranuclear Zinc Complex as an Efficient Multitask Catalyst for CO_2 Conversion, Eur. J. Inorg. Chem., 2021, 1057–1064. n) K. I. Assaf, A. K. Qaroush, I. K. Okashah, F. M. Al-Qaisi, F. Alsoubani, A. F. Eftaiha, Activation of β-diketones for CO_2 capture and utilization, React. Chem. Eng., 2021, 6, 2364–2375. o) K. Naveen, H. Ji, T. S. Kim, D. Kim, D.-H. Cho, C_3-symmetric zinc complexes as sustainable catalysts for transforming carbon dioxide into mono- and multi-cyclic carbonates, Appl. Catal. B: Environ., 2021, 280, 119395. p) K. Yin, L. Hua, L. Qu, Q. Yao, Y. Wang, D. Yuan, H. You, Y. Yao, Heterobimetallic rare earth metal–zinc catalysts for reactions of epoxides and CO_2 under ambient conditions, Dalton Trans., 2021, 50(4), 1453–1464. q) J. Ma, Y. Wu, X. Yan, C. Chen, T. Wu, H. Fan, Z. Liu, B. Han, Efficient synthesis of cyclic carbonates from CO_2 under ambient conditions over $Zn(betaine)_2Br_2$: Experimental and theoretical studies, Phys. Chem. Chem. Phys., 2022, 24(7), 4298–4304. r) M. Navarro, S. Sobrino, I. Fernández, A. Lara-Sánchez, A. Garcés, L. F. Sánchez-Barba, Exploring Enantiopure Zinc-Scorpionates as Catalysts for the Preparation of Polylactides, Cyclic Carbonates, and Polycarbonates, Dalton Trans., 2024, 53, 13933–13949.

4. a) J. E. Herweh, W. J. Kauffman, 2-Oxazolidones via the Lithium Bromide Catalyzed Reaction of Isocyanates with Epoxides in Hydrocarbon Solvents, Tetrahedron Lett., 1971, 12, 809–812. b) I. Shibata, A. Baba, H. Iwasaki, H. Matsuda, Cycloaddition Reaction of Heterocumulenes with Oxiranes Catalyzed by an Organotin Iodide-Lewis Base Complex, J. Org. Chem., 1986, 51, 2177–2184. c) A. Baba, M. Fujiwara, H. Matsuda, Unusual cycloaddition of oxiranes with isocyanates catalyzed by tetraphenylstibonium iodide; selective formation of 3,4-disubstituted oxazolidinones, Tetrahedron Lett., 1986, 27, 77–80. d) C. Qian, D. Zhu, A Facile Synthesis of Oxazolidinones via Lanthanide-Catalyzed Cycloaddition of Epoxides with Isocyanates, Synlett, 1994, 2, 129–130. e) L. Aroua, A. Baklouti, Synthesis of α,ω-Bis(oxazolidinone)polyoxyethylene via a Lithium Bromide–Catalyzed Reaction of Oligoethylene Glycol Diglycidyl Ethers with Isocyanates, Synth.

Commun., 2007, 37, 1935–1942. f) M. T. Barros, A. M. Faísca Phillips, The first enantioselective [3+2] cycloaddition of epoxides to arylisocyanates: asymmetric synthesis of chiral oxazolidinone phosphonates, Tetrahedron: Asymmetry, 2010, 21, 2746–2752. g) T. Baronsky, C. Beattie, R. W. Harrington, R. Irfan, M. North, J. G. Osende, C. Young, Bimetallic Aluminum(salen) Catalyzed Synthesis of Oxazolidinones from Epoxides and Isocyanates, ACS Catal., 2013, 3, 790–797. h) R. L. Paddock, D. Adhikari, R. L. Lord, M.-H. Baik, S. T. Nguyen, [(Salcen)CrIII + Lewis base]-Catalyzed Synthesis of N-Aryl-Substituted Oxazolidinones from Epoxides and Aryl Isocyanates, Chem. Commun., 2014, 50, 15187–15190. i) C. Beattie, M. North, Vanadium(V)(salen) Catalysed Synthesis of Oxazolidinones from Epoxides and Isocyanates, RSC Adv., 2014, 4, 31345–31352. j) P. Wang, J. Qin, D. Yuan, Y. Wang, Y. Yao, Synthesis of Oxazolidinones from Epoxides and Isocyanates Catalyzed by Rare-Earth-Metal Complexes, ChemCatChem, 2015, 7, 1145–1151. k) J. A. Castro-Osma, A. Earlam, A. Lara-Sánchez, A. Otero, M. North, Synthesis of Oxazolidinones from Epoxides and Isocyanates Catalysed by Aluminium Heteroscorpionate Complexes, ChemCatChem, 2016, 8, 2100–2108. l) X. Wu, J. Mason, M. North, Isocyanurate Formation During Oxazolidinone Synthesis from Epoxides and Isocyanates Catalysed by a Chromium (Salphen) Complex, Chem. Eur. J., 2017, 23, 12937–12943. m) Y. Toda, S. Gomyou, S. Tanaka, Y. Komiyama, A. Kikuchi, H. Suga, Tetraarylphosphonium Salt-Catalyzed Synthesis of Oxazolidinones from Isocyanates and Epoxides, Org. Lett., 2017, 19, 5786–5789. n) M. Yang, N. Pati, G. Bélanger-Chabot, M. Hirai, F. P. Gabbaï, Influence of the catalyst structure in the cycloaddition of isocyanates to oxiranes promoted by tetraarylstibonium cations, Dalton Trans., 2018, 47, 11843–11850. o) H. J. Altmann, M. Clauss, S. König, E. Frick-Delaittre, C. Koopmans, A. Wolf, C. Guertler, S. Naumann, M. R. Buchmeiser, Synthesis of Linear Poly(oxazolidin-2-one)s by Cooperative Catalysis Based on N-Heterocyclic Carbenes and Simple Lewis Acids, Macromolecules, 2019, 52, 487–494. p) Y. Toda, S. Tanaka, S. Gomyou, A. Kikuchi, H. Suga, 4-Hydroxymethyl-substituted oxazolidinone synthesis by tetraarylphosphonium salt-catalyzed reactions of glycidols with isocyanates, Chem. Commun., 2019, 55, 5761--5764 q) P. Yingcharoen, W. Natongchai, A. Poater, V. D'Elia, Intertwined Chemistry of Hydroxyl Hydrogen-Bond Donors, Epoxides and Isocyanates in the Organocatalytic Synthesis of Oxazolidinones versus Isocyanurates: Rational Catalytic Investigation and Mechanistic Understanding, Catal. Sci. Technol., 2020, 10, 5544–5558. r) R. Nishiyori, K. Okuno, S. Shirakawa, Triethylamine Hydroiodide as a Bifunctional Catalyst for the Solvent-Free

Synthesis of 2-Oxazolidinones, Eur. J. Org. Chem., 2020, 2020, 4937–4941. s) A. Rostami, A. Ebrahimi, J. Husband, M. U. Anwar, R. Csuk, A. Al-Harrasi, Squaramide–Quaternary Ammonium Salt as an Effective Binary Organocatalytic System for Oxazolidinone Synthesis from Isocyanates and Epoxides, Eur. J. Org. Chem., 2020, 2020, 1881–1895. t) D.-X. Cui, Y.-D. Li, P. Huang, Z. Tian, Y.-Y. Jia, P.-A.Wang, Bifunctional phase-transfer catalysts for synthesis of 2-oxazolidinones from isocyanates and epoxides, RSC Adv., 2020, 10, 12360–12364. u) A. Rostami, A. Ebrahimi, N. Sakhaee, F.Golmohammadi, A. Al-Har, Microwave-Assisted Electrostatically Enhanced Phenol-Catalyzed Synthesis of Oxazolidinones, J. Org. Chem. 2022, 87, 40−55. v) M. P. Caballero, F. Carrascosa, F. de la Cruz-Martínez, J. A. Castro-Osma, A. M. Rodríguez, M. North, A. Lara-Sánchez, J. Tejeda, 4-(2-Hydroxyphenyl)imidazolium Salts as Organocatalysts for Cycloaddition of Isocyanates and Epoxides to Yield Oxazolidin-2-ones, ChemSelect, 2022, 7, e202103977. w) Z. Zhang, Y. Ni, Z. Li, J. He, X. Zou, X. Yuan, Z. Liu, S. Cao, C. Ma, K. Guo, Amino-cyclopropenium H-bonding organocatalysis in cycloaddition of glycidol and isocyanate to oxazolidinone, Mol. Catal., 2023, 548, 113425.

5. S. Bachmann, B. Gernert, D. Stalke, Chem Commun. 2016, 52, 12861−12864. For further information regarding ECCs and the methodology see: R. Neufeld, D. Stalke, Chem. Sci. 2015, 6, 3354−3364. S. Bachmann, R. Neufeld, M. Dzemski, D. Stalke, Chem. Eur. J. 2016, 22, 8462−8465.

6. Bruker, SAINT+ v8.38A Integration Engine, Data Reduction Software, Bruker Analytical X-ray Instruments Inc., Madison, WI, USA, 2015.

7. Bruker, SADABS 2014/5, Bruker AXS area detector scaling and absorption correction, Bruker Analytical X-ray Instruments Inc., Madison, Wisconsin, USA, 2014/5.

8. Rigaku OD (2023). CrysAlis PRO. Rigaku Oxford Diffraction, Yarnton, Englan.

9. G.M. Sheldrick, Acta Crystallogr. Sect. A: Found. Crystallogr. 2015, 71, 3-8.

10. G.M. Sheldrick, Acta Crystallogr. Sect. A: Found. Crystallogr. 2008, 64, 112-122.

11. G.M. Sheldrick, Acta Crystallogr. Sect. C: Struct. Chem. 2015, 71, 3-8.

12. O.V. Dolomanov, L. J. Bourhis, R. J. Gildea, J. A. K. Howard, H. J. Puschmann, Appl. Crystallogr. 2009, 42, 339-341.

13. M.J. Frisch, G.W. Trucks, H.B. Schlegel, G.E. Scuseria, M.A. Robb, J.R. Cheeseman, G. Scalmani, V. Barone, G.A. Petersson, H. Nakatsuji, X. Li, M. Caricato, A.V. Marenich, J. Bloino, B.G. Janesko, R. Gomperts, B. Mennucci, H.P. Hratchian, J.V. Ortiz, A.F. Izmaylov, J.L. Sonnenberg, D. Williams-Young, F. Ding, F. Lipparini, F. Egidi, J. Goings, B. Peng, A. Petrone, T. Henderson, D. Ranasinghe, V.G. Zakrzewski, J. Gao, Rega, N.; G. Zheng, W. Liang, M. Hada, M. Ehara, K. Toyota, R. Fukuda, J. Hasegawa, M. Ishida, T. Nakajima, Y. Honda, O. Kitao, H. Nakai, T. Vreven, K. Throssell, J.A. Montgomery, Jr., J.E. Peralta, F. Ogliaro, M.J. Bearpark, J.J. Heyd, E.N. Brothers, K.N. Kudin, V.N. Staroverov, T.A. Keith, R. Kobayashi, J. Normand, K. Raghavachari, A.P. Rendell, J.C. Burant, S.S. Iyengar, J. Tomasi, M. Cossi, J.M. Millam, M. Klene, C. Adamo, R. Cammi, J.W. Ochterski, R.L. Martin, K. Morokuma, O. Farkas, J.B. Foresman, D.J. Fox, Gaussian 16, Revision A.03, Gaussian, Inc., Wallingford CT, USA, 2016.

14. J.-D. Chaia, M. Head-Gordon, Long-range corrected hybrid density functionals with damped atom–atom dispersion corrections, Phys. Chem. Chem. Phys. 2008, 10, 6615-6620.

15. a) A. D. McLean and G. S. Chandler, Contracted Gaussian-basis sets for molecular calculations. 1. 2nd row atoms, Z=11-18, J. Chem. Phys., 1980, 5639-5648. b) Krishnan, J. S. Binkley, R. Seeger, J. A. Pople Self-consistent molecular orbital methods. XX. A basis set for correlated wave functions, J. Chem. Phys., 1980, 72, 650–654. c) T. Clark, J. Chandrasekhar, G. W. Spitznagel, P. v. R. Schleyer, Efficient diffuse function-augmented basis sets for anion calculations, J. Comput. Chem., 1983, 4, 294–301. d) A. J. H. Wachters, Gaussian basis set for molecular wavefunctions containing third-row atoms, J. Chem. Phys., 1970, 52, 1033-1036. d) P. J. Hay, Gaussian basis sets for molecular calculations. The representation of 3d orbitals in transition-metal atoms. J. Chem. Phys., 1977, 66, 4377-4384. e) K. Raghavachari, G. W. Trucks, Highly correlated systems: Excitation energies of first row transition metals Sc-Cu, J. Chem. Phys., 1989, 91, 1062-1065.